

2013

Scanning Electron Microscope (SEM) as a means to determine dispersibility

Erica Velasco
Iowa State University

Follow this and additional works at: <https://lib.dr.iastate.edu/etd>

 Part of the [Geotechnical Engineering Commons](#), and the [Soil Science Commons](#)

Recommended Citation

Velasco, Erica, "Scanning Electron Microscope (SEM) as a means to determine dispersibility" (2013). *Graduate Theses and Dissertations*. 13396.
<https://lib.dr.iastate.edu/etd/13396>

This Thesis is brought to you for free and open access by the Iowa State University Capstones, Theses and Dissertations at Iowa State University Digital Repository. It has been accepted for inclusion in Graduate Theses and Dissertations by an authorized administrator of Iowa State University Digital Repository. For more information, please contact digirep@iastate.edu.

Scanning Electron Microscope (SEM) images as a means to determine dispersibility

by

Erica Susan Velasco

A thesis submitted to the graduate faculty
in partial fulfillment of the requirements for the degree of
MASTER OF SCIENCE

Major: Civil Engineering (Geotechnical Engineering)

Program of Study Committee:
Vernon R. Schaefer, Major Professor
David J. White
Richard Cruse

Iowa State University
Ames, Iowa
2013

Copyright © Erica Susan Velasco, 2013. All rights reserved.

DEDICATION

For my family, Rick, Sue, and Rose Velasco.

TABLE OF CONTENTS

LIST OF TABLES	viii
LIST OF FIGURES.....	x
ACKNOWLEDGEMENTS	xiv
ABSTRACT.....	xv
CHAPTER 1. INTRODUCTION	1
Industry problem.....	1
Industry concerns	1
Impact on industry.....	2
Technical problem	2
Objectives	3
Significance of the research.....	3
Organization of the document.....	4
CHAPTER 2. BACKGROUND	5
Literature review.....	5
Dispersive clay properties	5
Dispersive clay identification test methods.....	12
Dispersive clay treatment options	20
Scanning electron microscopy (SEM) analysis.....	24
Preliminary work	36
Dispersive clay study for Los Esteros Lake Project; Santa Rosa, NM	36
Consolidation of a flocculated illite	37
CHAPTER 3. METHODS	38
Research design	38
Crumb test.....	38
Equipment	39
Preparation of samples	39
Procedure.....	40
Interpretation of data	41

Pinhole test.....	42
Equipment	42
Preparation of samples	44
Procedure.....	45
Interpretation of data	51
Double hydrometer test.....	51
Particle size analysis of soils	52
Dispersive characteristics of clay soil by double hydrometer.....	55
Percent dispersibility calculation.....	59
Modified free swell index	60
Equipment	60
Preparation of samples	60
Procedure.....	60
Interpretation of data	61
SEM testing.....	61
Equipment	62
Sample preparation.....	64
Procedure.....	68
Interpretation of data	71
Lime treatment.....	74
Equipment	75
Preparation of samples	75
Procedure.....	75
CHAPTER 4. MATERIALS.....	76
Oxidized glacial till.....	76
Laboratory test results	76
Alluvial top stratum	77
Laboratory test results	78
Western Iowa loess	79
Laboratory test results	80
Bentonite.....	81
Laboratory test results	81

Kaolinite.....	83
Laboratory test results	83
Santa Rosa clay	84
Laboratory test results	86
Prepared sodium illite	87
Laboratory test results	89
CHAPTER 5. RESULTS AND DISCUSSION	91
Oxidized glacial till.....	93
Crumb test	93
Pinhole test	94
Double hydrometer test	95
Modified free swell index test	96
SEM images	97
Ultimate sample classification.....	99
Alluvial top stratum	99
Crumb test	99
Pinhole test	100
Double hydrometer test	102
Modified free swell index test	103
SEM images	103
Ultimate sample classificaation.....	105
Western Iowa loess	105
Crumb test	105
Pinhole test	106
Double hydrometer test	108
Modified free swell index test	109
SEM images	109
Ultimate sample classification.....	111
Bentonite - untreated.....	111
Crumb test	111
Pinhole test	112
Double hydrometer test	114

Modified free swell index test.....	115
SEM images	115
Ultimate sample classification.....	117
Bentonite – treated with 4% lime	117
Crumb test	117
Pinhole test	118
Modified free swell index test.....	120
SEM images	120
Ultimate sample classification.....	122
Kaolinite.....	122
Crumb test	122
Pinhole test	123
Double hydrometer test	125
Modified free swell index test.....	126
SEM images	127
Ultimate sample classification.....	129
Santa Rosa clay	129
Crumb test	129
Pinhole test	130
Double hydrometer test	131
Modified free swell index test.....	132
SEM images	133
Ultimate sample classification.....	135
Sodium illite - untreated	135
Crumb test	136
Pinhole test	136
Double hydrometer test	138
Modified free swell index test.....	139
SEM images	140
Ultimate sample classification.....	143
Sodium illite – treated with 4% lime	143
Crumb test	143

Pinhole test	144
Modified free swell index test	145
SEM images	146
Ultimate sample classification.....	149
Discussion of SEM images by classification.....	149
Nondispersive soil images.....	149
Moderately dispersive soil images	151
Dispersive soil	154
SEM comparison of treated Soils to untreated.....	155
CHAPTER 6. CONCLUSIONS AND RECOMMENDATIONS	160
Conclusions.....	160
Dispersive clay properties	160
Dispersive clay identification test methods.....	161
Dispersive clay treatment effects	161
Dispersive clay microstructure observation using SEM technology.....	162
Recommendations for future research.....	163
REFERENCES	165
APPENDIX. TEST RESULTS	169
Oxidized glacial till.....	169
Alluvial top stratum	173
Western Iowa loess	177
Bentonite.....	181
Kaolinite.....	188
Santa Rosa clay	194
Sodium illite.....	198
Crumb Test Results.....	204

LIST OF TABLES

Table 1. Summary of properties by clay mineralogy	9
Table 2. Degree of dispersion by percent dispersivity	15
Table 3. Swelling potential based on modified free swell index.....	17
Table 4. Table of dispersive clay classification by ESP.....	18
Table 5. Temperature correction values	59
Table 6. Swelling potential based on modified free swell index.....	61
Table 7. Particle size and Atterberg test summary for oxidized glacial till	77
Table 8. Particle size and Atterberg test summary for alluvial top stratum	78
Table 9. Particle size and Atterberg test summary for Western Iowa loess	80
Table 10. Particle size and Atterberg test summary for bentonite	82
Table 11. Particle size and Atterberg test summary for kaolinite	83
Table 12. Table of Santa Rosa clay properties as performed by HWS, Inc.....	85
Table 13. Particle size and Atterberg test summary for Santa Rosa clay.....	86
Table 14. Particle size and Atterberg test summary for prepared sodium illite	90
Table 15. Test results and classification summary.....	92
Table 16. Crumb test results for oxidized till.....	93
Table 17. Double hydrometer test results for oxidized till.....	96
Table 18. Modified free swell Index results for oxidized till.....	97
Table 19. Summary table of dispersivity tests for oxidized glacial till.....	99
Table 20. Crumb test results for alluvial top stratum	99
Table 21. Double hydrometer test results for alluvial top stratum.....	102
Table 22. Modified free swell index results for alluvial top stratum	103
Table 23. Summary table of dispersivity tests for alluvial top stratum.....	105
Table 24. Crumb test results for Western Iowa loess.....	106
Table 25. Double hydrometer test results for Western Iowa loess.....	108
Table 26. Modified free swell index results for Western Iowa loess	109
Table 27. Summary table of dispersivity tests for Western Iowa loess	111
Table 28. Crumb test results for untreated bentonite	111
Table 29. Double hydrometer test results for untreated bentonite	114
Table 30. Modified free swell index results for untreated bentonite.....	115
Table 31. Summary table of dispersivity tests for untreated bentonite	117
Table 32. Crumb test results for treated bentonite	118
Table 33. Modified free swell index results for treated bentonite.....	120
Table 34. Summary table of dispersivity tests for treated bentonite	122
Table 35. Crumb test results for kaolinite	123
Table 36. Double hydrometer test results for kaolinite	126
Table 37. Modified free swell index results for kaolinite	127
Table 38. Summary table of dispersivity tests for kaolinite.....	129
Table 39. Crumb test results for Santa Rosa clay.....	129
Table 40. Double hydrometer test results for Santa Rosa clay	132
Table 41. Modified free swell Index results for Santa Rosa clay.....	133
Table 42. Summary table of dispersivity tests for Santa Rosa clay	135

Table 43. Crumb test results for sodium illite	136
Table 44. Double hydrometer test results for sodium illite	139
Table 45. Modified free swell index results for sodium illite	140
Table 46. Summary table of dispersivity tests for sodium illite.....	143
Table 47. Crumb test results for treated sodium illite	143
Table 48. Modified free swell index results for treated sodium illite	146
Table 49. Summary table of dispersivity tests for treated sodium illite.....	149

LIST OF FIGURES

Figure 1. Schematic view of montmorillonite structure.....	6
Figure 2. Schematic view of illite structure	8
Figure 3. Schematic view of kaolinite structure.....	9
Figure 4. Simplified chart portraying how to determine classification in pinhole test	14
Figure 5. Chart depicting percent dispersion in double hydrometer test.....	15
Figure 6. Dispersive clay classification by SAR and TDS by percent sodium	20
Figure 7. Schematic of three-lens electron column that may be used in a SEM.....	25
Figure 8. Cross section of a SEM electron column with discussed pieces highlighted ...	26
Figure 9. Visual of SE emission differing with topographic features	27
Figure 10. Illustration of SE detection from a specimen with varying features.....	27
Figure 11. Relationship between backscattering coefficient and atomic number	28
Figure 12. Schematic diagram of an inner atomic electron shell	29
Figure 13. Illustration showing the creation of a characteristic X-ray.	30
Figure 14. Example of histogram produced by energy dispersive X-ray spectrometry ...	31
Figure 15. Modes of particle associations in clay suspension systems	32
Figure 16. SEM images of flocculated kaolin	34
Figure 17. SEM images of dispersed kaolin.....	34
Figure 18. SEM images of bentonite with and without treatment.....	35
Figure 19. SEM images of bentonite with and without treatment.....	36
Figure 20. Crumb test data form for dispersibility of clayey soils.....	41
Figure 21. Complete assembled pinhole dispersion system.....	43
Figure 22. A complete picture of the pinhole test specimen apparatus.....	44
Figure 23. Harvard miniature compaction equipment.....	46
Figure 24. Schematic view of pinhole test specimen	47
Figure 25. Schematic view of final assembled apparatus	48
Figure 26. Pinhole test data form	49
Figure 27. Air-jet dispersion tube use for mechanical agitation in ASTM D 422-63	53
Figure 28. Hydrometer test data sheet.....	53
Figure 29. Particle size distribution curve for a Des Moines County soil.....	55
Figure 30. Vacuum used for de-airing of sample in ASTM D 4221-99	57
Figure 31. Q150 T Turbo-Pumped Sputter Coater/Carbon Coater	63
Figure 32. FEI Quanta 250 SEM in the Iowa State MARL	64
Figure 33. Graphite coating and brush used to affix soil sample to carbon stud	65
Figure 34. Sample platform for sputter coating	66
Figure 35. Touch screen control for Q150T sputter coater	66
Figure 36. Sputter coating chamber during sputtering	67
Figure 37. Coated samples for SEM testing from (a) side and (b) top view	67
Figure 38. Image of soil samples placed in SEM machine for testing.....	68
Figure 39. Working distance of SEM used for analysis from Nav-Cam	69
Figure 40. Nav-Cam image recording sample locations in SEM.....	69
Figure 41. Knob set used to focus SEM on sample.....	70
Figure 42. SEM image of a montmorillonite	72

Figure 43. SEM image of an illite	73
Figure 44. SEM image of a kaolinite	74
Figure 45. Grain size distribution for oxidized glacial till	77
Figure 46. Grain size distribution for alluvial top stratum	79
Figure 47. Grain size distribution for Western Iowa loess.....	81
Figure 48. Grain size distribution for bentonite	82
Figure 49. Grain size distribution for kaolinite	84
Figure 50. Grain size distribution for Santa Rosa clay.....	87
Figure 51. View of compaction permeameter system used to compress sodium illite	89
Figure 52. Grain size distribution for prepared sodium illite	90
Figure 53. Crumb test for oxidized till at increasing times	93
Figure 54. Effluent from pinhole test for oxidized till	94
Figure 55. Aerial size of hole after pinhole test completion for oxidized till	95
Figure 56. Inner size of hole compared with drill needle for oxidized till.....	95
Figure 57. Double hydrometer particle size distributions for oxidized till	96
Figure 58. Final swell volume for modified free swell test for oxidized till.....	97
Figure 59. SEM images of oxidized till in order of increasing magnification.....	98
Figure 60. Crumb test for alluvial top stratum at increasing times	100
Figure 61. Effluent from pinhole test for alluvial top stratum	101
Figure 62. Aerial size of hole after pinhole test completion for alluvial top stratum	101
Figure 63. Inner size of hole compared with drill needle for alluvial top stratum.....	101
Figure 64. Double hydrometer particle size distributions for alluvial top stratum	102
Figure 65. Final swell volume for modified free swell test for alluvial top stratum.....	103
Figure 66. SEM images of alluvial top stratum in order of increasing magnification...	104
Figure 67. Crumb test for Western Iowa loess at increasing times	106
Figure 68. Effluent from pinhole test for Western Iowa loess	107
Figure 69. Aerial size of hole after pinhole test completion for Western Iowa loess	107
Figure 70. Inner size of hole compared with drill needle for Western Iowa loess.....	107
Figure 71. Double hydrometer particle size distributions for Western Iowa loess	108
Figure 72. Final swell volume for modified free swell test for Western Iowa loess.....	109
Figure 73. SEM images of Western Iowa loess in order of increasing magnification...	110
Figure 74. Crumb test for untreated bentonite at increasing times	112
Figure 75. Effluent from pinhole test for untreated bentonite.....	113
Figure 76. Aerial size of hole after pinhole test completion for untreated bentonite.....	113
Figure 77. Inner size of hole compared with drill needle for untreated bentonite	113
Figure 78. Double hydrometer particle size distributions for untreated bentonite.....	114
Figure 79. Final swell volume for modified free swell test for untreated bentonite	115
Figure 80. SEM images of untreated bentonite in order of increasing magnification ...	116
Figure 81. Crumb test for treated bentonite at increasing times	118
Figure 82. Effluent from pinhole test for treated bentonite.....	119
Figure 83. Aerial size of hole after pinhole test completion for treated bentonite.....	119
Figure 84. Inner size of hole compared with drill needle for treated bentonite	119
Figure 85. Final swell volume for modified free swell test for treated bentonite	120
Figure 86. SEM images of treated bentonite in order of increasing magnification	121

Figure 87. Crumb test for kaolinite at increasing times	123
Figure 88. Effluent from pinhole test for kaolinite	124
Figure 89. Aerial size of hole after pinhole test completion for kaolinite.....	124
Figure 90. Inner size of hole compared with drill needle for kaolinite	125
Figure 91. Double hydrometer particle size distributions for kaolinite	125
Figure 92. Final swell volume for modified free swell test for kaolinite.....	126
Figure 93. SEM images of kaolinite in order of increasing magnification	128
Figure 94. Crumb test for Santa Rosa clay at increasing times.....	130
Figure 95. Effluent from pinhole test for Santa Rosa clay.....	131
Figure 96. Aerial size of hole after pinhole test completion for Santa Rosa clay	131
Figure 97. Inner size of hole compared with drill needle for Santa Rosa clay	131
Figure 98. Double hydrometer particle size distributions for Santa Rosa clay.....	132
Figure 99. Final swell volume for modified free swell test for Santa Rosa clay	133
Figure 100. SEM images of Santa Rosa clay in order of increasing magnification.....	134
Figure 101. Crumb test for sodium illite at increasing times	136
Figure 102. Effluent from pinhole test for sodium illite	137
Figure 103. Aerial size of hole after pinhole test completion for sodium illite	137
Figure 104. Inner size of hole compared with drill needle for sodium illite.....	138
Figure 105. Double hydrometer particle size distributions for sodium illite	138
Figure 106. Final swell volume for modified free swell test for sodium illite.....	139
Figure 107. SEM images of sodium illite with salt by increasing magnification	141
Figure 108. SEM images of sodium illite without salt by increasing magnification	142
Figure 109. Crumb test for treated bentonite at increasing times	144
Figure 110. Effluent from pinhole test for treated sodium illite	145
Figure 111. Aerial size of hole after pinhole test completion for treated sodium illite..	145
Figure 112. Inner size of hole compared with drill needle for treated sodium illite	145
Figure 113. Final swell volume for modified free swell test for treated sodium illite...	146
Figure 114. SEM images of treated sodium illite with salt; increasing magnification ..	147
Figure 115. SEM images of treated sodium illite no salt; increasing magnification	148
Figure 116. SEM images of clays classified as nondispersive.....	150
Figure 117. SEM images of clays classified as moderately dispersive.....	152
Figure 118. SEM images of clay classified as dispersive (bentonite).....	154
Figure 119. SEM images of bentonite with and without 500x magnification	156
Figure 120. SEM images of bentonite with and without treatment.....	156
Figure 121. SEM images of treated and untreated illite at 500x magnification.....	158
Figure 122. SEM images of untreated and treated illite at 1,500x magnification.....	158
Figure 123. SEM images of dispersed and flocculated illite.....	159
Figure 124. Atterberg limits for oxidized glacial till.....	169
Figure 125. Pinhole test data for oxidized glacial till.....	170
Figure 126. Hydrometer analysis in a dispersant for oxidized glacial till.....	171
Figure 127. Particle size distribution in a dispersant for oxidized glacial till	171
Figure 128. Hydrometer analysis in water for oxidized glacial till.....	172
Figure 129. Particle size distribution in water for oxidized glacial till	172
Figure 130. Atterberg limit results for alluvial top stratum	173

Figure 131. Pinhole test data for alluvial top stratum	174
Figure 132. Particle size analysis in a dispersant for alluvial top stratum	175
Figure 133. Particle size distribution in a dispersant for alluvial top stratum.....	175
Figure 134. Particle size analysis in water for alluvial top stratum	176
Figure 135. Particle size distribution in water for alluvial top stratum.....	176
Figure 136. Atterberg test results for Western Iowa loess	177
Figure 137. Pinhole data form for Western Iowa loess.....	178
Figure 138. Particle size analysis in a dispersant for Western Iowa loess	179
Figure 139. Particle size distribution in a dispersant for Western Iowa loess.....	179
Figure 140. Particle size analysis in water for Western Iowa loess	180
Figure 141. Particle size distribution in water for Western Iowa loess.....	180
Figure 142. Atterberg limit results for bentonite.....	181
Figure 143. Pinhole test results for bentonite.....	182
Figure 144. Particle size analysis in a dispersant for bentonite.....	183
Figure 145. Particle size distribution in a dispersant for bentonite	184
Figure 146. Particle size analysis in water for bentonite.....	185
Figure 147. Particle size distribution in water for bentonite	186
Figure 148. Pinhole test data form for bentonite with 4% lime	187
Figure 149. Atterberg limit results for kaolinite.....	188
Figure 150. Pinhole test data form for kaolinite.....	189
Figure 151. Particle size analysis in a dispersant for kaolinite	190
Figure 152. Particle size distribution in a dispersant for kaolinite.....	191
Figure 153. Particle size analysis in water for kaolinite.....	192
Figure 154. Particle size distribution in water for kaolinite	193
Figure 155. Atterberg limit results for Santa Rosa clay	194
Figure 156. Pinhole test data form for Santa Rosa clay	195
Figure 157. Particle size analysis in a dispersant for Santa Rosa clay	195
Figure 158. Particle size distribution in a dispersant for Santa Rosa clay	196
Figure 159. Particle size analysis in water for Santa Rosa clay	196
Figure 160. Particle size distribution in water for Santa Rosa clay	197
Figure 161. Pinhole test data form for sodium illite.....	198
Figure 162. Particle size analysis in a dispersant for sodium illite	199
Figure 163. Particle size distribution in a dispersant for sodium illite.....	200
Figure 164. Particle size analysis in water for sodium illite	201
Figure 165. Particle size distribution in water for sodium illite.....	202
Figure 166. Pinhole test data form for sodium illite treated with 4% lime	203
Figure 167. Crumb test results for all samples.....	204

ACKNOWLEDGEMENTS

I would like to take a moment to thank everyone who helped me through the course of this research. To my committee chair, Dr. Vernon Schaefer, thank you for suggesting research that was exciting and thought-provoking. I could never have thought of something this interesting myself. Thank you for entrusting me with the study and allowing me to use every resource you had available. Thank you to Stephen H. Nickel, who allowed me to borrow ideas and samples from his original research in 1972. Knowing I had someone else invested in this research inspired me to try my hardest. To my committee members, Dr. David White and Dr. Richard Cruse, thank you for your flexibility and willingness to be on my committee. I really respect both of your work and am lucky to have you on my committee.

In addition, I would like to thank my friends who kept me sane throughout this process. At times it got stressful and I truly appreciated having them around. Kara Ekholm and Maggie Klein – thank you for putting up with me. You were truly my stress relievers and I cannot imagine my last year here without you a bike ride away!

To my colleagues and the civil engineering department faculty and staff, thank you for making my time at Iowa State University a wonderful adventure. It has been six years since I first started my education here and I can't imagine being anywhere else.

Finally, thanks to my family for their encouragement and continued patience as I finished my education. My original four years of undergraduate studies quickly turned into six, with the addition of a major and a master's degree, and it meant a lot to have a supportive family who encouraged me and were proud of me no matter what degree I ended up earning. Thank you for your unrelenting support and I'm so grateful to have such a wonderful sister and compassionate parents in my life.

ABSTRACT

There is no one definitive test to determine the dispersivity of a soil. The ones that are available carry some uncertainty and need to be compared against one another. Even so, clays may be misclassified. This error can produce hazardous results if these clays are used, for example, in levee or dam systems. However, if there was a feature characteristic of all dispersive clays, some doubt could be eliminated and clays could be used without fear of dispersivity. Scanning electron microscope (SEM) images are able to look at soil surfaces on microscopic levels and note distinct particle associations. In viewing clays of various dispersivity classifications with an SEM, samples with the same dispersivity classifications can be compared and common features can be recorded. This could eliminate some of the uncertainty that arises from any single dispersion test and minimize the time needed to make an accurate classification.

The report includes a discussion of the factors influencing the formation of a dispersive clay, the tests used to detect dispersivity, the technology behind an SEM, and the results and images obtained from the analyses. The report identifies conclusions and recommendations based on the research objectives; (1) classify samples per available dispersivity tests, (2) compare the results and assign a classification, (3) use SEM technology to view the substructure, (4) establish a relationship between a soil's substructure and its dispersivity, and (5) note the effects of a chemical additive on dispersivity using physical tests and SEM imagery.

CHAPTER 1. INTRODUCTION

This chapter introduces the industry and technical problems with dispersive soils, the goal of the research, and its overall significance. The chapter concludes with a discussion on the thesis organization.

Industry problem

In a levee or dam system, clays are often used as an impervious center core in order to prevent the leakage of water to the opposite side. If a dispersive clay is unknowingly used in the levee core, instead of resisting the flow of water through the dam, the clay could instead be promoting it. Additional concerns include the fact that there is no set indicator of a clay's dispersivity. Few tests exist to determine a soil's dispersivity and even those contain some uncertainty. Therefore, there is some unpredictability in the selection of a clay as an impervious core. This research examined the physical testing methods used to classify a clay as dispersive and compared these results to one another as well as scanning electron microscope (SEM) images of the soil's substructure. As no classification criteria have been developed solely on the soil substructure, this study focused on discovering topography that may be characteristic of dispersive soils.

Industry concerns

Unless specified, the dispersivity of a soil is generally not tested. When the dispersivity is tested, there are both chemical and physical tests that can be performed to make an informed classification of the soil. However, as concerned with the chemical tests, there is no set chemical composition of a soil that dictates its dispersivity. Although clays high in sodium tend to be dispersive, the sodicity of a sample can be affected by external factors such as pore water fluid which may increase or reduce the likelihood of dispersion. Concerning the physical tests, no one test should be performed by itself. At least two tests should be performed in conjunction with each other and the results compared. The pinhole test is known to be the most reliable but the classification depends highly on the ionic concentration of the water as well as the technician. A large

component of the pinhole test, as well as other physical tests, requires visual observation of the turbidity of a soil. The scale of turbidity is described only in words and thus the actual classification can vary depending on the interpretation of the technician.

Considering these issues, it would be advantageous to investigate the soils of various dispersibilities (classified by one technician) and look at their structure microscopically to see if any relationships exist on that level.

Impact on industry

Because dispersivity classification tests are not always conclusive and may provide erroneous results, the resulting impervious dam design could unknowingly be susceptible to erosion. If a connection were made between dispersivity and a soil's substructure, some of the uncertainty behind the existing tests could be eliminated. The safety of a dam system could be improved and additional information could be garnered in relating soil classification tests with the substructure. If a soil appeared to exhibit associations typical of a dispersive clay, that sample could be eliminated from construction consideration or treated accordingly with a chemical additive to ensure standard safety practices.

Technical problem

The technical issue at hand is that no one test exists to classify dispersive clay conclusively. Several tests are available, but they exist with some uncertainty as well as a strong dependence on visual interpretation, which likely varies from technician to technician. By examining the substructure of a soil, some of the guesswork may be eliminated. The sample is not classified as dispersive per its discoloration but rather its microscopic interparticle associations. By comparing dispersive clay images with other nondispersive or moderately dispersive samples, one can examine the physical differences and define associations that may promote or inhibit dispersion.

Other studies have been performed on comparing one type of soil (typically a pure clay mineral) in its dispersed form with that of its flocculated, noting the structural changes. Additionally, studies have been undertaken to compare naturally dispersed soil

images with that same soil treated with a chemical additive. However, no study has compared SEM images of soils with different levels of dispersiveness and made conclusions on dispersivity based on their surface topography.

This study attempts to find relationships concerning dispersive behavior based on the microscopic topography a soil sample.

Objectives

The objectives of the research are to

- use physical tests to classify the dispersivity of a soil;
- compare classification results and determine dispersivity;
- use SEM technology to view soil substructure;
- relate soil structures to one another according to dispersivity classification;
- and
- treat soil with chemical additive and note structural changes as well as similarities to soils with similar dispersivities.

Significance of the research

Physical and chemical tests of dispersive clay can be time intensive. Additionally, more than one test must be performed due to uncertainties that exist in their classifications. It would be beneficial if soil samples could be taken from their in-situ state and observed using SEM technologies. If dispersive associations were identified on microscopic levels, the soil could be excluded from construction considerations or treated with an additive to minimize its dispersive tendencies. This would save time in the testing process, as SEM imaging can be performed rather quickly, and eliminate some uncertainty in a soil's classification. SEM testing may be difficult based on equipment availability; however, if it is an option, SEM images could provide beneficial insights to the true dispersive nature of a soil. This has the potential to save time and ensure safety against erosion in a levee or dam system.

No research has focused solely on this means of classification. With research using SEM technology on soils of differing compositions and dispersivities,

relationships can be using the particle associations present on a sample's surface. This has the potential to produce more knowledge on the factors influencing a soil's dispersivity and provide insight into its microscopic organization.

Organization of the document

The thesis is organized into five chapters; background, methods, materials, results and discussion, and conclusions and recommendations. The background provides a review of relevant research, summary of current practices, and discussion of preliminary work performed by others. The methods chapter describes the various physical tests and SEM imaging processes performed on the samples. It also discusses the addition of lime to the soil. Materials provides a description of the soil evaluated by each test. The results and discussion contain the dispersivity classification based on the physical tests performed and an analysis using the SEM images with those determinations. The final chapter, conclusion and recommendations, summarizes the outcomes and benefits of the study and provides recommendations for future research and practices.

CHAPTER 2. BACKGROUND

This chapter presents a review of relevant research literature as well as a summary of current practices concerning dispersive clay testing. The chapter serves as an overview to the relevance to the research performed.

Literature review

This section presents a review of literature as it relates to the research and discusses the following topics; dispersive clay properties, dispersive clay identification test methods, dispersion clay treatment options, Scanning Electron Microscopy (SEM) analysis, and dispersive clay microstructure observation using SEM technology.

Dispersive clay properties

Dispersive clays are natural clay soils whose particles deflocculate and separate from one another when in the presence of relatively pure, practically still water. This property makes them highly susceptible to piping and erosion and creates hazardous problems when used in construction applications (Sherard and Decker, 1977). The act of dispersion in a soil occurs when the repulsive forces between the clay particles are greater than their attractive forces (Bell and Maud, 1994). Clay dispersion is influenced by a variety of soil chemical and physical properties including clay mineralogy, soil sodicity, electrolyte concentration, soil charge, pH level, clay content, and geologic origin among others. For the purpose of this research, work was performed on clays with varying types of mineralogy and geologic origins. Accordingly, although the above factors are all important in the classification of a dispersive clay, the clay mineralogy and geologic origin are the only factors discussed in more detail below.

Clay mineralogy

This section discusses the three common minerals in clay structures; montmorillonite, illite, and kaolinite. A summary table is also presented at the end of the clay mineralogy discussion in Table 1.

Montmorillonite

Typically, clays high in montmorillonite are be classified as dispersive. Montmorillonite has a 2:1 mineral composition; that is, two silica tetrahedral sheets surrounding one octahedral sheet containing mainly aluminum cations. This structure is shown schematically in Figure 1 (Ranjan and Rao, 2005). In between these layers, bonding occurs through van der Waals forces and cations. The cations serve to balance the charge deficiencies present in the structure (clay particles have a tendency to have a net negative charge). The van der Waals bonds are the attractive forces in a molecule that exist due to the distribution of electrons around a nucleus. This distribution fluctuates creating a weak instantaneous dipole which results in oppositely charged ends that are attracted to one another. These bonds are weak and can be separated easily by liquid adsorption or cleavage (Fell et al., 2005).

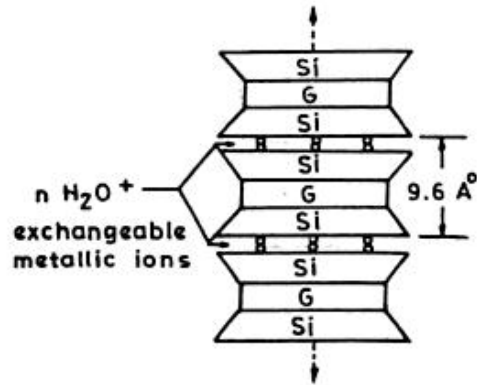


Figure 1. Schematic view of montmorillonite structure (after Ranjao and Rao, 2005)

There also exists extensive isomorphous substitution in montmorillonites. Isomorphous substitution refers to “the substitution of ions of one kind by ions of another type, having either the same or different valence, but the same crystal structure (Mitchell and Soga, 2005).” This essentially means the soil structure will remain the same; however, the chemical composition and charge may vary. The particles in the structure makeup tend to appear as thin equidimensional flakes that have a film-like appearance (Mitchell and Soga, 2005).

In montmorillonites, isomorphous substitution typically occurs in an exchange of magnesium for aluminum creating a net negative charge. This charge deficiency due to isomorphous substitution is balanced by exchangeable cations present between the unit cell layers and on the particle surfaces. Due to the large amount of substitution in these minerals, the cation exchange capacity of montmorillonites tends to be high. Cation exchange capacity refers to the quantity of exchangeable cations present on the montmorillonite particle surfaces. In montmorillonites, the presence of relatively high amounts of exchangeable cations is due to the large negative surface charge that is balanced (Mitchell and Soga, 2005).

Finally, montmorillonites tend to have a large specific surface. Specific surface refers to the amount of surface area per material unit mass. In a dispersed system, this can be defined as the surface area per gram or surface area per unit volume of the system (Jury and Horton, 2004). As montmorillonites have the largest specific surface among the major clay minerals, montmorillonitic soil layers can easily be penetrated by exchangeable ions and water. This causes the layers to separate and the soil experiences relatively large volume changes (Ranjan and Rao, 2005).

Illite

Clays high in illite tend to be classified as moderately dispersive. Illite has a 2:1 mineral composition of two silica tetrahedral sheets sandwiching one octahedral sheet containing mainly aluminum cations. The schematic sketch is shown in Figure 2. In between the layers, the sheets are bonded by a potassium ion. The gaps between the structures have the precise diameter for the potassium ions. As such, the bond created is much stronger than that of the van der Waals forces in montmorillonite. Illite particles are usually present in the form of very small, flaky particles intermixed with other clay and nonclay materials (Ranjan and Rao, 2005).

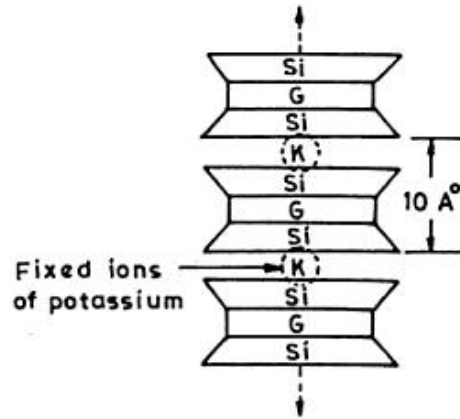


**Figure 2. Schematic view of illite structure
(after Ranjao and Rao, 2005)**

Illites experience extensive isomorphous substitution. A charge deficiency is created, as in montmorillonites, but it is partially balanced by the nonexchangeable potassium ions bonding the sheets together. As such, the cation exchange capacity of illites is less than that of montmorillonites as is the specific surface area. This indicates illites are less susceptible to swelling in the presence of water (Ranjan and Rao, 2005).

Kaolinite

Kaolinitic clays are classified as nondispersive. Kaolinite has a 1:1 structure consisting of alternating layers of one silica tetrahedral sheet to one alumina octahedral sheet. A schematic figure is shown in Figure 3. The layers are bonded by hydrogen bonds. Hydrogen bonds occur between oppositely charged ends of a permanent dipole. Since the dipoles are permanent (unlike those in montmorillonite), the attraction between the molecules is much stronger (Fell et al., 2005). Due to this strong attraction, kaolinite particles are well-crystallized and appear to be well-formed plates (Mitchell and Soga, 2005).

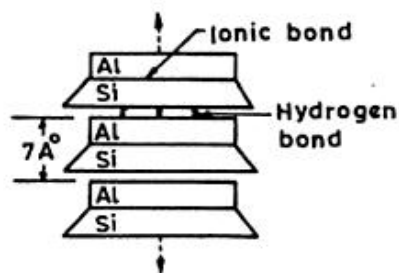


**Figure 3. Schematic view of kaolinite structure
(after Ranjao and Rao, 2005)**

Kaolinites experience the least amount of isomorphous substitution in layers; however, they still experience a net negative charge. Broken bonds between layers may be a source of cation exchange. Nonetheless, interlayer separation does not occur in these minerals and accordingly, the cation exchange capacity and specific surface of kaolinites is the lowest of the three major clay minerals discussed (Mitchell and Soga, 2005).

Table 1. Summary of properties by clay mineralogy

Mineral	Kaolinite	Illite	Montmorillonite
Classification	Nondispersive	Moderately Dispersive	Dispersive
Type	1:1	2:1	2:1
Interlayer Bond	Hydrogen Bonds	Potassium ions	Van der Waals forces
Cation Exchange Capacity	Lowest	Intermediate	Highest
Specific Surface Area	Lowest	Intermediate	Highest

Geologic origin

There are no definitive geologic origins associated with dispersive clays; however, most have been found to be alluvial clay present in the following forms; flood plain deposits, lake bed deposits, slope wash, and loess deposits. Additionally, in some areas, claystones and shales in marine deposits share the same pore water salts as dispersive clays. Thus, their residual soils are classified as dispersive (Sherard et al., 1977).

In steep topographic areas where dispersive clays exist, a distinct surface erosion pattern can be observed. Jagged, winding ridges and deep, rapidly forming channels and tunnels indicate possible sites of dispersive clay. In a rolling or flat topographic area, there is generally little surface evidence of dispersive clays. This is due to a protective layer of topsoil, vegetation, or silty sand from which the dispersive particles may have been removed. However, a lack of erosion pattern does not indicate a nondispersive area. Dispersive clays can be a variety of colors (red, brown, gray, yellow) or a combination of colors. Highly organic clays (typically black) however, are not dispersive (Bureau of Reclamation, 1991). It should be noted though that all fine-grained soil formed from in-situ weathering of metamorphic and igneous rocks have been found to be nondispersive. Residual soils formed from limestone are also known to be nondispersive (Sherard et al., 1977).

Early studies found dispersive clays were associated only with arid or semiarid climates and in basic soils (having a pH higher than 8.5). However, more recent studies have found dispersive clay problems in humid climates as well. Dispersive clays have been found in such countries with varying climates as Australia, the United States, Thailand, India, Spain, and Canada (Sherard et al., 1977). With this wide set of locations, it is difficult to pinpoint one distinct area or climate indicative of dispersive clay.

Other factors in clay dispersivity

Other factors in determining whether a soil may display dispersive tendencies include a soil's sodicity, electrolyte concentration, soil charge, pH level, and clay content.

Soil sodicity

A high dissolved sodium ion content increases the possibility of dispersivity in a soil. Studies performed by Velasco-Molina et al. (1971) found just that correlation. They looked at two different montmorillonite samples; one sample was saturated with sodium while the other with calcium. Montmorillonite is known to be dispersive and by varying

the predominant element, they were able to focus on the effects of sodicity. Tests on the sodium-rich montmorillonite soil found these samples tended to expand and disperse indefinitely in distilled water. This phenomenon occurred due to the adsorption of water into the interlayer spaces. The calcium-rich sample however, experienced limited expansion in their interlayer space (Velasco-Molina et al., 1971). The effects caused by the exchangeable sodium are further confirmed through the use of the exchangeable sodium percentage (ESP) to define dispersivity. This test (discussed later) provides a delineation of dispersive to nondispersive clays of 10%, which higher percentages indicating a higher exhibition of dispersive behavior (Bell and Maud, 1994).

Electrolyte concentration, negative charge, and pH level

Chorum et al. (1994) found a correlation between electrolyte concentration and pH level with dispersivity. Generally, dispersive clays are known to have high pH levels (levels as high as 8 to 8.5 have been recorded) making the soil very alkaline. Taking a soil with a known pH, Chorum et al. (1994) added alkali and acid and recorded the effects on the soil's dispersivity. They found when acid was added to the system and the soil's pH decreased to below 6, there was a drastic increase in electrolyte concentration. This reduced the net negative charges present on the soil and caused flocculation of the particles. With this decrease in pH, more dissolution of iron and aluminum particles onto the clay sample were allowed to occur.

With the addition of alkali, the electrolyte content also increased, but only slightly, and there was an increase in net negative charge. This increase in charge generated high repulsive forces on the sample surface and hence, high flocculation values were recorded. The results of their experiment showed that with changes in pH values, the electrolyte concentration varied but the range from dispersed clays was below 4.0 millimoles per liter (mmol/L) whereas flocculated clays showed much higher ranges varying from 100 to 210 mmol/L (Chorum et al., 1994).

Clay content

Dispersive soils are known to have a moderate to high clay content. There are no set distinctions between the amounts of dispersive to nondispersive clay content in a sample; however, soils with less than 10% clay particles may not contain enough clay colloid particles to inhibit dispersive behavior (Sherard et al., 1976).

Dispersive clay identification test methods

Dispersive clays can be identified via laboratory and chemical test methods. For the purposes of this research, only laboratory test methods were performed and, as such, they will be discussed in the most detail below with a brief section discussing chemical methods after. The crumb test, pinhole dispersion test, double hydrometer test, and modified free swell index test can all be used in the laboratory to classify clays as dispersive, nondispersive, or intermediately dispersive. This section discusses the development of these tests in more detail. An in depth procedure of each test will also be examined in Chapter 3: Methods.

Crumb test

The crumb test was developed by W. W. Emerson as a way to identify dispersive clay in the field. He made observations based on whether dry aggregates slaked when immersed in water. Once the aggregates are immersed, an osmotic stress is induced between the negatively charged clay particles. As the soluble salts initially present in the aggregates diffuse out, the stress on the particles continues to increase. In some cases, the increase may cause dispersion in the clay. Based on this observation, he initially classified clay aggregates that slaked into three classes; complete dispersion, some dispersion, and no dispersion, classes one, two, and three, respectively (Emerson, 1967).

To perform the test in the lab, a cubical specimen with sides of approximately 15 mm is placed in 250 milliliters (mL) of distilled water. The specimen can either be in the form of a natural, irregularly shaped crumb or in a remolded form, prepared from moist soil passing a 2 millimeter (mm) or No. 10 sieve. Once placed in water, the soil is

monitored after two minutes, one hour, and six hours and classified based on the tendency of the colloidal particles to deflocculate and go into suspension. Observations are made at each time interval and the soil is classified into four grades; 1 – Nondispersive, 2 – Intermediate, 3 – Dispersive, 4 – Highly Dispersive (Bureau of Reclamation, 1991). The crumb test is one of the simplest to perform but does not always yield a consistent result. The test depends heavily on the pH of the pore water as well as the type of clay minerals present. In some cases, a dispersive soil may in fact yield a nondispersive reaction. However, that being stated, a classification as dispersive by this test most likely indicates a soil is dispersive (Bell and Maud, 1994).

Pinhole test

The pinhole test was developed in 1976 to measure the dispersibility (colloidal erodibility) of fine-grained soils under the optimum unit weight and water content specified for construction. Because dispersive clay first became problematic in dam and levee systems, this test simulates a leak in dispersive clay in such a structure. In this test, a small hole is punched through a compacted sample and the color and flow rate of the effluent is recorded at various times and heights of hydraulic head. The dispersivity of the soil is then classified in six different grades based on these criteria. The six grades, in order of decreasing dispersivity, include dispersive (grades D1 and D2), intermediate (ND4 and ND3), and nondispersive (ND2 and ND1) (Sherard et al., 1976). Figure 4 presents the dispersive grade classification based on the varying flow rates and turbidity of effluent (Bureau of Reclamation, 1991). Fundamentally, a dispersive clay will produce a cloudy colored suspension of particles whereas a nondispersive clay resistant to erosion will emit a completely clear stream of water.

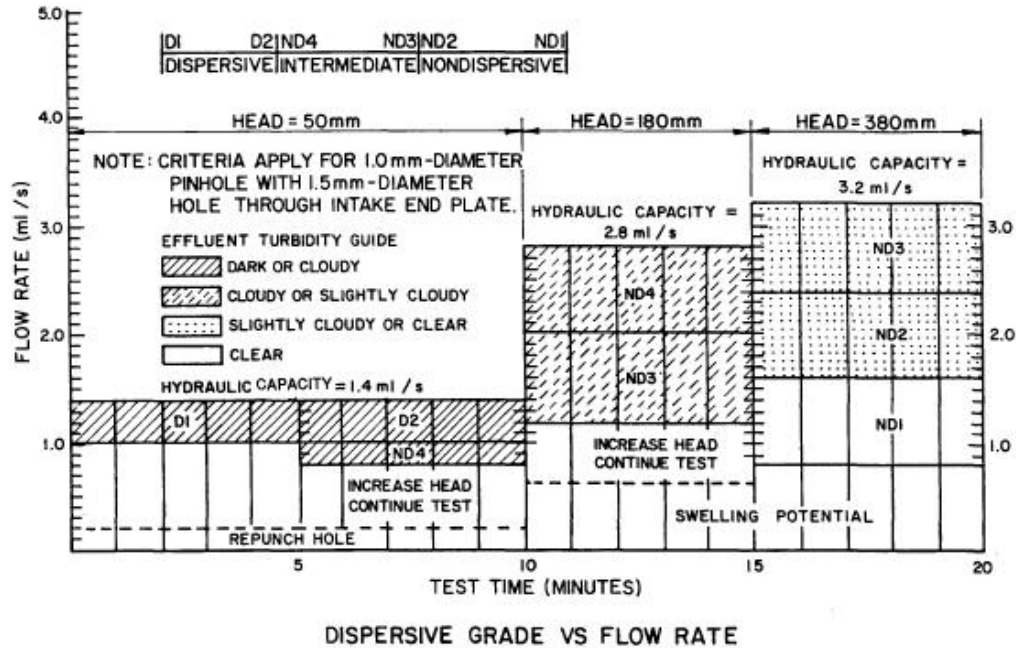


Figure 4. Simplified chart portraying how to determine classification in pinhole test (after ASTM Standard D 4647-06)

The pinhole test is generally considered to be the most reliable of the classification tests used in the laboratory as it is a direct physical test. Additionally, it is fairly simple to perform and the results can be reproduced easily. This is important as, in some cases, individual test results may not agree with one another. It is thus imperative that all tests be performed independently of each other and the results be compared in order to obtain the most correct and reliable information (Bureau of Reclamation, 1991).

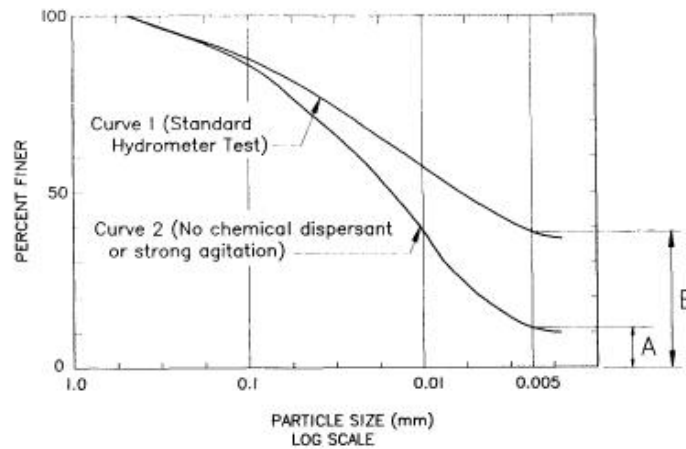
Double hydrometer test

The double hydrometer Test was created by G.M. Volk in 1937 and was adopted by the United States Soil Conservation Service (SCS) in 1940. It has since been used extensively to assign a percent dispersion to soils. In this test, a particle size distribution test is performed on a soil under two conditions. The first being the standard hydrometer test where the soil sample is dispersed using strong mechanical agitation as well as a chemical dispersant. The second test is performed similarly but with neither strong mechanical agitation nor a chemical dispersion (Fernando, 2010). The percent dispersion

can then be calculated based on the dry mass of particles smaller than five nanometers (5 μm) in diameter from both. The equation used is shown below in equation 1 from the American Society for Testing and Materials (ASTM) standard D 4221-99 (2005).

$$\% \text{ Dispersion} = \frac{\% \text{ passing } 5 - \mu\text{m without dispersant}}{\% \text{ passing } 5 - \mu\text{m with dispersant}} \times 100 \quad (1)$$

The percent passing 5 μm can be determined graphically based on the particle sized distribution test results. This is shown in Figure 5 presented below. Using this method the degree of dispersion is determined based on the following percentages of dispersion in Table 2 (United Bureau of Reclamation, 1991).



$$\text{DEFINITION: PERCENT DISPERSION} = \frac{A}{B} (100)$$

Figure 5. Chart depicting percent dispersion in double hydrometer test (after US Bureau of Reclamation, 1991)

Table 2. Degree of dispersion by percent dispersivity (after US Bureau of Reclamation, 1991)

Percent Dispersivity	Degree of Dispersion
< 30	Nondispersive
30 to 50	Intermediate
> 50	Dispersive

It should be noted that the test can vary based on the settings present in the laboratory during the time of testing. In the 1950's and 1960's, as the test was becoming more popular as a classification method, it was found that tests performed in different laboratories on the same soil yielded different results. To explore these discrepancies, in 1977 Sherard et al. researched the effects on the percent dispersion based on varying test conditions. Their research found the results varied due to differences in the quality of water used in the hydrometer as well as the moisture state of the soil at the time of testing. Thus, they compared tests by varying the type of water (distilled or demineralized) and the sample treatment (at in-situ natural water content, air-dried, or oven-dried). From their study, they concluded that the double hydrometer test was most effective when the test was performed using distilled water and soil at its natural moisture content (Sherard et al., 1977).

Modified free swell index test

The modified free swell index test was developed in 1987 by Sivapullaiah et al.. It follows the same procedures for a free swell test but employs a different formula to classify the swelling potential of soil. The formula was developed as a nondimensional alternative to the original test. In the original free swell index test, problems arose due to difficulties in soil measurements as well as occasionally producing a negative index value. The modified equation eliminates these errors and correlates more closely to a soil's engineering properties (Sivapullaiah et al., 1987).

To perform a free swell test, 10 grams of an oven-dried soil is measured and transferred into a 100 mL graduated cylinder of water. The sample is thoroughly agitated and stoppered for 24 hours. This allows the clay particles to disperse and then settle in the cylinder. After 24 hours, the swollen volume is measured according to the gradations on the side of the cylinder. The free swell index is then calculated using the following equations:

$$\text{Modified Free Swell Index} = \frac{V - V_s}{V_s} \quad (2)$$

where V is the soil volume after swelling;

V_s is the volume of soil solids calculated from the formula below

$$V_s = \frac{W_s}{G_s * \gamma_w} \quad (3)$$

where W_s is the weight of dry soil;

G_s is the specific gravity of the solids; and

γ_w is the unit weight of the water. The modified free swell index can then be used to determine the swelling potential, presented below in Table 3 (Sivapullaiah, 1987).

**Table 3. Swelling potential based on modified free swell index
(after Sivapullaiah, 1987)**

Modified Free Swell Index	Swelling Potential
< 2.5	Negligible
2.5 to 10.0	Moderate
10.0 to 20.0	High
> 20.0	Very High

Although the free swell test correlates most directly to the swelling capacity of a soil, it can also be related to the dispersivity as well. When a clay soil is introduced to a water system, the soil tends to swell due to the ion concentration gradient and the net interparticle forces present on the sample. C.C. Ladd in 1960 found in clay systems there is a concentration gradient between the clay particles and the ionic solution. Additionally, in such a system there is an electric field that exists around the charged clay particles that acts as a semipermeable membrane. The above discussed osmotic pressure gradient promotes swelling in the clay particles while the net interparticle forces oppose it. Using this concept and comparing dispersive and nondispersive samples under the test parameters, it was found a dispersive soil tends to lose its cohesion due to swelling in its layers. A flocculated or nondispersive sample meanwhile, is more resistant to swelling (Arulanandan and Heinzen, 1977).

In 1976, Heinzen performed free swell tests on ten natural samples, two of which were highly dispersed. During his test, Heinzen note the two dispersive clays underwent extreme swelling. The samples swelled so much that it lost its original shape completely and seemed to change consistencies into a liquid form. He concluded dispersive clays

would lose its cohesion during swelling and high extreme swelling values (Arulanandan and Heinzen, 1977). Using these studies, the correlation was made that the higher the swelling potential for a soil (determined from the modified free swell index), the higher the likelihood that soil is dispersive.

Chemical test methods

Including the above physical tests, chemical test methods are available to classify the dispersivity of the soil. Popular chemical tests include the exchangeable sodium percentage (ESP), sodium absorption ratio (SAR), and total dissolved salts (TDS) tests.

Exchangeable sodium percentage (ESP)

As discussed above, researchers have found there is a direct correlation between the presence of exchangeable sodium with dispersive clay behavior; that is, the higher the sodium content, the increased likelihood of dispersivity. Accordingly, the follow equation has been used to determine the exchangeable sodium percentage (ESP) in relation to the cation exchange capacity of a sample (discussed earlier in clay mineralogy).

Table 4 follows the equation indicating the criteria for soil classification (Bureau of Reclamation, 1991).

$$ESP = \frac{\text{exchangeable sodium}}{\text{Cation Exchange Capacity (CEC)}} \times 100 \quad (4)$$

Table 4. Table of dispersive clay classification by ESP (after the US Bureau of Reclamation, 1991)

ESP	Degree of Dispersion
< 7	Nondispersive
7 to 10	Intermediate
> 10	Dispersive

Sodium absorption ratio (SAR) and total dissolved salts (TDS)

The sodium absorption ratio (SAR) is used when free salts are present in the pore water volume. As such, if no free salts are present in the water this method is not applicable. This method is based on the knowledge that naturally occurring soils are in equilibrium with their environment. Specifically, there is a relationship between the electrolyte concentration of the pore water and the exchangeable ions in any given clay layer. The following equation represents the percent sodium in a sample with SARs greater than 2 indicating a dispersive soil.

$$SAR = \frac{Na}{0.5 * (Ca + Mg)} \times 100 \quad (5)$$

Where Na indicates the amount of sodium cations in a sample;

Ca is the amount of calcium ions; and

Mg is the amount of magnesium ions present in a soil sample in terms of milliequivalents per liter (meq/L). A related method based on similar ideas is the total dissolved salts (TDS) test. The equation is similar and shown below

$$Percent\ Sodium = \frac{Na}{Total\ Dissolved\ Salts\ (TDS)} \times 100 \quad (6)$$

Where TDS is represented by the following equation,

$$TDS = Na + Ca + Mg + K \quad (7)$$

Where K is the amount of potassium ions present in the soil sample.

The cation values for each of these tests are determined by vacuuming out the pore water from a soil sample. Chemical tests are then performed to determine the amounts of each of these main cations in terms of milliequivalents per liter (meq/L). The TDS test classifies dispersivity into three zones A, B, C of dispersive, nondispersive, and intermediate behavior, respectively. A chart for classification using both SAR and TDS tests have been developed and are presented below in Figure 6 in terms of percent sodium (Bureau of Reclamation, 1991). In a study in 1976, Sherard et al. compared

results of pinhole tests with the sample's pore-water sodium contents. They found a strong correlation between the classification of a soil as dispersive (per the pinhole test) and a high sodium pore-water content (Sherared et al. 1976).

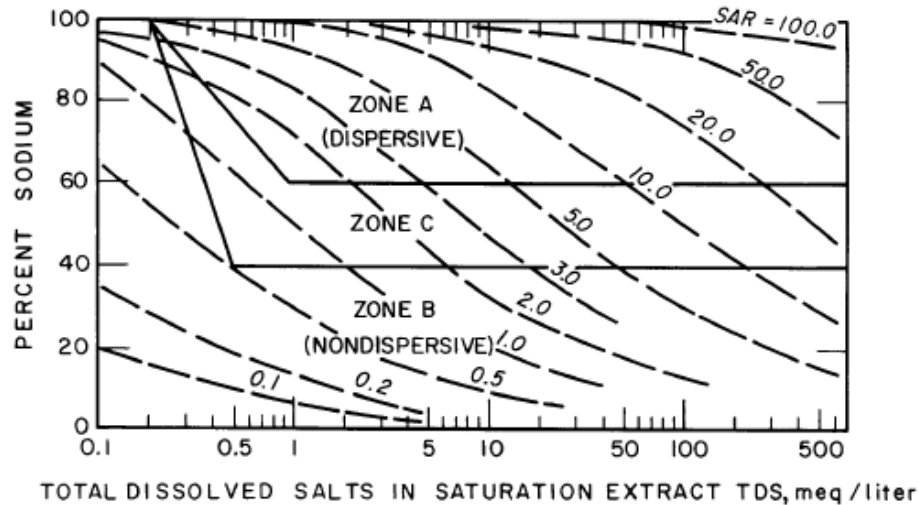


Figure 6. Dispersive clay classification by SAR and TDS by percent sodium (after US Bureau of Reclamation, 1991)

Dispersive clay treatment options

If a soil is found to have dispersive tendencies, there are several chemical additives that can be used to inhibit the dispersive behavior. Common additives include alum, fly ash, lime, and gypsum. Each additive has a unique effect on the properties characteristic of dispersive clays. As it pertains to the scope of this research, the lime additive is discussed in the most detail below as it was the additive most readily available for testing. The other treatment options are briefly examined following that section.

Lime

Lime is an additive composed of calcium hydroxide (CaOH_2). With the addition of this chemical to clay, cation exchange begins to occur on the surface of the clay particles. That is, the metallic ions associated with the clay interact with the calcium ions from the lime. Surrounding the clay particle surface is a diffuse hydrous double layer

that is additionally affected by the calcium ion exchange. In the presence of the calcium ions, the electric charge density of the original clay particles is altered as the problematic sodium and potassium ions of montmorillonite and illite, respectively, are replaced by calcium or magnesium (Kavak and Baykal, 2010). This in turn leads the clay particles to become more closely attracted to each other, or flocculated to one another. The flocculation produced is the primary reason for the addition of lime to a clay system (Bell, 1996).

Additionally, once lime is introduced to the system, there is an immediate increase in the pH of the soil. This now highly basic system promotes the mixing of calcium ions with the reactive hydrous silica and/or aluminates in the soil. The new alumino-silicate solution can then be precipitated as a hydrated cementitious reaction product. The pozzolanic reaction further bonds soil particles together and contributes to increased flocculation of the soil. Pozzolanic reactions are also time dependent. With a long curing period, the strength of the treated soil will continue to develop (Kavak and Baykal, 2010). Lime can alter almost all fine-grained soils, but has the most effect on clay soils ranging from moderate to high plasticity. With the addition of lime, these plastic clays will experience a reduction in the following engineering parameters; plasticity, moisture-holding capacity, and swelling (National Lime Association, 2010).

To effectively alter the dispersive behavior of a clay, various research has been performed on the amount of lime to use. In a study on the dispersive clay that caused failure at the Los Esteros Dam in New Mexico in 1979, dispersive clay was treated with various lime contents and then their dispersivity was determined using a pinhole test (described above). In this study, the samples were treated with lime, compacted at optimum moisture content to near-maximum density and cured for two and four days. From the pinhole test, it was found all soils were nondispersive at both curing times. However at 2% and 3% lime content, the effluent produced from the pinhole test displayed a slight cloud from the top indicating some dispersive behavior was present. At a lime content of 4% by mass, the discharge from the pinhole test was completely clear and there was no enlargement of the hole punched in the sample. Thus, it was

determined that to produce the most effective, nondispersive, erosion-resistant soil, a lime content of 4% was ideal (McDaniel and Decker, 1979).

The addition of lime to a soil can be problematic. First, not all dispersive soils can be stabilized with lime. Proper stabilization depends highly on the cation exchange reaction of the soil (adsorption of the calcium hydroxide onto the clay surface) as well as the hydration reactivity between the clay and the lime. As such, kaolinite with a lower cation exchange capacity will experience lesser property changes as compared to montmorillonite (Indraratna, 1996). Additionally, if only a small amount of lime is needed to stabilize a soil, the resulting mixture may not be homogenous. Problems with stabilization of the soil may then occur which disrupts work and can cause shrinkage cracks (Bell and Maud, 1994). Finally, if lime is mixed on site, mixing may be problematic due to windy conditions. However, this problem can be countered by employing a lime slurry in place of a powder (McDaniel and Decker, 1979).

Other chemical additives

Other chemical additives available for dispersive clay treatment include aluminum sulfate (alum), fly ash, and gypsum. The selection of the additive depends on project specific characteristics including costs and equipment available on site. Each has a unique effect on a dispersive clay.

Aluminum sulfate (alum)

As an additive, alum has a low cost of application (as compared to lime) and is less dangerous to handle. In a study in 2006, Ouhadi and Goodarzi investigated the effects of adding alum to a dispersive bentonite soil sample. The bentonite, which is of similar composition to montmorillonite, originally had a sodium absorption ratio (discussed above) of 46%. With the addition of alum, the aluminum ion concentration increases in the pore fluid. This encourages the replacement of sodium ions, which are characteristic of dispersive behavior, with aluminum ions. In their tests, they found the SAR decreased to 0% with an addition of 5% alum by weight to the sample. This decrease in sodium causes a decrease in the clay double layer. A decrease in this layer

further decreases the repulsive forces present in the dispersed sample and promotes flocculation. Additionally, the pH of the soil sample was monitored. With the addition, the pH decreased from about 10 to 7.3. As discussed earlier, a decrease in pH level reduces the negative charges present in the soil and increased the flocculation of particles (Ouhadi and Goodarzi, 2006).

Fly ash

Fly ash is the by-product of pulverized coal combustion in thermal power plants. Fly ash is primarily composed of spherical non-crystalline silicate, aluminum and iron oxides, free lime, and unburned carbon. Due to the presence of the calcium and aluminum ions, with the inclusion of fly ash to a dispersed soil, cation exchange may occur within the materials and the dispersive sodium ions may be substituted with the aluminum and calcium cations in the fly ash. This would promote flocculation of the dispersed clay particles (Indraratna et al., 1991).

In 1991, Indraratna and his team investigated the results of fly ash in a dispersive soil sample. They used a low plasticity, silty highly dispersed clay with contents of montmorillonite, chlorite, and kaolinite. To test dispersibility, their sample was treated with fly ash then pinhole tests and crumb tests. In the crumb test, the untreated sample was classified as grade 3-4 (dispersive to highly dispersive). After 5% treatment of fly ash by weight, the soils were classified as nondispersive. The pinhole test showed similar results. Initially, the soil was classified as D1 or D2 dispersiveness. After 5-8% fly ash contents, the soil became nondispersive (classification ND1). It was interesting to note though, that after 8% fly ash content, the flow rate of the soil increased. The researchers speculated that this could be due to a lack of cohesion with an overwhelming amount of fly ash. From their study, it was found a 5% by weight fly ash treatment would drastically reduce the dispersiveness of a soil (Indraratna et al., 1991).

Gypsum

Gypsum is a soft sulfate mineral composed of calcium sulfate. With its inclusion to a dispersive soil, sodium ions in the soil can be exchanged with calcium cations. This

substitution reduces the ESP of a soil and causes the subsequent reduction in dispersivity. Additionally, gypsum is readily soluble in water. Accordingly, it could be applied to water in a reservoir so that if seepage were to occur, the soil would receive a gypsum treatment as well (Bell and Maud, 1996). As it pertains specifically to dispersive clay, more research is needed to determine the optimum amount of gypsum to use and its direct effects on a clay's dispersivity.

Scanning electron microscopy (SEM) analysis

A scanning electron microscope (SEM) is used to generate surface images of a specimen on a microscopic level. It does this by scanning a specimen with a beam of high energy electrons in an optical column. The electrons emitted by the beam then interact with the atomic structure of the specimen and generate topographic images. Different types of electrons are produced from the beam, secondary and backscattered, and are discussed in more detail below. If the microscope is also equipped with X-ray capabilities, the equipment can generate information about the elemental make-up of the structure as well as the specific location of those elements. The section serves to further discuss the processes occurring in the SEM optical column, the images produced by secondary and backscattered electrons, and complementary analyses using an energy-dispersive X-ray spectroscope (EDS).

Scanning electron microscope optical column

To magnify the surface of a specimen and generate detailed images about the microstructure, a probe-forming column is used to focus the electron beam on a finely focused spot. That intensified spot then produces electron deflections (discussed in further sections) which provide detailed information to the user (Wischnitzer 1970).

Referencing Figure 7 from Reed (1996), the electron column uses magnetic electron lenses on the sides of the column to project an image of the electron beam onto the specimen. Throughout the length of the column, the beam is demagnified by a factor of 100 to 1000 times its original size and is focused on the specimen. The lenses used to concentrate the beam are the condenser lenses and the final lens. The condenser lens (the

top two lenses in the bottom figure for a three-lens probe-forming column) is used to focus the illumination produced by the electron gun. The final lens, sometimes known as objective lens, forms the magnified image from the specimen. It usually has a tapered form, unlike the condenser lens, so as to leave space for electron detectors. Also shown in the figure are apertures. These are used to intercept any unwanted parts of the reflected electron beam (Reed, 1996).

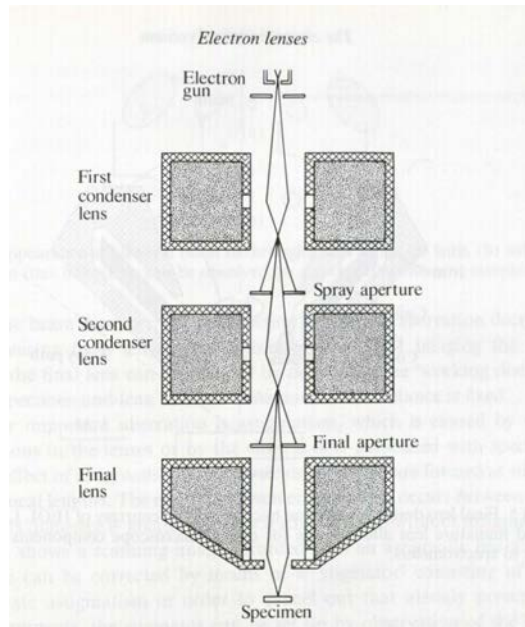


Figure 7. Schematic of three-lens electron column that may be used in a SEM (after Reed, 1996)

A cross-section of the SEM column is presented below in Figure 8 to illustrate the location of the above mentioned lenses as well as the location of the electron gun, electron detectors, and specimen holder. All the parts of the column are labeled with those discussed here highlighted in red.

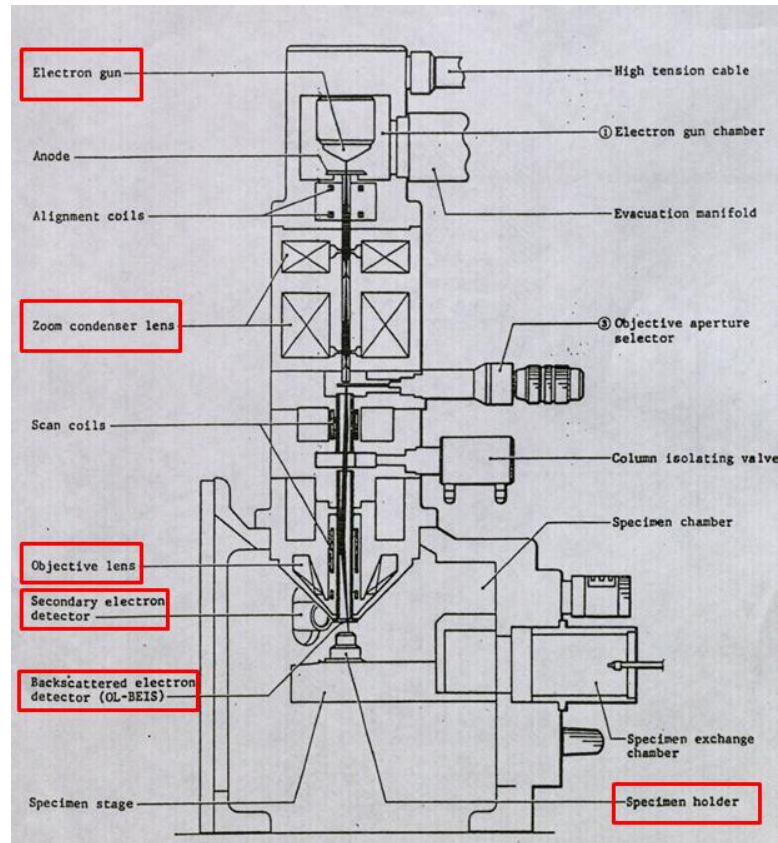


Figure 8. Cross section of a SEM electron column with discussed pieces highlighted (after White CE 565 Course Notes, Scanning Electron Microscopy Lecture, 3/26/2012)

Secondary electron images

The reflection of secondary electrons is helpful in creating the topographic imagery of a sample. Secondary electrons (SEs) are created when electrons, originally located in the sample, are ejected due to impact with the electron beam. The SEs are distinguished from the backscattered electrons as they have much lower energies, typically less than 50 electron volts (eV). These electrons are created along all the electrons in the specimen; however, only the SEs within the top few nanometers of the sample surface are able to escape. As such, only these electrons are emitted and detected by the secondary electron detector in the SEM (Reed, 1996). The SEs are sensitive to

curvatures in the sample topography and reflect as much, as seen below in Figure 9 and Figure 10.

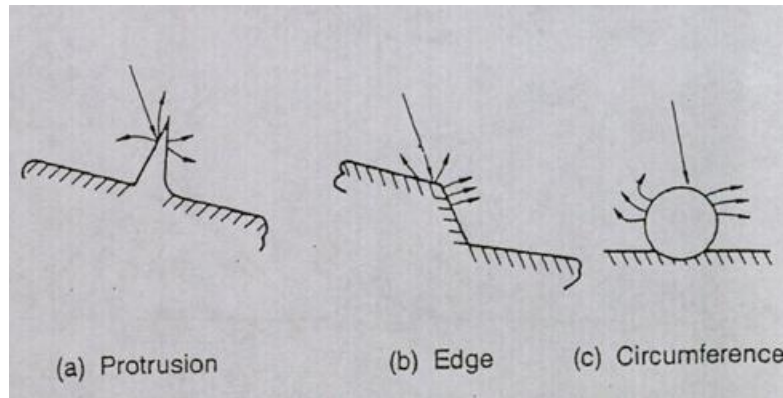


Figure 9. Visual of SE emission differing with topographic features
(after White CE 565 Course Notes, Scanning Electron Microscopy Lecture,
3/26/2012)

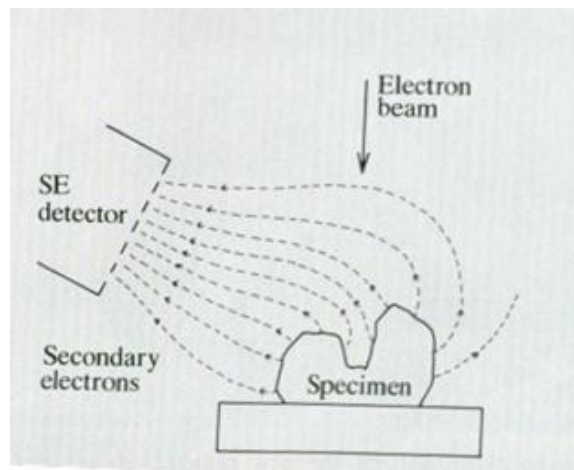


Figure 10. Illustration of SE detection from a specimen with varying features
(after Reed, 1996)

SE emissions can carry some information about the composition of the sample, but these emissions are often caused because of incident secondary electrons created by backscattered electrons. Accordingly, it is more prudent to use the data produced by the backscattered electron emissions to evaluate a sample's composition.

Backscattered electron images

As mentioned above, backscattered electrons (BSEs) are mainly used to learn about the composition of the sample and have energies measured at thousands of electron volts. The backscattering of electrons occurs as a result of multiple deflections through small angles on a sample. BSEs are scattered from the sample with little energy loss and are able to travel greater depths within the sample (as compared to the weaker SE). The generation of electrons from deflection off the sample depends highly on the atomic number of the specimen (White CE 565 Course Notes, Scanning Electron Microscopy Lecture, 3/26/2012). As shown in Figure 11, the greater the coefficient of backscattering (the fraction of incident electrons deflected from the surface), the greater the atomic number. This then provides a way to estimate the elements present in the sample.

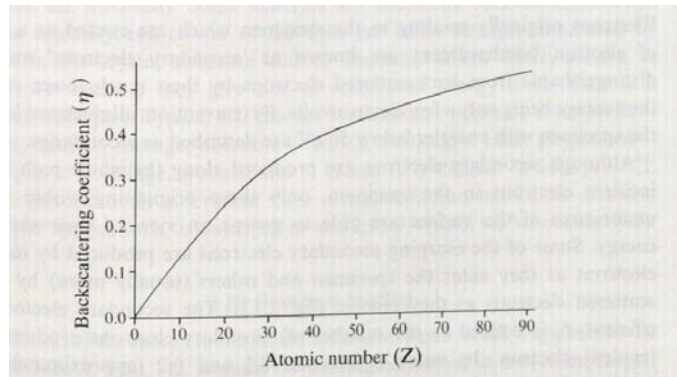


Figure 11. Relationship between backscattering coefficient and atomic number (after Reed, 1996)

Like the SE emissions, the BSE emissions are also affected by the angle of the surface. The detector ‘sees’ different electrons produced from various angles on the surface and a topographic image can be generated. However, the topographic image produced by BSEs tends to have a lower resolution than that produced by SE emission.

Energy-dispersive X-ray spectroscope

When a particle is bombarded with an electron beam, several different types of electron emissions are created (including backscattered and secondary as discussed above). Of importance in an energy dispersive X-ray spectrometry (EDS) analysis, auger

electrons and consequently, characteristic X-rays, are emitted from the specimen. These X-rays are produced by the movement of electrons within an atom.

Looking at the inner atomic electron shell in Figure 12, in a single atom, the positive nucleus (black circle) is orbited by negative electrons located in various shells (K, L, M, etc. as labeled). The electrons in the shells nearest the nucleus (K-shell) have lower energy levels but tighter bonds (Introduction to Energy Dispersive X-Ray Spectrometry (EDS), 2011). When the shells are bombarded with electrons, an electron in one of the shells may be removed. This creates an imbalance in the atomic system. With the removal of an electron in a shell, another electron from a further orbit must switch shells in order to return the atom to its normal state. This transition releases energy in the form of an X-ray photon, or characteristic X-ray (Reed, 1996). The sequence is illustrated in Figure 13(a) and (b) of Kevex. The illustration also shows the creation of an auger electron due to the filling of an inner-shell gap in c. This phenomenon is not discussed in this study.

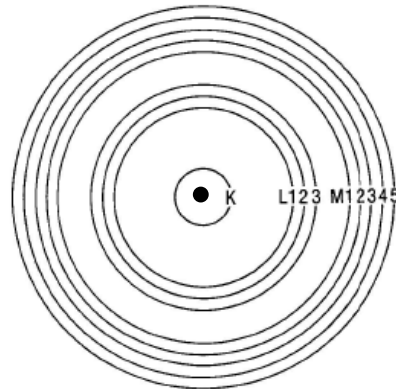


Figure 12. Schematic diagram of an inner atomic electron shell
(after Introduction to Energy Dispersive X-Ray Spectrometry (EDS), 2011)

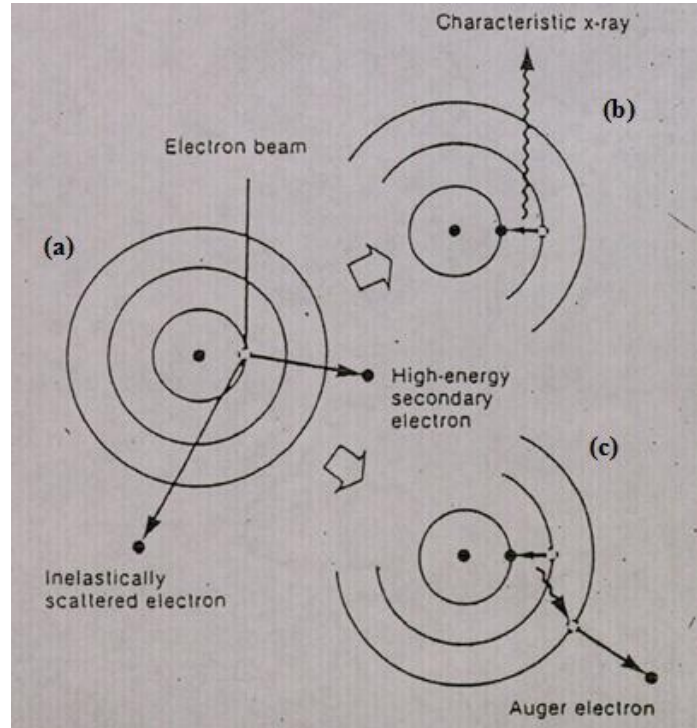


Figure 13. Illustration showing the creation of a characteristic X-ray. In (a), an atom is struck with an electron beam and electrons are knocked out of their shells. To fill this gap, an electron from a lower shell (as shown in (b)), must move to return the atom to its normal state. This movement produces a characteristic X-ray from the element atom. Additionally, when an electron is transferred to a lower shell, an auger electron may be emitted, shown in (c). (after White CE 565 Course Notes, Scanning Electron Microscopy Lecture, 3/26/2012)

To identify the elements present in a sample, EDSs uses pulse height analysis. A detector emits pulses to the sample proportional in height to the characteristic X-ray energy. Characteristic X-rays produced from the transition of electrons due to pulses create ionization in the detector which induces an electrical charge. These charges are amplified and then converted into a spectrum using a multichannel pulse-height analyzer (Introduction to Energy Dispersive X-Ray Spectrometry (EDS), 2011). The analyzer measures the energies of the incoming pulses and creates a histogram of the number of occurrences (counts) by energy height. The energy height can be calibrated with

references to known X-ray lines and classified as certain elements (Reed, 1996). An example of a histogram with element classification is shown below in Figure 14.

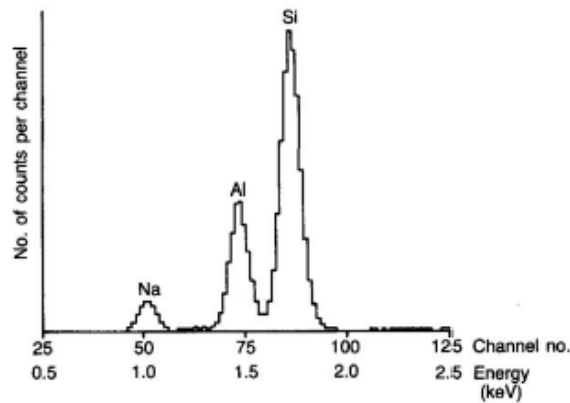
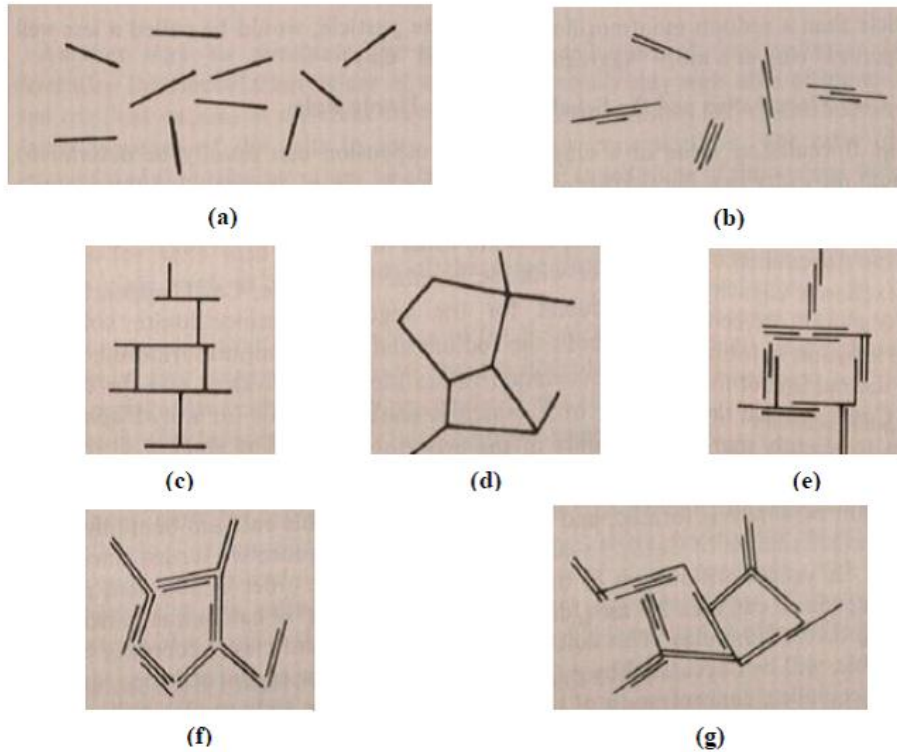


Figure 14. Example of histogram produced by energy dispersive X-ray spectrometry
(after Introduction to Energy Dispersive X-ray Spectrometry (EDS), 2011)

Dispersive clay microstructure using scanning electron microscopy (SEM)

In a clay system, the particles are allowed to associate in various forms. The three modes of particle association are face-to-face (FF), edge-to-face (EF), and edge-to-edge (EE). These associations can combine in various ways, shown in Figure 15. There is a brief explanation below the figure of the suspensions shown in terms of dispersion compared to aggregation and flocculation compared to deflocculation (Van Olphen, 1977).



**Figure 15. Modes of particle associations in clay suspension systems
(after Van Olphen, 1977)**

- (a) Dispersed and deflocculated**
- (b) Aggregated but deflocculated (FF associations)**
- (c) Flocculated but dispersed (EF associations)**
- (d) Flocculated but dispersed (EE associations)**
- (e) Flocculated and aggregated (EF associations)**
- (f) Flocculated and aggregated (EE associations)**
- (g) Flocculated and aggregated (EF and EE associations)**

The term “dispersion” as used in terms of clay microstructure, describes soil in which the net electrical force between particles encourages repulsion from one another. Dispersed structures contain parallel oriented particles as shown in Figure 15c and are composed of FF particle associations (Sides and Barden, 1970). “Aggregation” is used to distinguish the degree of layer stacking in a particle. For example, a dispersed clay could include more particle layers (as shown in Figure 15b) and could still be described as

dispersed; however, it would be classified as a “less well dispersed” or a “more aggregated.” “Flocculation” is meanwhile used to describe soil in which the net electrical force encourages attraction. A soil with an EE or EF association is described as flocculated as shown in Figure 15c, d, e, f, and g. Conversely, deflocculated is used to express structures in which the linked particles are dissociated and split as seen in Figure 15a and b (Van Olphen, 1977).

Through the use of a scanning electron microscope (SEM), discussed above, the soil structures of various clay types can be observed. In 1971, Sides and Barden did just that with clays of three distinct mineralogies; kaolinite, illite, and montmorillonite (the importance of these distinctions is discussed in an earlier section). In their study, SEM imaging was used to look at the clay structures of each sample in its flocculated and dispersed form. As illustrated schematically above in Figure 15, it was concluded a flocculated sample should show no set particle orientation and there should be a preponderance of edges, planes, and cavities in both the vertical and horizontal sections of the sample. Conversely, in a dispersed sample, particle edges would be a predominant feature in a vertical section while particle planes would be more prominent in the horizontal view (Sides and Barden, 1971). Sample images generated by Sides and Barden illustrating these concepts are presented below for kaolin in both flocculated (Figure 16) and dispersed form (Figure 17) and horizontal and vertical sections (as specified).

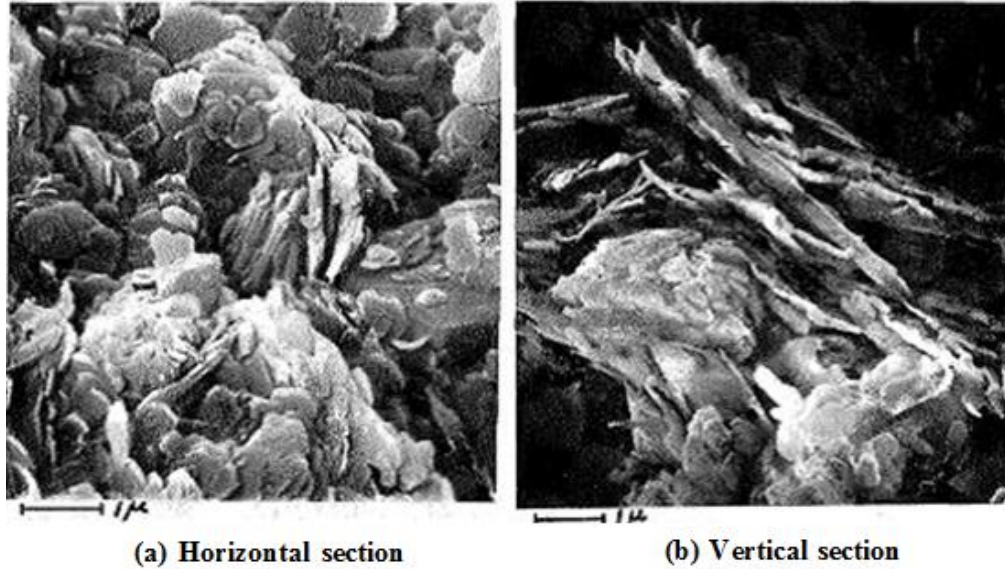


**Figure 16. SEM images of flocculated kaolin
(after Sides and Barden, 1971)**

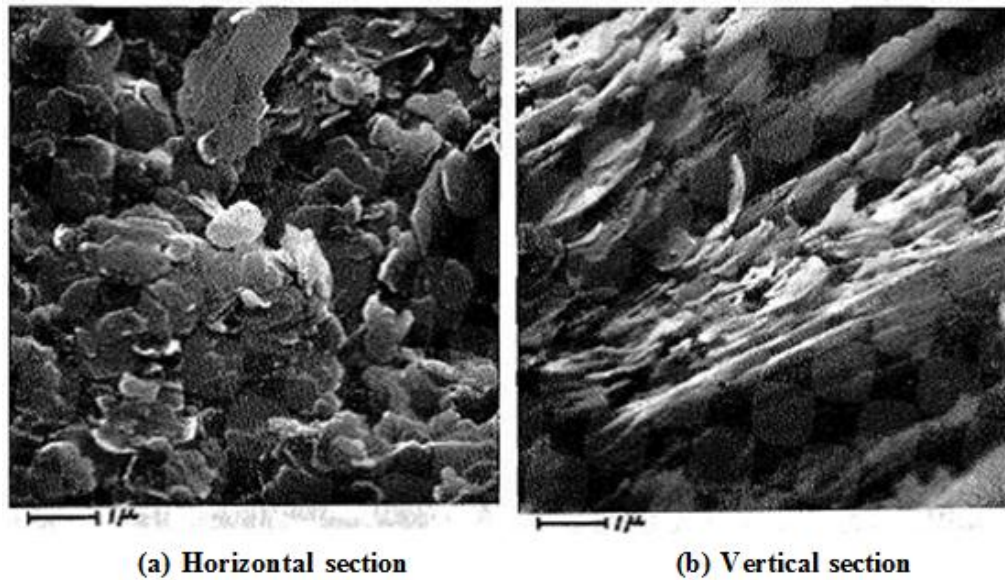


**Figure 17. SEM images of dispersed kaolin
(after Sides and Barden, 1971)**

In closely related studies, a bentonite soil has been treated with chemical additives and the differences noted using SEM testing. In 2007, Bhuvaneshwari et al.

generated images of a natural bentonite soil and soil treated with 5% lime. These images are presented in Figure 18. After treatment with lime, the figures were compared and the researchers noted clay aggregates present in the second image in coherent masses. The generation of these masses was due to the stimulation of pozzolanic reactions and ion exchange reactions (Bhuvaneshwari et al., 2007).

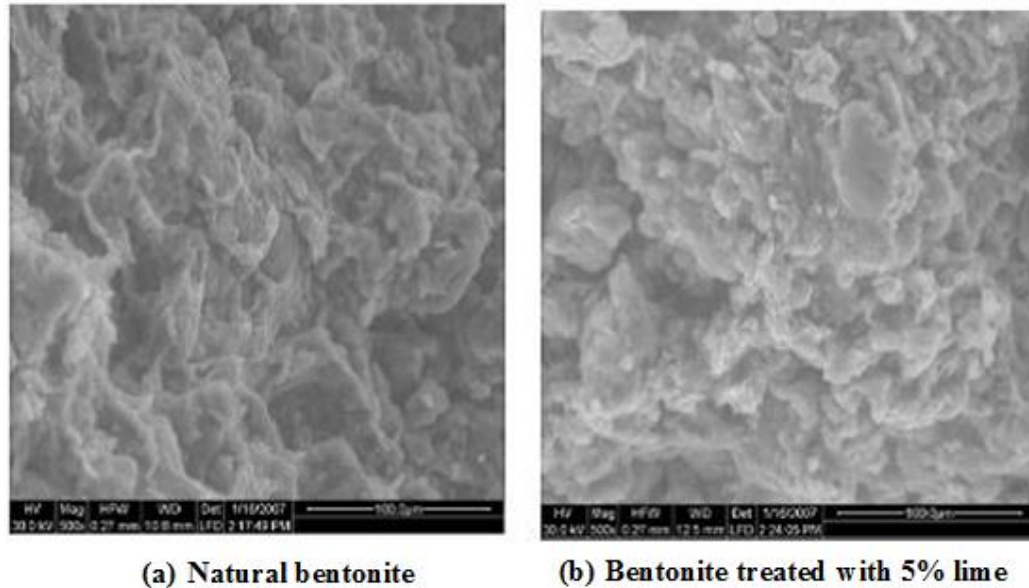
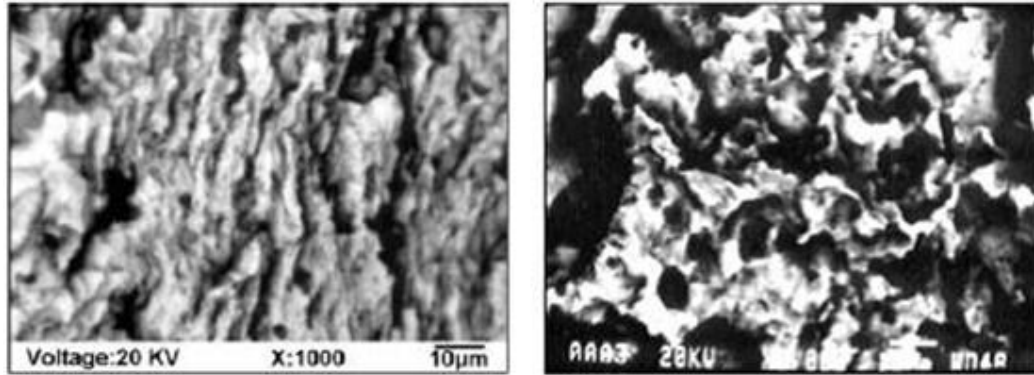


Figure 18. SEM images of bentonite with and without treatment (after Bhuvaneshwari et al, 2007)

In 2006, Ouhadi and Goodarzi also performed SEM testing on a natural bentonite and a bentonite treated with 3% alum. These images are shown in Figure 19. After the inclusion of alum, there was an increase in basal spacing of the sample due to the substitution of sodium ions with aluminum ions. This effect can be noted on the substructure in the below images.



(a) Natural bentonite (b) Bentonite treated with 3% alum
**Figure 19. SEM images of bentonite with and without treatment
 (after Ouhadi and Goodarzi, 2006)**

The above images from Sides and Barden (1971), Bhuvanshwari et al. (2007), and Ouhadi and Goodarzi (2006) are presented as a comparison to the images generated in this study. Their results will also be used as references when evaluating the resulting SEM images of different clay soil samples.

Preliminary work

This section discusses specifically the work performed on two samples included in this research. The two samples include dispersive clay from the Los Esteros Lake Project in New Mexico and an illite created for the analysis of consolidation of flocculated illite used in an earlier thesis.

Dispersive clay study for Los Esteros Lake Project; Santa Rosa, NM

After dispersive clay problems were found in the impervious core section of the Los Esteros Dam Embankment in 1977 in Santa Rosa, New Mexico, Hoskins-Western-Soderegger, Inc. (HWS) performed an analysis on the problematic soil. At this date, the concept of dispersive clay was relatively new and tests were just being created to determine clay dispersibility. In their analysis, HWS performed index tests, pinhole tests, and filter tests on select soil samples. They used the results from these tests to determine the dispersibility of the impervious core and to make recommendations to the contractor in order to continue construction (Hoskins-Western-Soderegger, 1977).

Although their analysis also included a cation analysis which aids in the classification of dispersibility, gaps still exist. As dispersive tests were still in their early stages and because tests are not always accurate as a stand-alone method (as discussed in an earlier section), other tests should have been performed and cross-referenced before making a strict classification on the samples. Thus, a sample from the Los Esteros dam project was included in this research to analyze the dispersibility using other laboratory tests and SEM imagery.

Consolidation of a flocculated illite

A soil sample initially used for a thesis from 1972 was also included in this research. In 1972, Nickel prepared a flocculated sodium illite-water system and analyzed it. For his research, the illite soil was consolidated under controlled conditions. The sample was subject to various consolidation rates and Nickel recorded the void ratios of the samples throughout testing. These results could then be compared with already defined mathematical floc models (specifically the parallel plate model floc and the double-T model floc). With this knowledge, the behavior of his prepared flocculated illite could be predicted. He hypothesized that his research could potentially aid in the prediction of how other flocculated clays may behave (Nickel, 1972).

In his work with the soil, consolidation tests, Atterberg limit tests, and an X-ray diffraction (XRD) were performed. He also determined the cation exchange capacities of the soil (Nickel, 1972). Little to no analysis was performed on the sample in terms of defining the dispersibility of the sample. Due to the uniqueness of the soil and its mineralogical composition, the sodium illite soil sample was included in this research and its dispersibility was analyzed.

CHAPTER 3. METHODS

The tests used in this study were selected to address the following objectives: to conduct laboratory tests; to evaluate a variety of soil types; to determine the dispersibility of a soil; to make a comparison of soil structure and properties; and to evaluate the effects of a lime additive on a soil.

Research design

The research objectives are to:

- determine soil dispersibility using a variety of laboratory tests;
- compare results and make a comprehensive classification;
- use SEM imagery to view soil structure on dispersive and nondispersive samples;
- relate the sample soil structure with the dispersivity classification;
- treat dispersive soil with lime additive and observe changes in soil behavior in laboratory tests and soil structure using SEM images.

To accomplish the above objectives, four laboratory tests were performed on seven different soil samples. The four tests conducted included the crumb test, pinhole test, double hydrometer test, and modified free swell index test. All laboratory tests were carried out in the Gerald and Audrey Olson Soil Mechanics Laboratory (Olson laboratory) in the Town Engineering Building at Iowa State University. The test results were analyzed using Excel spreadsheets created specifically for this research. After the tests were run on each sample, SEM imaging was performed in the Materials Analysis and Research Laboratory, also located in the Town Engineering Building at Iowa State University. A FEI Quanta FE-SEM (field emission scanning electron microscope) was used to analyze the soil structures of the samples.

Crumb test

The crumb test was performed in accordance with the American Society for Testing and Materials (ASTM) standard designated D 6576 –06, Standard Test Methods

for Determining Dispersive Characteristics of Clayey Soils by the Crumb Test. The test procedures are summarized below according to this standard.

This test provides a quick and simple method to identify a dispersive clay soil. In this test, essentially, a soil crumb sample is placed in a water setting and its turbidity in relation to time is observed. It is a popular test as it can be easily utilized in the field or in a laboratory setting. While the test can be a quick and easy indicator of dispersive clay, it should be run in combination with additional tests such as the pinhole or double hydrometer test.

Equipment

The equipment necessary for the completion of this test was found in the Olson laboratory in the Town Engineering Building. The only items of equipment needed were the respective soil specimens as well as a porcelain evaporating dish, thermometer, and timer. Depending on the soil color (for example if the specimen was white as with kaolinite), a beaker was substituted so as to get a better view of the sample throughout the test.

Preparation of samples

A representative sample of each soil must be obtained prior to the test. The sample may be at its natural water content (Test Method A) or in a remolded state passing a 2-mm aperture (No. 10) sieve (Test Method B). For this study, the state of the soil during the time of sample determined the sample preparation method. The method for each sample is noted in a later chapter, Chapter 5: Results and Discussion.

Test method A

In Test Method A, a natural, irregularly shaped soil crumb that has been preserved at natural moisture content or a crumb that has been subject to air drying only is selected. The crumb selected should resemble a cubic shape with equal sides of approximately 15 mm. Smaller cubes of 7 mm in size may be used if a larger sample cannot be found.

Test method B

In Test Method B, a 15 mm sided cube is prepared from moist soil that has passed a No. 10 sieve. Distilled water should be used to remold the sample into a usable cube form.

Procedure

1. Place a 300 milliliter (mL) porcelain evaporating dish on a level working surface that will be devoid of vibration for at least the next 6 hours.
2. Fill the porcelain dish with 250 mL of distilled water and allow the temperature to stabilize.
3. Prepare a test specimen as necessary (refer to methods A and B described above).
4. Set the cubic specimen in the water and place directly on the bottom of the dish. Be wary not to move or vibrate the dish during placement or after until the test has been completed.
5. Allow the crumb to absorb water and note the tendency for the colloidal particles to deflocculate and go into suspension.
6. At set time intervals of 2 minutes, 1 hour, and 6 hours, determine the dispersion grade of the sample and temperature of the water and record on a prepared data form (as shown in Figure 20). The criteria for each dispersion grade are discussed further below in the interpretation of data subtopic.

CRUMB TEST FOR DISPERSIBILITY OF CLAYEY SOILS

Sample No. _____ Disturbed _____ Date _____
 Soil Type _____ Undisturbed _____
 Color _____ Natural moisture content (as received) _____ %
 Specimen Type: _____ Natural irregularly shaped crumb _____ Remolded crumb cube _____
 Moisture Content: _____ Natural Moisture _____ Air-Dried _____ Distilled water added to remold specimen _____
 Curing Time _____ min _____ Water used: _____ Distilled _____ Distilled and demineralized _____
 Initial Water T _____ °C _____ Time at beginning of test _____ am _____ pm
 Tested by _____ Date _____

Specimen Number	Dish Number	2 minutes		1 hour		6 hours		Remarks
		Grade	°C	Grade	°C	Grade	°C	

**Figure 20. Crumb test data form for dispersibility of clayey soils
(after ASTM D6576-06)**

7. Make a final determination of the dispersive grade of the clay. Generally, if the grade changes throughout the test, the 1 hour reading is normally used. However, if the grade increases from a 2 to 3 or 3 to 4 between the 1 hour and 6 hour readings, the 6 hour reading should be used.

Interpretation of data

The following criteria should be used to classify the sample at each respective time interval:

Grade 1 (nondispersive)

There is no soil reaction with the water. The sample may crumble, slake, diffuse, or spread out but the water will not appear cloudy when viewed from above. All soil particles settle within the first hour.

Grade 2 (intermediate)

There is a slight soil reaction with the water. In this transition grade, a faint and barely visible cloudy surface can be seen near portions of the soil crumb surface or all around the surface. If the cloud is easily seen, the higher grade of 3 should be assigned to

the soil. If the cloud is faintly seen and is confined to one small area, a designation of Grade 1 should be given.

Grade 3 (dispersive)

A moderate soil reaction is noted with the water. A suspended clay colloid cloud is easily seen around the entire outer soil crumb surface. In some cases, the colloid cloud can extend up to 10 mm from the soil crumb mass in the bottom of the evaporating dish.

Grade 4 (highly dispersive)

A strong reaction can be seen between the soil and water. A large, dense cloud can be seen around the entire bottom of the dish. At times, it may be difficult to distinguish the extent of the original soil crumb from the now present colloidal suspensions. In highly dispersive soils, the turbid cloud is often also easily seen on the sides of the evaporating dish.

Pinhole test

The pinhole test was performed in accordance with the ASTM standard designated D 4647-06, Standard Test Method for Identification and Classification of Dispersive Clay Soils by the Pinhole Test. The test procedures are summarized below following this standard.

This test is highly recommended as it provides a direct, qualitative analysis of the soil. Through performing this test, one can determine a qualitative dispersibility measurement as well as the colloidal erodibility of a clay soil.

Equipment

To complete this test, the proper equipment is essential. This research used pinhole test equipment produced by the Karol Warner Company. The complete system is shown below in Figure 21 with certain pieces of equipment highlighted for increased discussion. In addition to the pieces below, a timer is needed as well.



Figure 21. Complete assembled pinhole dispersion system

Pinhole test apparatus

The pinhole test apparatus (highlighted in red) is the most important piece of equipment for the correct implementation of the test. A detailed picture of all the parts of the apparatus is shown below in Figure 22. This apparatus includes the test mold, wire screens, truncated cone centering guide (located inside the test mold), and wire punch needle. The placement of the soil sample inside the apparatus will be discussed in a further section entitled Procedure.



Figure 22. A complete picture of the pinhole test specimen apparatus

Constant head tank

The tank (highlighted in blue in Figure 21) is used to supply distilled water to the system. The water should have a pH of 5.5 to 7.0.

Graduated cylinder

A graduated cylinder (highlighted in green in Figure 21) is placed under the test apparatus to catch the effluent from the test. The cylinder is used to calculate the effluent flow rate as well as observe the turbidity.

Preparation of samples

Soil samples can be prepared based on whether samples were delivered in the disturbed form at natural water content, disturbed, pulverized form after being air-dried, or an undisturbed form taken from a core or block specimen. All of the soil samples analyzed were delivered in a disturbed, pulverized form at their air-dried water content. As such, the preparation for only this type of sample specimen is described below.

For a disturbed sample at an air-dried water content, first all particles greater than 2-mm (No. 10) sieve are removed. Distilled water is then be added to the specimen to achieve a water content within 2 percentage points of optimum. The optimum water content was determined based on research (as discussed during the Results portion of this paper) or based on standard industry practices. The soil will then be compacted using ASTM Test Method D 698 (Laboratory Compaction Characteristics of Soil Using

Standard Effort (12,400 ft-lb/ft³ (600 kN-m/m³))). For this study, this standard was modified through the use of a Harvard miniature compaction apparatus discussed below.

Following the above standard, the Harvard miniature mold was used to compact soil passing a 4.75 mm (No. 4) sieve in three layers at 25 blows per layer (apparatus is further discussed in Figure 23 below). After the soil was compacted, it was extruded, and allowed to cure for 24 to 48 hours. Once cured for the desired time, the compacted soil was broken up and screened through a 2-mm (No. 10) sieve. It should be noted the sample will be compacted twice using different standards: first to cure the sample using ASTM D698 (discussed in this Preparation of Samples section) and again to perform the pinhole test using ASTM D4647-06 (discussed below in Procedure).

Procedure

There are three methods that can be used to perform the pinhole test. All are essentially the same but have various modifications in the criteria for classifying the sample in terms of dispersibility. The method options include Method A, B, and C, respectively. For this purposes of this study, Method A was used on all the soil specimens. The following procedure was followed:

1. Compact the 38-mm (1.5 in) specimen into the pinhole test cylinder on top of the truncated centering guide. Use Harvard compaction equipment to compact the soil in the apparatus in five lifts with 16 tamps on each lift. To comply with the standards, use Harvard compaction tamper with a 6.8 kg (15-lb) spring. The Harvard compaction equipment is shown below Figure 23 and is comprised of the following parts:
 - a. The blue outline highlights the compaction mold.
 - b. The red outline shows the tool used to extract the mold collar.
 - c. The yellow outline displays the tamper used to compact the sample.
 - d. The green outline shows the tool used to extract the compacted sample.

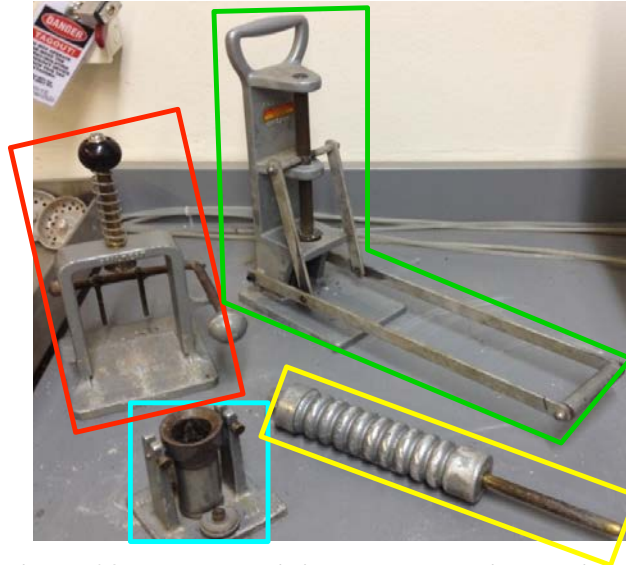


Figure 23. Harvard miniature compaction equipment

2. After the specimen has been compacted into the apparatus, insert the 1.0-mm (0.039 in) diameter wire punch through the truncated centering guide and punch a hole through the soil specimen. Remove once a hole has been punched all the way through the sample. After placement of the hole, the compacted clay will look similar to the illustration below schematically in Figure 24.

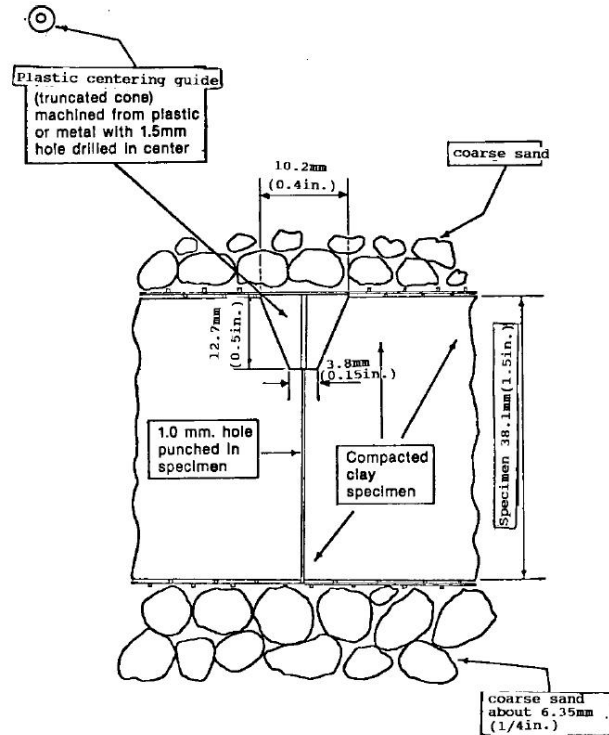


Figure 24. Schematic view of pinhole test specimen

3. Place the wire screen on top of the specimen and fill the top of the test cylinder with coarse sand. The sand used for the procedure was a concrete sand stored in the Iowa State University teaching laboratory in Town Engineering.
4. Once the sand is in place, assemble the top plate of the apparatus and connect the distilled water head source to the device. Schematically, the assembled apparatus should appear as shown in Figure 25.

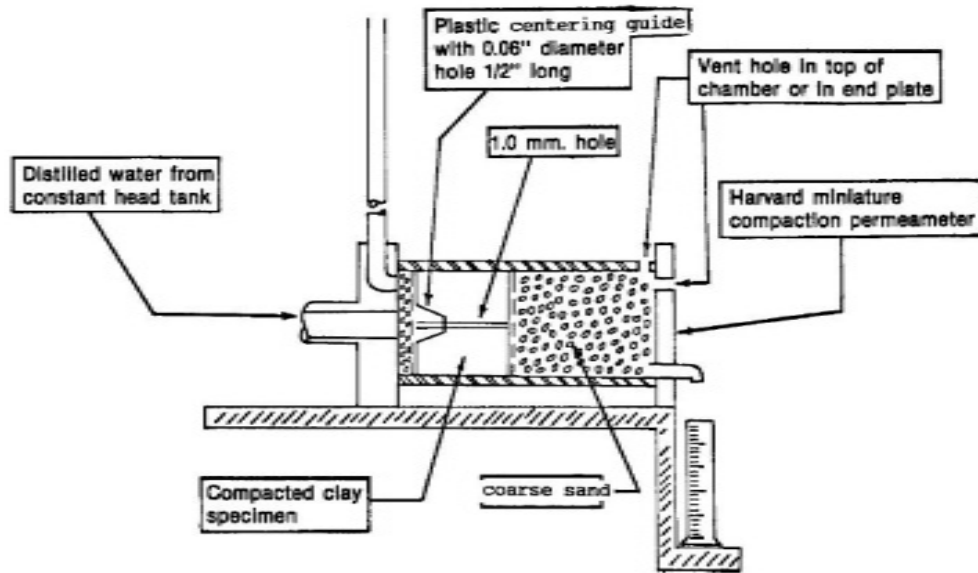


Figure 25. Schematic view of final assembled apparatus

5. Begin the test by introducing distilled water into the pinhole dispersion apparatus. A hydraulic head at the level of the pinhole should be 50 mm (2 in). This height can be altered by raising or lowering the pinhole apparatus as connected to the stand (complete system shown above).
6. Start the stopwatch to begin the test.
7. Using a graduated cylinder at the output of the system, take measurements of the effluence as it flows through the specimen. If no flow upon test startup; stop the water source, disassemble the apparatus, and repunch the hole.
 - a. Measurements may be made in terms of effluent collection (25, 50, or 100 mL) or at a set time interval.
8. For each measurement, observe and record the cloudiness of the discharge. Observe the cloudiness of the discharge from both the side of cylinder as well as the top through the fluid column. Use the data sheet shown in Figure 26 to record the time and color of the discharge. Record cloudiness using the following distinctions in order of decreasing cloudiness:
 - a. Very dark

less than twice the initial punching diameter, the test results are inconsistent with the standard and the test should be redone.

10. If after 5 minutes under the 50-mm (2 in) head the water is distinctly dark and the flow rate is less than 1.0 mL/s, the test should be continued for an additional 5 minutes under this head. If after the 10 minutes the soil is still dark and the flow rate is between 1.0 and 1.3 mL/s, stop the test and measure the final hole size. Under these criteria, the soil should be classified as dispersive, D2.
11. If after 10 minutes under the 50-mm (2 in) head the water is clear or very slightly dark and the flow rate is 0.4 to 0.8 mL/s, raise the water head to 180-mm (7 in) above the pinhole. Under this head, note the effluent color and flow rate. If the discharge has become distinctly dark and the flow rate has increased to 1.4 to 2.7 mL/s, stop the test and examine the hole diameter. If the diameter is equal or greater than 1.5 to 2 times the initial needle diameter, the soil is classified as slightly to moderately dispersive, ND3.
12. If after 5 additional minutes under the 180-mm (7 in) hydraulic head the flow is completely clear or barely visible and the flow rate is 0.8 to 1.4 mL/s, the head should be raised to 380-mm (15 in). After 5 minutes under this increased head, note the darkness and flow rate. If the darkness has increased and flow rate has increased to 1.8 to 3.2 mL/s, the test should be stopped and the soil is classified as slightly dispersive, ND4.
13. If after 5 minutes under the 380-mm (15 in) head the flow is completely clear and the rate is 1.0 to 1.8 mL/s, the head should further be increased to 1020-mm (40 in). Maintain this head for 5 additional minutes and note the darkness and flow rate.
 - a. If the flow shows a very slight discoloration from the top or the flow rate is greater than 3.0 mL/s, the soil is classified as nondispersive, ND2.

- b. If the flow shows no discoloration and the flow rate is less than 3.0 mL/s, the soil is classified as nondispersive, ND1. Additionally, under this classification, the final hole diameter should not be much larger than the needle punch.

Interpretation of data

In simplified form the dispersibility of a sample is determined based on the following criteria (in terms of increasing nondispersivity):

Dispersive D1, D2

The clay fails rapidly under a 50-mm (2 in) head. The discharge is discolored and the flow rate is faster than 1.0 mL/s.

Slightly to moderately dispersive (ND4, ND3)

The clay erodes slowly under a 50-mm (2 in), 180-mm (7 in), or 380-mm (15 in) head. With increasing hydraulic head, the discoloration of the effluent increases as does the flow rate.

Nondispersive (ND1, ND2)

The clay shows little to no colloidal erosion. Under heads of 380-mm (15-in) or 1020-mm (40 in), the flow through the specimen is only slightly discolored if that and the flow rate only increases under the final highest hydraulic head of 1020-mm (40 in).

Double hydrometer test

The double hydrometer test was performed in accordance with the ASTM standards designated D 422-63 and D 4221-99, Standard Test Method for Particle-Size Analysis of Soils and Standard Test Method for Dispersive Characteristics of Clay Soil by Double Hydrometer, respectively. The test procedures for both tests, per their standards, are summarized below in separate subsections.

This test calculates the percent dispersion of a sample by comparing the percent of sample passing the 5- μ m size as determined by both above test methods. The first method, standard D 422-63 for particle-size analysis, determines the percent finer using

mechanical agitation and a chemical dispersant. The second method, standard D 4221-99 for dispersive clay characteristics, uses neither mechanical agitation nor a chemical dispersant to determine this fraction. The comparison of the two methods is based on the concept that dispersive clays tend to deflocculate when exposed to water whereas aggregated, nondispersive clays would remain flocculated. As such, a dispersed sample when exposed to water would disperse and settle in a similar manner as when exposed to a chemical dispersant. The final percent dispersion is calculated based on this idea; the percent passing 5- μm in a water solution is compared to the percent finer than 5- μm in a dispersant and a higher percentage indicates a higher likelihood of dispersion.

According to the ASTM standard, this test method is purported to have about 85% reliance in predicting the dispersive clay behavior of a sample. However, as with the other laboratory tests, the double hydrometer test may not identify all dispersive clays. Hence, another test should be run in conjunction with this one and both analyses should be used to classify the sample.

Particle size analysis of soils

The first particle size analysis was performed following ASTM D422 Test Method for Particle-Size Analysis of Soils. This ASTM standard describes how to determine the percent finer of different diameters using mechanical agitation and a chemical dispersant on the soil. The standard was followed with one exception; an air-jet dispersion tube (shown below in Figure 27) was used to mechanically agitate the soil. To record the readings from the hydrometer (in this study, a 152H hydrometer), the data sheet in Figure 28 below was used.

Interpretation of data

In order to effectively use the data garnered from the particle size analysis using the 152 hydrometer, the following corrections and calculations need to be performed. In terms of corrections, the reading was subject to a hygroscopic moisture correction, hydrometer reading correction (zero correction), and temperature correction. After the readings were adjusted accordingly, the percent of soil in suspension and their corresponding diameters were calculated. All these procedures were performed in accordance with the ASTM standard.

Particle size distribution chart

Using the above described calculations to find the percent finer at each time interval and the corresponding diameter of the suspended solution, a particle size distribution chart can be created. The spreadsheet used to calculate these values is presented in the Appendix. The particle size distribution chart for each respective soil sample is presented in Chapter 5: Results and Discussions. A sample graph is shown below illustrating an example soil particle distribution. The graph, shown in Figure 29, also highlights the demarcation needed at the 5- μm particle size necessary for the double hydrometer analysis. The blue line indicates the percent finer of the soil by diameter in both inches and millimeters.

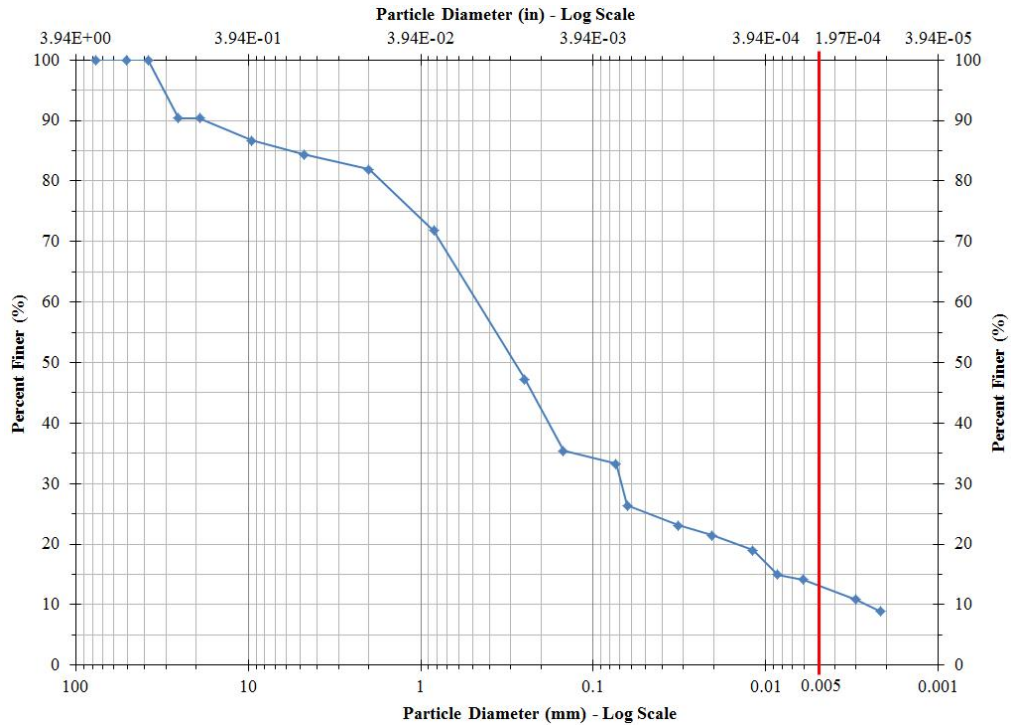


Figure 29. Particle size distribution curve for a Des Moines County soil

Dispersive characteristics of clay soil by double hydrometer

This ASTM standard describes how to determine the percent finer of a suspended soil in a distilled water solution without the use of mechanical agitation or a chemical dispersant.

Equipment

For the completion of the fine particle size analysis using without a dispersant, the following specialized pieces of equipment are needed. Similar to the above procedure with a dispersant, a 1000 mL graduated cylinder, thermometer, and timer are also required.

Vacuum pump and filtering flask

Both these pieces of equipment are necessary to evacuate entrapped air within the sample. The filtering flask used should have a rubber stopper and a side tube able to

withstand forces initiated from a vacuum. The vacuum pump should have capabilities to pull 10 to 12.3 pounds per square inch (psi) to completely de-air the sample.

Hydrometer

A 152H hydrometer was used for this procedure, similar to the above particle size analysis equipment.

Preparation of samples

For this test, the sample must pass the 2-mm (No. 10 sieve) and be in air-dried form.

Procedure

1. Weigh out 25 g of soil passing the 2-mm (No. 10) sieve. Place the sample in a 250-mL beaker and cover with 125 mL of distilled water. Allow the sample to soak for a minimum of 2 hours.
2. After soaking, move the soil to the filtering flask, place a stopper in the top, and connect to the vacuum pump, shown in Figure 30. Start the pump and apply full vacuum using 10 to 11.3 psi – ensure bubbles appear. If bubbles make no appearance, the vacuum is insufficient.



Figure 30. Vacuum used for de-airing of sample in ASTM D 4221-99

3. At 3, 5, and 8 minutes after initiation of vacuum, swirl the flask to ensure entrapped air is being removed.
4. Disconnect flask and wash suspension into a 1000 mL graduated cylinder. Using a rubber stopper placed on the top of the cylinder, agitate the slurry for 1 minute by rotating the cylinder upside down and back.
5. As in the previous standard, set the cylinder on a stable surface and take hydrometer and temperature readings at set time intervals or as needed. For this research, the first reading was taken after 30 seconds and the following (in minutes) were approximately taken at 1, 2, 5, 15, 30, 60, 135, 270, 525, 960, and 1400. A data sheet as shown in Figure 28 above was again used to record the hydrometer reading and temperature at each time interval.

Interpretation of data

In order to effectively use the data garnered from the particle size analysis using the 152 hydrometer, the following corrections and calculations need to be performed.

Water content correction

Similar to the above standard, the oven-dried sample mass must be corrected. To make this correction the oven-dried weight is multiplied by the water content in the below equation.

$$W_s = W_d \times \left(1.0 + \frac{w}{100}\right) \quad (8)$$

Where W_s is the mass of the moist soil;

W_d is the mass of the oven-dried soil (taken as 50 g); and

w is the water content of the sample in a percentage form. This value is then used as the weight of soil used to calculate the percent finer of the solution.

Hydrometer reading corrections

As in the earlier procedure, the hydrometer must be corrected due to the temperature of the solution. However, since the solution is only composed of distilled water, only the temperature correction should be applied to the solution. As such, the corrected hydrometer reading is calculated using the following equation.

$$R_C = R + C_T \quad (9)$$

Where R_C is the corrected hydrometer reading;

R is the actual hydrometer reading as taken from the hydrometer; and

and C_T is the temperature correction value which may be interpolated if between values from Table 5 below.

**Table 5. Temperature correction values
(after Bowles Table 6-3)**

Temperature (°C)	Temperature Correction, C _T
20	0.00
21	0.20
22	0.40
23	0.70
24	1.00
25	1.30
26	1.65
27	2.00
28	2.50

Calculations

After making the above corrections, percentage of soil in suspension and diameter of soil particle calculations can be made in the same manner as above. Refer to ASTM D422-63 for the equations. A similar particle size distribution is then created with the 5- μ m delineation highlighted.

Percent dispersibility calculation

Through the determination of the soil particle percentage passing 5- μ m in each respective test, the percent dispersibility can be calculated using the following equation, presented earlier as Equation 1 in Chapter 2: Background.

$$\% \text{ Dispersion} = \frac{\% \text{ passing } 5 - \mu\text{m without dispersant}}{\% \text{ passing } 5 - \mu\text{m with dispersant}} \times 10 \quad (1)$$

The standard states that a clay sample is defined as dispersive if more than 35% dispersion is calculated.

Modified free swell index

The modified free swell index test was performed in accordance with the research produced by Sivapullaiah et al. (1987). The test procedures are summarized below according to this standard. This test was used as it provided solutions to problems common with free swell tests. No ASTM standard exists for either of these tests.

This test provides a quick and simple method to identify the swelling potential of a clay. In this test, essentially, a known mass of a soil sample is placed in a graduated cylinder filled with water and is allowed to settle for a day. It is an easy test to perform and can be a quick indicator of swelling potential. Although the test calculates the swelling potential of a soil rather than its dispersibility, swelling soils tend to indicate the likelihood of dispersion problems. When placed in a water setting, dispersive soils tend to lose their cohesion and exhibit swelling tendencies; therefore, it can be inferred dispersive soils yield higher swelling potentials as indicated by this test.

Equipment

The equipment necessary for this test was found in the Olson laboratory. The only items of equipment needed were the respective soil specimens as well as a 100 mL graduated cylinder of water.

Preparation of samples

A representative, oven-dried soil must be used for this procedure.

Procedure

1. Measure 10 grams of oven-dried clay. If the clay is known to be expansive, such as with bentonite, a lesser weight of 3 to 5 grams may be used.
2. Transfer the dry clay to a 100 mL graduated cylinder filled with distilled water.
3. Stir the cylinder to agitate the sample and ensure thorough mixing.
4. Find a stable surface, stopper the cylinder, and allow the solution to settle undisturbed for a period of 24 hours.

5. After 24 hours, estimate and record the swollen volume of the soil using the gradations on the side of the cylinder.

Interpretation of data

The percent of swelling is taken as a comparison of the change in volume as related to the dry volume of the soil. The equations used and their variables were presented earlier in Chapter 2: Background as Equations 2 and 3 shown again below.

$$\text{Modified Free Swell Index} = \frac{V - V_s}{V_s} \quad (2)$$

where V is the soil volume after swelling;

V_s is the volume of soil solids calculated from the formula below

$$V_s = \frac{W_s}{G_s * \gamma_w} \quad (3)$$

where W_s is the weight of dry soil;

G_s is the specific gravity of the solids; and

γ_w is the unit weight of the water. The modified free swell index is then related to Table 3 (earlier presented in Chapter 2) to determine the swelling potential.

Table 6. Swelling potential based on modified free swell index (after Sivapullaiah et al., 1987)

Modified Free Swell Index	Swelling Potential
< 2.5	Negligible
2.5 to 10.0	Moderate
10.0 to 20.0	High
> 20.0	Very High

Again, a soil with a high swelling potential is predicted to display dispersive tendencies. As a result, this test can then be used to provide an additional evaluation of a soil's dispersivity.

SEM testing

SEM testing was used to look at the microstructure at each of the samples. The testing procedures were performed per standard procedures as developed by the

Materials Analysis and Research Laboratory (MARL) at Iowa State University. The test procedures are summarized below per their previous work with the equipment.

SEM imaging is a relatively quick way to investigate the microstructure of a soil sample. To obtain such an image, the sample is prepared and mounted onto a stud and placed in the chamber of a machine with SEM capabilities. The technician can maneuver the observation lens and focus in on different areas as needed. A variety of images can be produced under different magnifications. Through the use of an energy-dispersive x-ray spectroscopy (EDS) as well, the elements predominant in the sample can be identified. In learning the elemental and microstructural composition of the sample, one can compare the properties with those of known specimens (such as the three unique clay mineralogies).

Equipment

In order to analyze the microstructure of the sample using SEM technology, the following pieces of equipment are required. For the purposes of this study, all the necessary equipment was located in the basement of the Town Engineering Building in the MARL offices. The most important equipment was the SEM equipment itself; however, care needed to be taken to adequately prepare the sample for imaging. To achieve this, a conductive graphite paint was used to mount the samples onto a non-contaminated surface. After the samples were secure, a coat of conductive material was applied to the sample in order to allow the SEM to generate electrons from the sample.

Conductive graphite

To mount the soil samples onto a carbon stud so as to fasten the sample to a stable surface during analysis, a conductive graphic paint was used. The paint available in the MARL offices was an “isopropanol based graphite resistive and dry film lubricant coating” produced by Ted Pella, Inc. (PELCO © Conductive Graphite Technical Notes, 2012). The paint secures the sample safely to the carbon stud without contaminating the working surface.

High resolution sputter coater

A high resolution sputter coater is used to coat the sample in a conductive material. As it stands, soil is a nonconductive material and the electron microscope functions by emitting electrons through a sample to emit a transfer of heat. Accordingly, the soil sample must be coated with a conductive material so as to allow the electron beam to be transferred to the sample. For this study, a Q150T Turbo-Pumped Sputter Coater/Carbon Coater was used; specifically, the Q150 T S (a high resolution sputter coater) shown below in Figure 31 (Quorum Technologies, 2012).

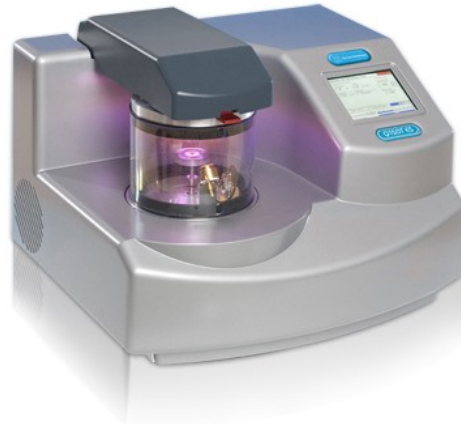


Figure 31. Q150 T Turbo-Pumped Sputter Coater/Carbon Coater (Quorum Technologies, 2012)

The coating material selected for this study was 5 nanometers (nm) of iridium (Ir). Iridium has become a more popular coating choice for SEM tests as the element produces thin films and is a non-oxidizing metal. The film thickness is important because if a thick film is used this texture may dominate the SEM pictures. The film produced by iridium has a very small grain structure and allows the user to see the sample texture rather than that of the metal. The non-oxidizing features of iridium are important as well for sample storage. Because it does not oxidize readily with air, the sample can be stored easily at atmospheric pressure for later use (Quorum Technologies, 2012).

Scanning electron microscope with energy-dispersive X-ray spectroscopy capabilities

To obtain an image of the soil microstructure and identify the elements present in its composition, a SEM with EDS capabilities is required. In this study, an FEI Quanta 250 FEG with EDS Capabilities located in the MARL at Iowa State University was utilized. The machine used is shown in Figure 32. The machine is equipped with standard secondary and backscattered electron detectors in order to obtain a topographic view of the soil structure. This machine also has a light-element x-ray detector and an Indium X-ray Fluorescence (IXRF) Systems EDS analysis system to able to allow for both quantitative and qualitative analysis of the soil. Using this advanced equipment, line scans of the soil and x-ray maps can be created to identify unique features and compositions of the samples (Quanta Scanning Electron Microscopes (SEM), 2013).



Figure 32. FEI Quanta 250 SEM in the Iowa State MARL

Sample preparation

After the performance of the pinhole test on each soil, the sample was extracted and split open (as detailed in the above section discussing the test). This sample was then stored and used for SEM imaging. The following procedure was performed to prepare the sample for the SEM machine.

1. Obtain a fairly flat particle for soil analysis. Using tweezers, extrude the sample from the container and set aside.
2. Using a brush, apply the conductive graphite coating to a carbon stud as seen in Figure 33.



Figure 33. Graphite coating and brush used to affix soil sample to carbon stud

3. Carefully set the selected soil flake on the painted stud and allow it to air-dry; drying should take no longer than 5 minutes.
4. After air-drying, place the sample(s) in the spaces available on the testing platform located in the chamber of the sputter coater shown in Figure 34.

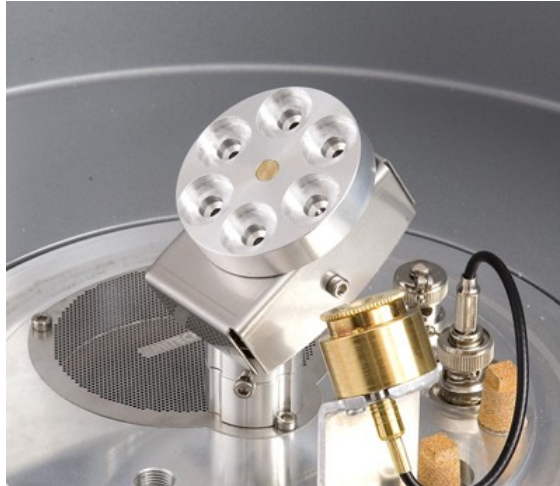


Figure 34. Sample platform for sputter coating (Quorum Technologies, 2012)

5. Specify the coating element and desired thickness using the touch screen control (seen in Figure 35). For this analysis 5 nm of iridium was used to coat the specimen.



Figure 35. Touch screen control for Q150T sputter coater (Quorum Technologies, 2012)

6. Allow the machine to run until coating of the samples is complete (time of coating depends on amount of sample and coating thickness). During running the chamber will emit a glowing light (Figure 36)

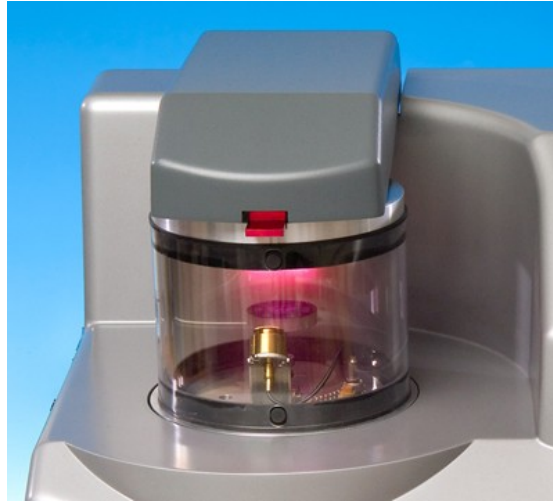
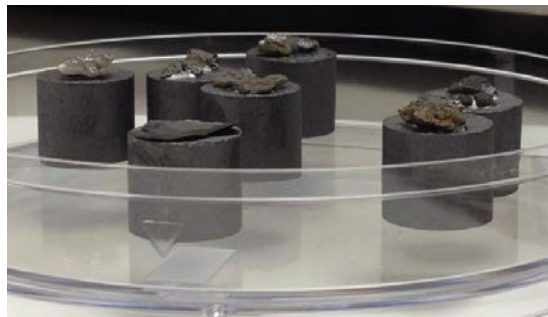


Figure 36. Sputter coating chamber during sputtering (Quorum Technologies, 2012)

7. Carefully remove samples from the sputter coater and place in a petri dish for easy transportation to the SEM equipment. The coated samples should look similar to the ones below in Figure 37 presented in both a side and top view.



(a)



(b)

Figure 37. Coated samples for SEM testing from (a) side and (b) top view

Procedure

1. Vent the chamber from the first tab (vacuum section of the beam control). Click ‘Vent’ and confirm the operation. Vacuuming of the chamber will take approximately 90 second.
2. Place and secure samples to sample holder shown below in Figure 38.

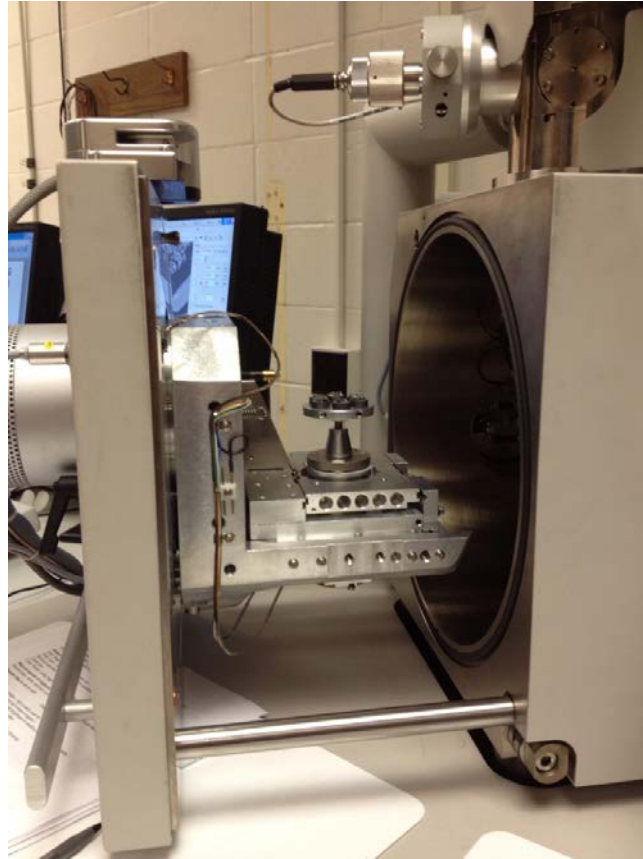


Figure 38. Image of soil samples placed in SEM machine for testing

3. Adjust sample holder and/or the stage height so the samples are oriented at a 10 mm working distance (distance between the bottom of the SEM column and top of samples). This is shown below in Figure 39.

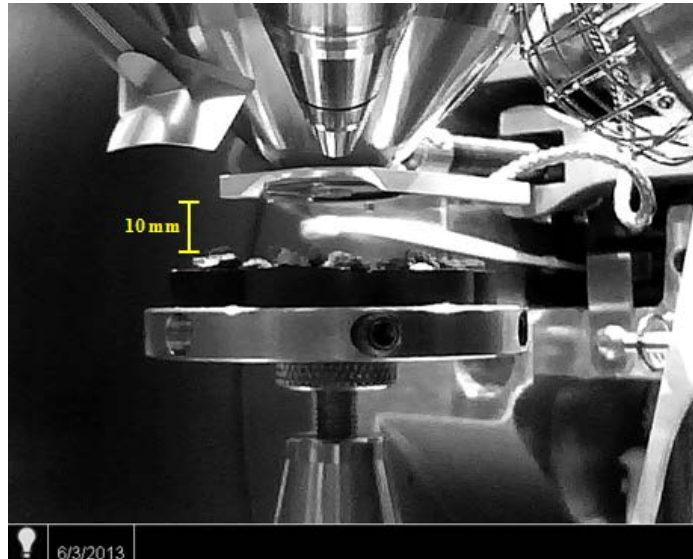


Figure 39. Working distance of SEM used for analysis from Nav-Cam

4. Record the sample locations with the navigation camera (Nav-Cam). This allows the user to know the location of each sample so as to navigate easily between samples. Select the third quadrant on the computer screen, turn off fluorescent lights, and rotate Nav-Cam 90° over the samples. Press the camera button to collect an image of the quadrant (shown in Figure 40). Return the Nav-Cam back to original idle position.

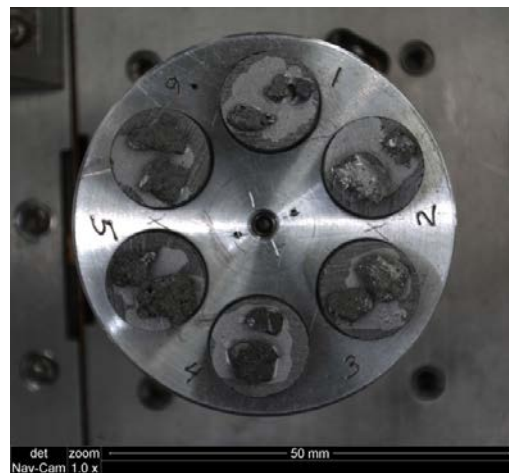


Figure 40. Nav-Cam image recording sample locations in SEM

5. Close the stage door.
6. Select the vacuum mode and level. For this analysis, a high vacuum was used with the Everhart-Thornley Detector (ETD) option to allow the best resolution for SEM imaging. Click 'Pump.'
7. Position the sample under the beam and wait until SEM icon turns green signifying a working vacuum in the chamber (pressure of less than $2.95e-2$ Pascals (Pa)).
8. Click 'Beam On.'
9. To begin taking images of a sample, first navigate to the image by double-clicking on it. This will center the Nav-Cam on a certain location.
10. To focus on an area, begin first at a low magnification (usually a magnification of 50) and move through fine focus and stigmator control at high magnifications. Use the below knob-set in Figure 41 to focus and fine-tune the sample image.



Figure 41. Knob set used to focus SEM on sample

11. To take a picture, zoom in on the area of interest. Focus at 2 to 3 times the magnification used for the image and set by double-clicking on the magnification value.
12. Set the brightness and contrast of an image.
 - a. Press F3 to open waveform.

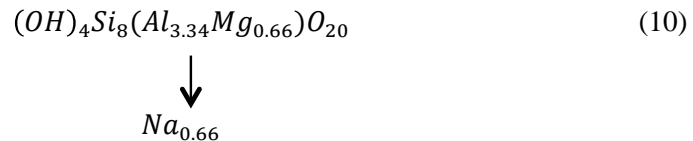
- b. Adjust the Brightness and Contrast knobs on above panel to set waveform between two dashed lines.
 - c. Turn off after adjustment by pressing F3 again.
13. Collect and save an image by pressing F2.
 14. Provide a unique name to the sample (including sample type and magnification) and save to the appropriate folder.
 15. Remove samples by selecting the Beam Control tab and turning the beam off by clicking the 'Beam on' option. Click 'Vent' and remove samples. Close the stage door.

Interpretation of data

Using the image output of the samples as well as the element composition, one can assess the mineral composition of the sample. This is important in reference to this research as it can be related to how likely certain materials tend to be dispersive over others. The clay minerals present in a sample can be identified using the atomic composition and SEM topography of the sample.

Montmorillonite

The montmorillonite mineral follows the following chemical formula (Mitchell and Soga, 2005):



As such, when looking at the elemental composition, it would be expected a material with high contents of magnesium and sodium contained some montmorillonite. Additionally, montmorillonite can be identified by its microstructure. Montmorillonites tend to occur in thin equidimensional flakes that have a film-like appearance. The particles can have thicknesses ranging from 1-nm to about 1/100 of the particle width. The long particle axis is usually less than 1 to 2- μ m. In addition to flakes, some platy or needle particles may be seen. This occurs when there is large isomorphous substitution

with the aluminum being exchanged for magnesium or iron. These ions are larger than the aluminum ions and are reflected as such in the microstructure (Mitchell and Soga, 2005). An example of a montmorillonite SEM image is presented below in Figure 42.

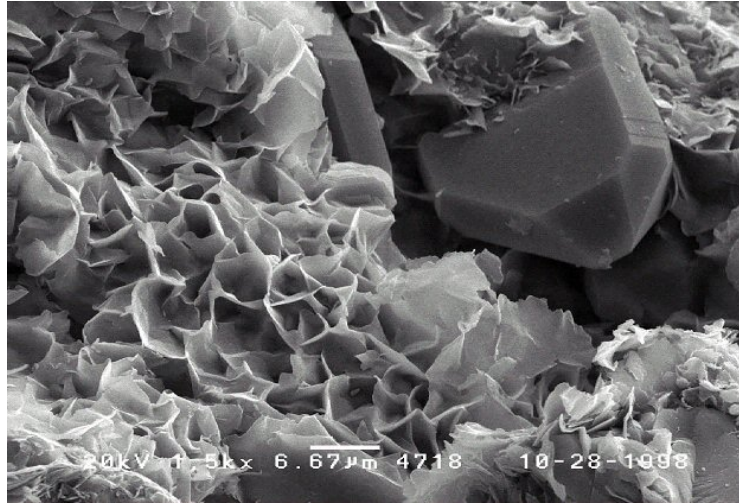


Figure 42. SEM image of a montmorillonite
(© OMNI Laboratories, Inc from Mineralogy Database, 2007)

Referencing the above figure, one can clearly see the filmy particles characteristic of montmorillonites on the left side of the image. The right side seems to have a more platy appearance which, as explained above, could be explained by extensive isomorphous substitution in the sample. Additionally, due to their dispersive tendencies, it would be assumed an image of a montmorillonite would mostly show particle edges rather than faces. The filmy particles all seem to be showing their edges which reaffirm the dispersivity of the mineral (Sides and Barden, 1971).

Illite

The illite mineral follows the following chemical formula (Mitchell and Soga, 2005):



Given the above, when looking at the elemental composition, it would be expected a material with high contents of potassium, magnesium, and iron had illite. When looking

at the microstructure, illites usually occur as small, flaky particles. If well crystallized, a hexagonal outline can be seen. The long axis of particles can range from 0.1- μm or less to several micrometers thick. The plate thickness varies as well and can be as small as 3 nm (Mitchell and Soga, 2005). An image of illite crystals is shown below in Figure 43.

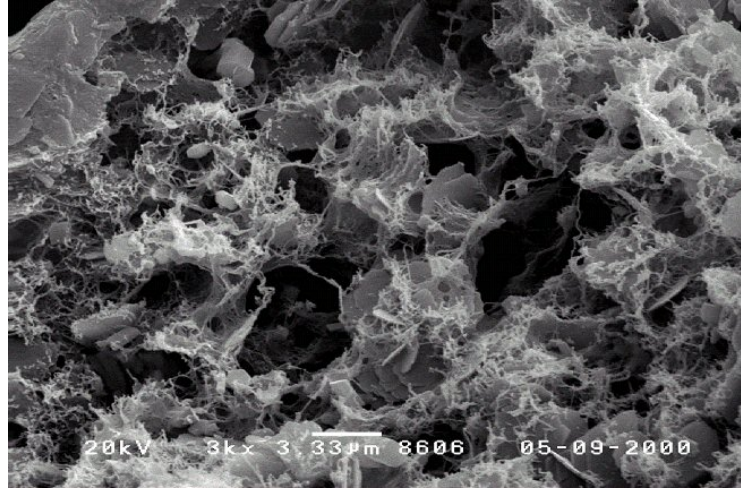


Figure 43. SEM image of an illite
 (© OMNI Laboratories, Inc from Mineralogy Database, 2007)

From the above figure, one can clearly see flaky particles dominating the image. Some hexagonal shapes can also be seen in the upper left corner of the image. These images, as described above, are characteristic of an illite's microstructure. Illites are also known to be moderately dispersive. This feature is reflected in the preponderance of particle edges visible in the image (Sides and Barden, 1971).

Kaolinite

The montmorillonite mineral follows the following chemical formula (Mitchell and Soga, 2005):



A compositional profile only showing the presence of silicon and aluminum elements would be indicative of a kaolinite. All three clay minerals contain these elements but kaolinite is the sole mineral without additional cations in its layers. The presence of 6-sided flakes in a sample's microstructure is typical of a kaolinite. In poorly crystallized

kaolinite, these flakes are still present but as less distinct plates. The long axis of particles can range from 0.1 to 4- μm while the thicknesses vary from 0.05 to 2- μm (Mitchell and Soga, 2005). Figure 44 below shows a SEM image of a typical kaolinite. This specific figure shows well-formed 6-sided shaped particles. Additionally, the particles shown are arranged as such to show a variety of edges, planes, and cavities. These features affirm the nondispersive properties of the clay mineral (Sides and Barden, 1971).

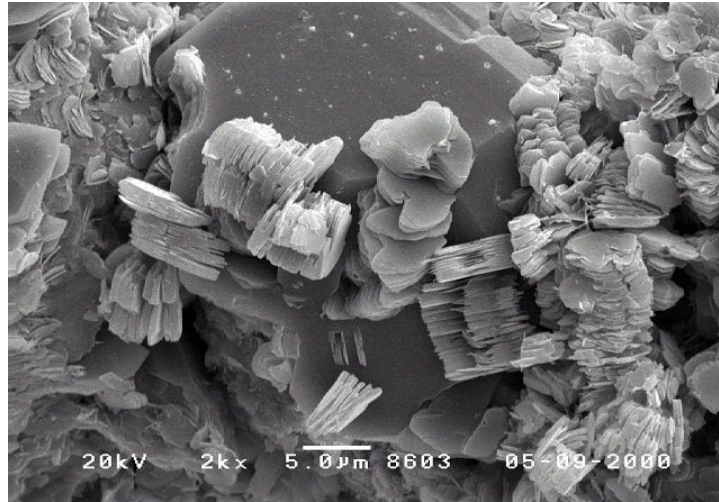


Figure 44. SEM image of a kaolinite
(© OMNI Laboratories, Inc from Mineralogy Database, 2007)

Lime treatment

Lime is a chemical additive used to improve the workability and strength of soils. When added to a sample, lime (or calcium hydroxide) induces a pozzolanic reaction which bonds soil particles together. In addition to this new strong bonding of particles, lime can also reduce a soil's plasticity, moisture-holding capacity, and tendency to swell. This reaction is time dependent and thus longer curing times result in higher strength gains and improvements in stability. Although lime can be utilized for most all fine-grained materials, the most improvement occurs on clays with moderate to high plasticity properties.

For this study, work performed earlier by McDaniel and Decker (1979) was referenced. In their study, clays were treated with varying amounts of lime by weight and cured for different time scales. The treated clays were then compacted and tested using a pinhole dispersion test (discussed above). From their tests, they found a lime content of 4% by weight and a cure time of two days was sufficient to reduce the dispersibility properties of the clay. This same procedure was then used for this research to analyze changes in dispersibility in clays before and after treatment.

Equipment

The equipment necessary for the completion of this test was found in the Olson laboratory in the Town Engineering Building. The necessary pieces included the Harvard miniature compaction apparatus (discussed in the pinhole dispersion test section) and Western Miracle type “s” hydrated masons lime produced by the Western Lime Corporation.

Preparation of samples

A representative soil sample at air-content is used for this procedure.

Procedure

1. Determine the water content of the sample as well as the optimum.
2. Weigh approximately 100 grams of soil sample to be treated.
3. Measure about 4 grams of lime (4% of the above sample weight) and add to the soil sample.
4. Determine the necessary water to be added to the sample to achieve the optimum moisture content. Add the water using a spray bottle and mix sample with spatula thoroughly in between layers of water.
5. Following ASTM Method D 698 and using a Harvard miniature compaction apparatus, compact the soil in three layers at 25 blows per layer. After compaction, extrude the sample and allow it to cure for a period of 48 hours.
6. After curing, prepare sample depending on test to be performed and follow procedures accordingly.

CHAPTER 4. MATERIALS

This chapter presents index property results for the soil used in this study. The soils used were obtained from material available at Iowa State University and from Stephen H. Nickel. The soils discussed below include oxidized glacial till, alluvial top stratum, Western Iowa loess, bentonite, kaolinite, Santa Rosa Dam clay, and a prepared sodium illite. Particle size distribution tests were performed on the samples and previous data from Atterberg tests were used. For the purposes of this study, the particle size distribution was classified based on the Unified Soil Classification System (USCS). Unless otherwise stated, the optimum moisture content was determined using standard industry practices based on the liquid and plasticity limit.

Oxidized glacial till

Till is sediment that has been transported and deposited directly by ice. Till can be highly variable and its composition depends greatly on the types of rock over which the initial glacier flowed. Typically, it is characterized by highly variable, unsorted angular debris composed of several different types of rock. Typically, tills are not known to be dispersive (Ritter et al., 2011).

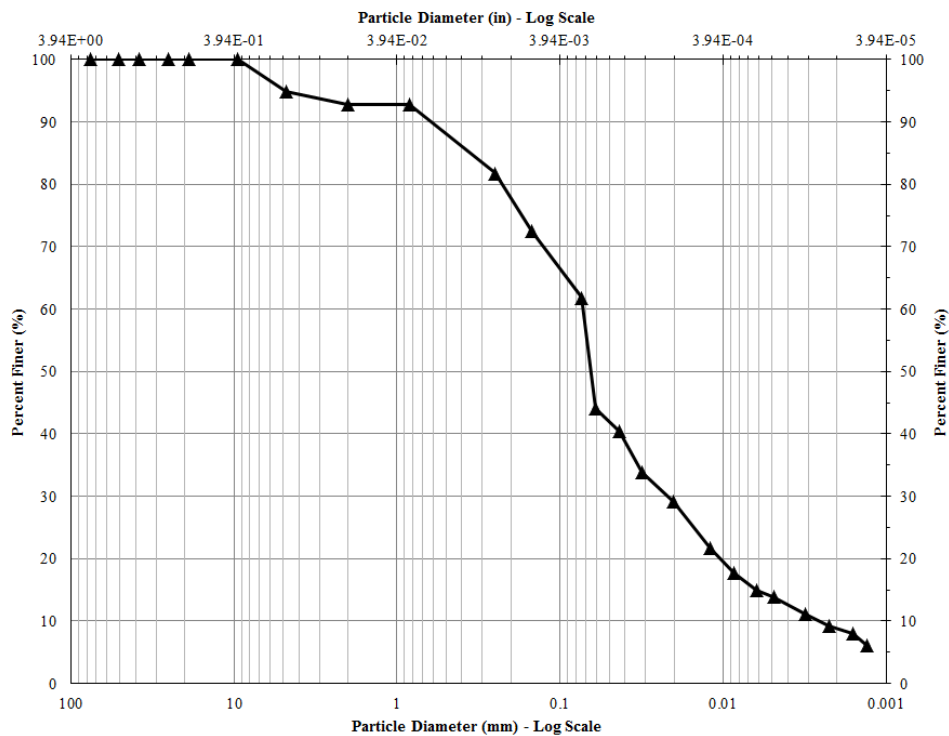
The oxidized glacial till sample for this study was collected from the soil bins located in the Teaching Laboratory in the Town Engineering Building at Iowa State University. The results of completed particle size analysis and Atterberg limits are show below.

Laboratory test results

The oxidized glacial till was subject to a particle size distribution analysis and Atterberg limit testing. The results are presented below in table and graph form, Table 7 and Figure 45, respectively. The tested oxidized glacial till was found to be clay.

Table 7. Particle size and Atterberg test summary for oxidized glacial till

Particle Size Summary	
Gravel	5.1%
Sand	33.0%
Silt and Clay	61.8%
Specific Gravity	2.70
Plastic Limit	13%
Liquid Limit	20%
Plasticity Index	7%
Natural Water Content	2%
Optimum Water Content	12%
Classification	CL-ML

**Figure 45. Grain size distribution for oxidized glacial till**

Alluvial top stratum

Alluvial refers to the transportation of soil by water. Sediment is typically transferred from one stream location to another through a stream medium. The sediment

sizes can be highly variable, from gravels to clays, depending on the velocity of the water (Ritter et al, 2011). Sherard et al. (1977) found alluvial clay to be prone to dispersive behavior.

The alluvial top stratum sample for this study was collected from the soil bins in the Teaching Laboratory in the Town Engineering Building at Iowa State University. The particle size analysis and Atterberg limit test results are shown below.

Laboratory test results

The results from the particle size distribution analysis and Atterberg limit tests on the alluvial top stratum are presented below in table and graph form, Table 8 and Figure 46, respectively. From the analysis, the alluvial top stratum was classified as a clay.

Table 8. Particle size and Atterberg test summary for alluvial top stratum

Particle Size Summary	
Gravel	0.3%
Sand	36.4%
Silt and Clay	63.3%
Specific Gravity	2.70
Plastic Limit	26%
Liquid Limit	41%
Plasticity Index	16%
Natural Water Content	4%
Optimum Water Content	18%
Classification	CL

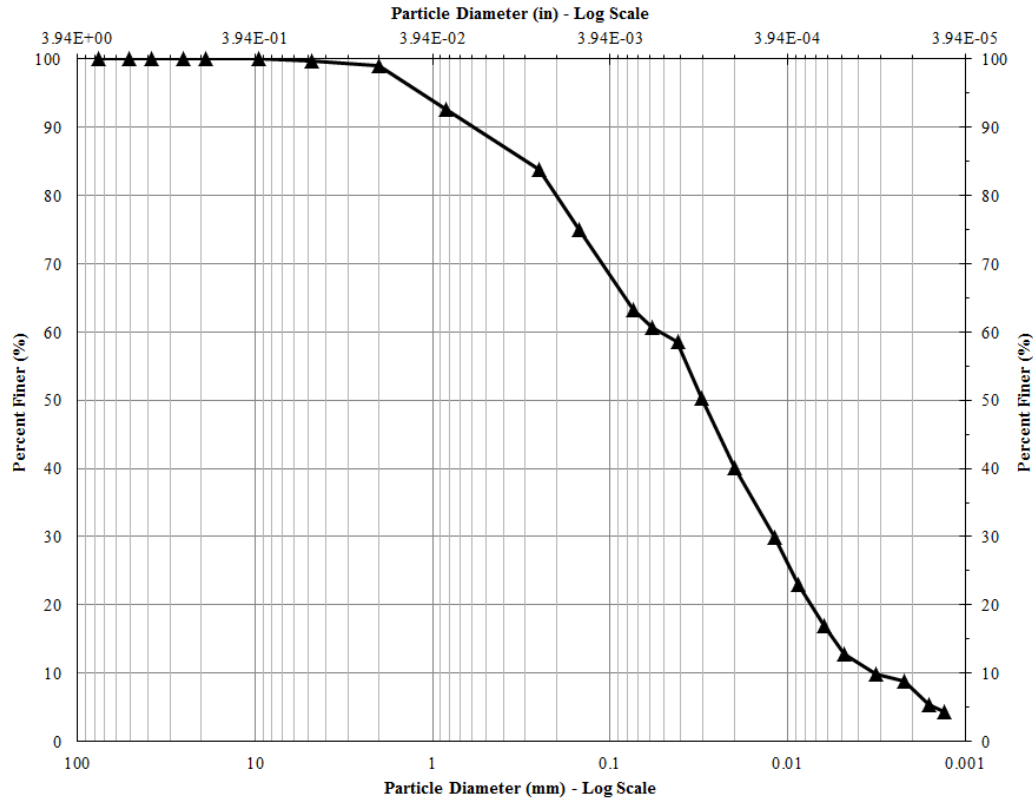


Figure 46. Grain size distribution for alluvial top stratum

Western Iowa loess

Loess is silt-sized sediment that has deposited by the wind. The structural characteristics of loess can vary dramatically depending on its moisture content at the time. The specific characteristics of loess vary depending on the geological location, but it can exist at a range of plasticity indices (depending on its mineralogy) and can be susceptible to collapsible if saturated and subject to a load. Although sensitive to water, loess is not known to be dispersive (Ritter et al., 2011).

The last sample obtained from the bins located in the Teaching Laboratory in the Town Engineering Building at Iowa State University was the Western Iowa loess. The results of the particle size analysis and Atterberg limits are show below. The analysis showed the Western Iowa loess to be a silt.

Laboratory test results

Results from particle size analysis and Atterberg limit testing on the Western Iowa loess are presented below in table and graph form, Table 9 and Figure 47, respectively.

Table 9. Particle size and Atterberg test summary for Western Iowa loess

Particle Size Summary	
Gravel	0.1%
Sand	1.0%
Silt and Clay	98.9%
Specific Gravity	2.70
Plastic Limit	25%
Liquid Limit	30%
Plasticity Index	5%
Natural Water Content	4%
Optimum Water Content	17%
Classification	ML

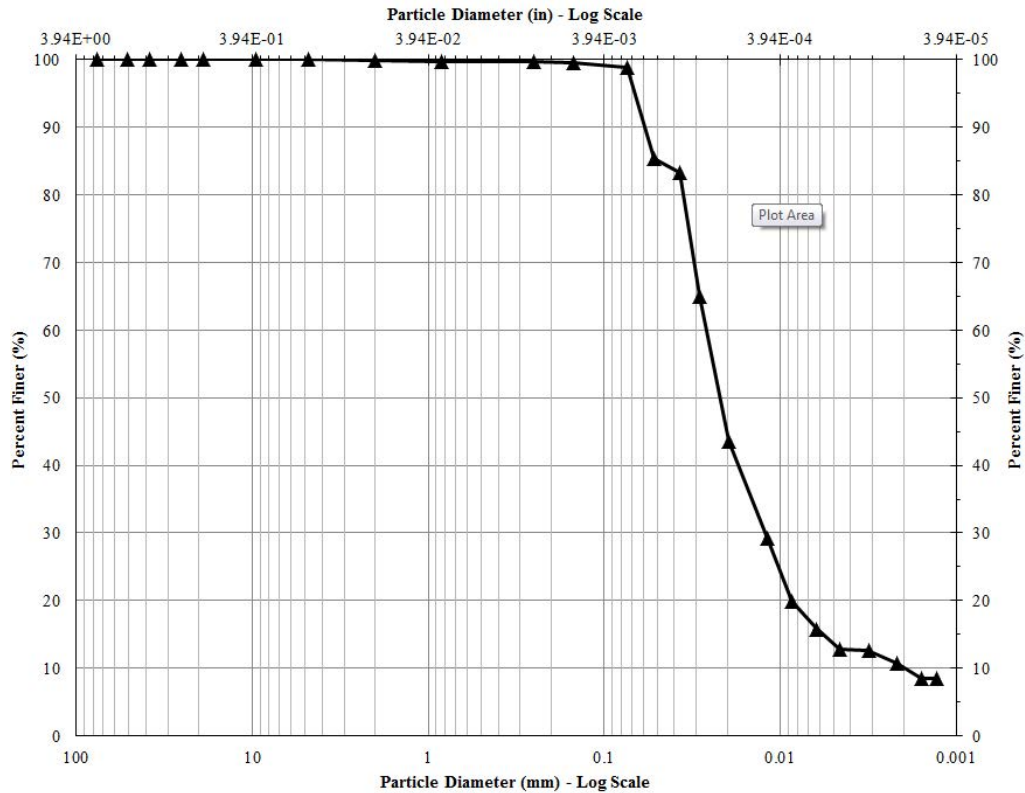


Figure 47. Grain size distribution for Western Iowa loess

Bentonite

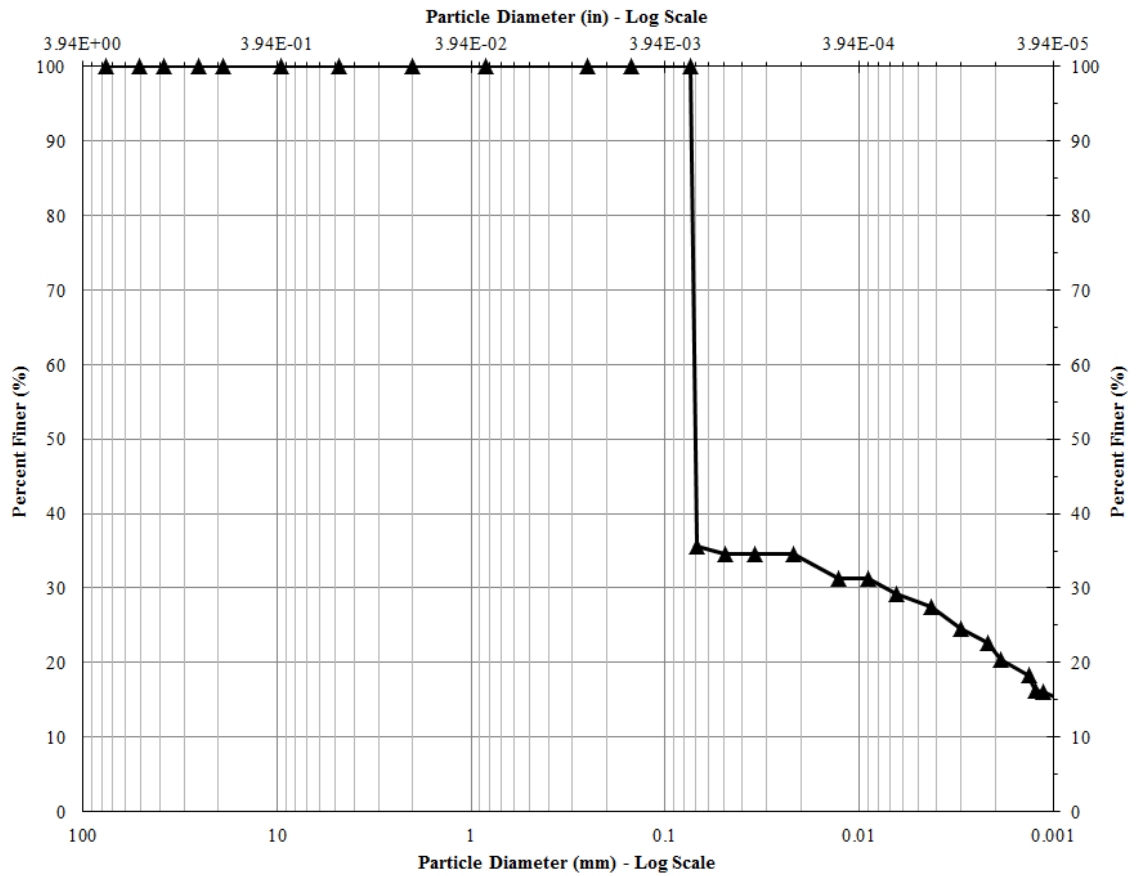
A bentonite soil sample was obtained from the Teaching Laboratory in the Town Engineering Building at Iowa State University. The results of the particle size analysis and Atterberg limits are shown below. Bentonite is known to be a high plasticity clay.

Laboratory test results

Results from particle size analysis and Atterberg limit testing on the bentonite sample are presented below in table and graph form, Table 10 and Figure 48, respectively. The specific gravity was produced from a study by Yilmaz in 2003 and 2004.

Table 10. Particle size and Atterberg test summary for bentonite

Particle Size Summary	
Gravel	0%
Sand	0%
Silt and Clay	100%
Specific Gravity	2.65
Plastic Limit	50%
Liquid Limit	452%
Plasticity Index	402%
Natural Water Content	6%
Optimum Water Content	47%
Classification	CH

**Figure 48. Grain size distribution for bentonite**

Kaolinite

A kaolinite soil sample was obtained from the Teaching Laboratory in the Town Engineering Building at Iowa State University. The kaolin was produced by Starwest Botanicals in Sacramento, California. A particle size analysis chart and table of Atterberg limits are show below. Kaolinite is known to be a clay.

Laboratory test results

Results from particle size analysis and Atterberg limit testing on the kaolinte sample are presented below in table and graph form, Table 11 and Figure 49, respectively. The specific gravity was produced in a study by Yilmaz in 2003 and 2004.

Table 11. Particle size and Atterberg test summary for kaolinite

Particle Size Summary	
Gravel	0%
Sand	0%
Silt and Clay	100%
Specific Gravity	2.55
Plastic Limit	30%
Liquid Limit	38%
Plasticity Index	8%
Natural Water Content	0%
Optimum Water Content	26%
Classification	CL

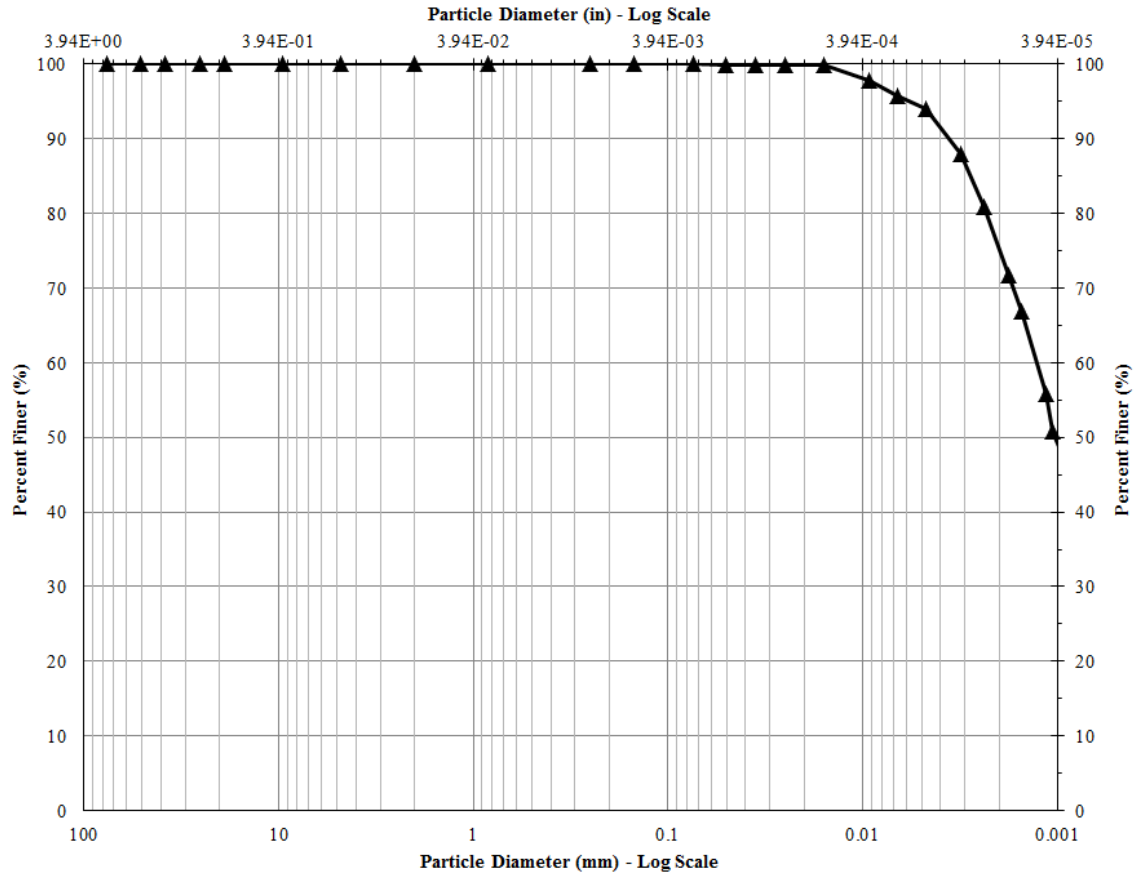


Figure 49. Grain size distribution for kaolinite

Santa Rosa clay

The Santa Rosa clay is a sample obtained from a failed dam in Santa Rosa, New Mexico. The samples were obtained from Stephen H. Nickel, a geotechnical engineering consultant in Lincoln, Nebraska. The dam began construction in 1975 and by the fall of 1976, dispersive clay erosion patterns had been noted in reservoir pits. Samples were taken from the area and subsequently classified as moderately to highly dispersive. An additional 14 samples were then taken from the area for classification tests. Half of the samples underwent pinhole classification tests and cation analysis a pinhole dispersion test was performed on all fourteen. Hoskins-Western-Soderegger (HWS), Inc. in Lincoln, Nebraska performed the testing on the soil samples (1977). The results from the

tests are presented below by sample number used in the paper in Table 12. The samples marked with an asterisk (*) were samples available for this study (Hoskins-Western-Soderegger, Inc, 1977).

Table 12. Table of Santa Rosa clay properties as performed by HWS, Inc.

Sample Number	% Dispersion by Double Hydrometer	Classification by Pinhole Test	% Sodium by Total Dissolved Salts test
C-1	44	Dispersive	75
C-2*	18		
C-3	57	Dispersive	84
C-4	74	Dispersive	77
C-5	39	Dispersive	64
C-6*	37		
C-7	28	Slightly dispersive	66
C-8*	29		
C-9*	43		
C-10	45	Dispersive	68
C-11*	25		
C-12*	27		
C-13*	31		
C-14	19	Dispersive	65

Of the 7 samples available for this study, sample C-13 was selected due to the amount of material available. It was one of the larger samples so all laboratory tests could be performed. Additionally, it had a previous dispersion percentage of 31% indicating an intermediately dispersive clay which relates well with this research.

Laboratory test results

Results from particle size analysis and Atterberg limit testing on the Santa Rosa clay sample are presented below in table and graph form, Table 13 and Figure 50, respectively.

Table 13. Particle size and Atterberg test summary for Santa Rosa clay

Particle Size Summary	
Gravel	0%
Sand	6.1%
Silt and Clay	93.9%
Specific Gravity	2.70
Plastic Limit	19%
Liquid Limit	34%
Plasticity Index	15%
Natural Water Content	2%
Optimum Water Content	16%
Classification	CL

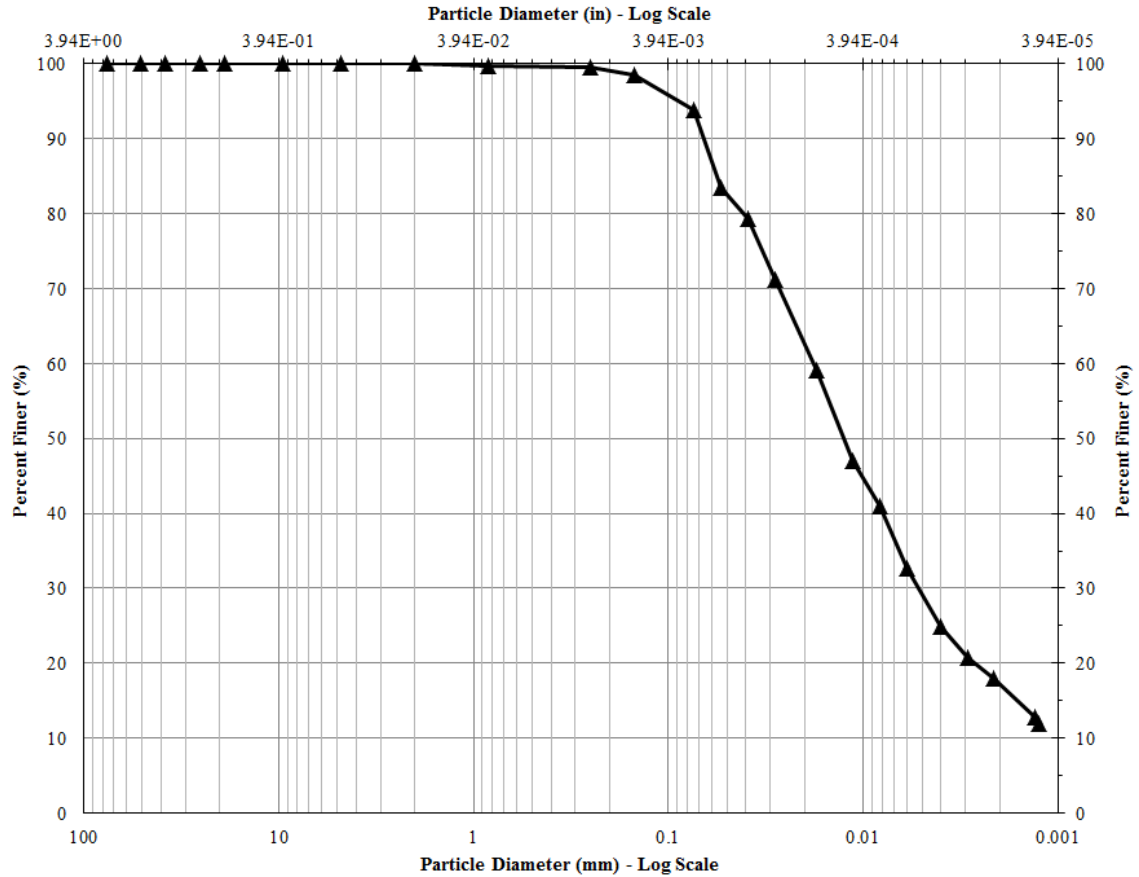


Figure 50. Grain size distribution for Santa Rosa clay

Prepared sodium illite

The sodium illite was acquired from Stephen H. Nickel who prepared the soil for his master's thesis, completed in 1972. To begin, 300 pounds of Grundite were obtained from the Illinois Clay Products Company and homogenized. The raw illite was then neutralized by adding 15 mL of 1.0 N potassium hydroxide (KOH) per 100 gram of ray clay to create a 1 part clay to 2 parts water slurry. After 5 to 7 days, the neutralization was complete.

The soil was then converted to a nonexpanding illite by treating the soil with a potassium chloride (KCl) which would replace sodium ions with potassium ions. The KCl solution was added in order to yield 40 liters of 1.5 N KCl. The new slurry was

agitated with the air and then allowed to settle before the KCL was decanted. Clay was then washed 6 times in 20 liters of distilled water to disperse the particles. Next, the pH was adjusted using a sodium hydroxide by passing the clay through ion exchange columns with medium porosity Amberlite exchange resin. After this process, the soil had been converted to the sodium illite form.

In the sodium illite form, the illite existed in a dispersed state at a water content of 5000%. The suspension was subsequently de-aired by vacuum and transferred to a large container. The suspended particles were then flocculated with the additional sodium chloride so as to produce a suspension at seawater concentration (35.0 grams of salt per liter). In its final form with the floc allowed to settle, the water content was 2000% (Nickel, 1972). It was in this state that the sodium illite sample was made available for testing.

In this state, the soil was allowed to settle and the top supernatant salt water was decanted. The remaining liquid was then pushed out of the sample using a compaction permeameter draining to a graduated cylinder (shown below in Figure 51). The sample was placed in the compaction permeameter with semipermeable plates above and below. On top of the sample, weights were slowly added in increasing weights to compress the sample and remove the liquid. Over a period of 10 days, the soil was compressed and the liquid was siphoned off the top and drained through the bottom. The resulting soil was a flocculated sodium illite. A portion of the clay sample was then oven-dried and sieved using a No. 10 sieve. The sample could then be used in the classification and dispersion tests.



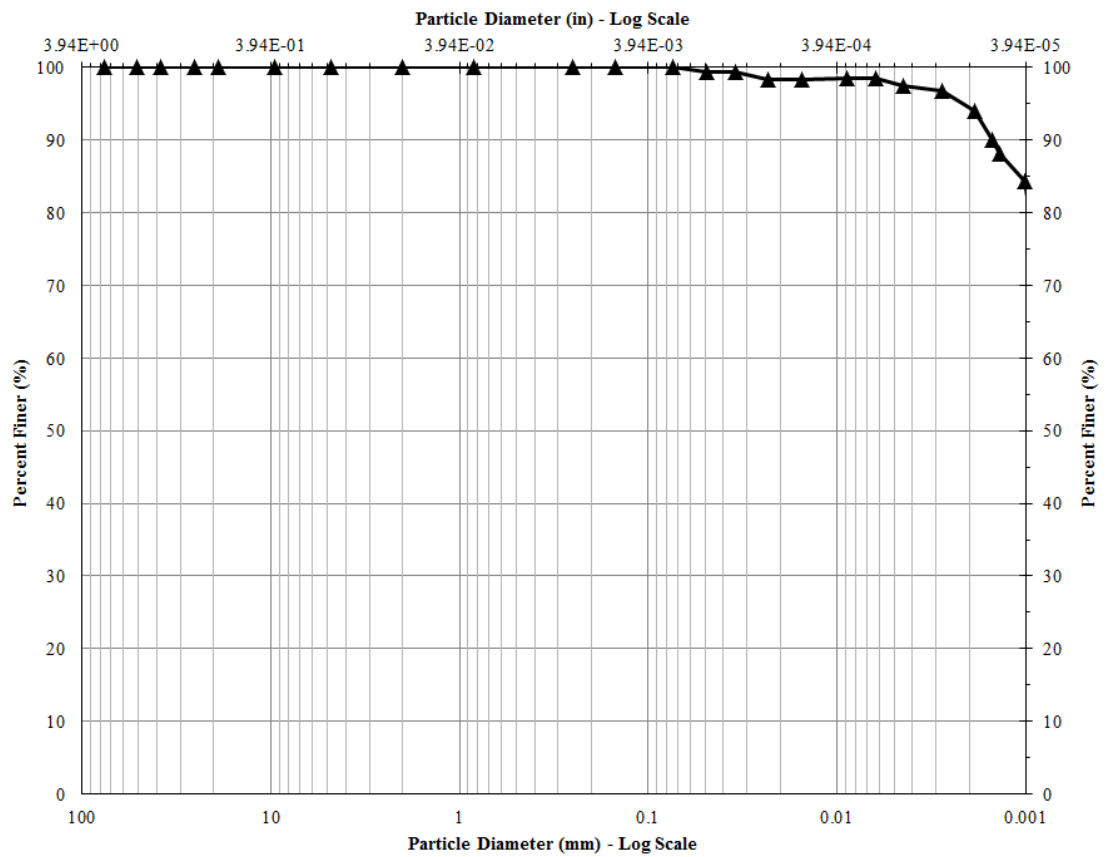
Figure 51. View of compaction permeameter system used to compress sodium illite

Laboratory test results

The particle size analysis and Atterberg limit results from the sodium illite are presented below in table and graph form, Table 14 and Figure 50, respectively. The clay fraction, specific gravity, and Atterberg limit results were determined by Nickel in his original thesis.

Table 14. Particle size and Atterberg test summary for prepared sodium illite

Particle Size Summary	
Gravel	0%
Sand	0%
Silt	2%
Clay	98%
Specific Gravity	2.82
Plastic Limit	32%
Liquid Limit	98%
Plasticity Index	66%
Natural Water Content	5%
Optimum Water Content	27%
Classification	CH

**Figure 52. Grain size distribution for prepared sodium illite**

CHAPTER 5. RESULTS AND DISCUSSION

This chapter provides the results and discussions from dispersivity testing and SEM imaging for seven different soil types. Dispersivity testing and SEM imaging on two treated samples are also presented and discussed. The chapter is organized by soil type: oxidized glacial till, alluvial top stratum, Western Iowa loess, bentonite (untreated and treated), kaolinite, Santa Rosa clay, and prepared sodium illite (untreated and treated). Within each chapter the test results are shown in the same order: crumb test, pinhole test, double hydrometer test, modified free swell index, and SEM images with a final dispersivity classification from the test results. Data sheets for each test are presented in the Appendix. A discussion of the SEM images by classification (nondispersive, moderately dispersive, and dispersive) follows the individual sample results.

Table 15 below presents a summary of the test results. Note ND, SD, MD, and D signify nondispersive, slightly dispersive, moderately dispersive, and dispersive, respectively. Additionally classification and percent dispersivity have also been abbreviated as “Class.” and “% Disp.”

Soil	Crumb Test		Pinhole Test		Double Hydrometer Test		Modified Free Swell Index		Ultimate Class.
	Grade	Class.	Grade	Class.	%Disp.	Class.	Modified Free Swell Index	Swell Potential	
Oxidized Glacial Till	1	ND	ND1	ND	26%	ND	2.0	Negligible	ND
Alluvial Top Stratum	1	ND	ND4	SD	26%	ND	2.4	Negligible	SD
Western Iowa loess	1	ND	ND1	ND	27%	ND	2.4	Negligible	ND
Bentonite	3	D	D2	D	66%	D	10.9	High	D
Treated Bentonite	2	MD	ND2	ND	N/A	N/A	14.2	High	ND
Kaolinite	3	D	ND3	MD	47%	MD	1.7	Negligible	MD
Santa Rosa Clay	1	ND	ND3	MD	21%	ND	2.5	Moderate	MD
Sodium Illite	3	D	ND3	MD	39%	MD	9.7	High	MD
Treated Sodium Illite	1	ND	ND2	ND	N/A	N/A	7.5	Moderate	ND

Table 15. Test results and classification summary

Oxidized glacial till

Four different laboratory tests for dispersivity were conducted on the oxidized glacial till. SEM imaging was also performed on the sample after the pinhole test was complete. The following is a presentation of the results.

Crumb test

The following table shows the grade of dispersion at each time interval. Figure 53 shows corresponding pictures for each of the readings at increasing time intervals. Table 16 shows the grade and temperature recorded for each reading.

Table 16. Crumb test results for oxidized till

Time Interval	Grade	Temperature (°C)
2 min	1	23.8
1 hour	1	23.8
6 hours	1	23.8

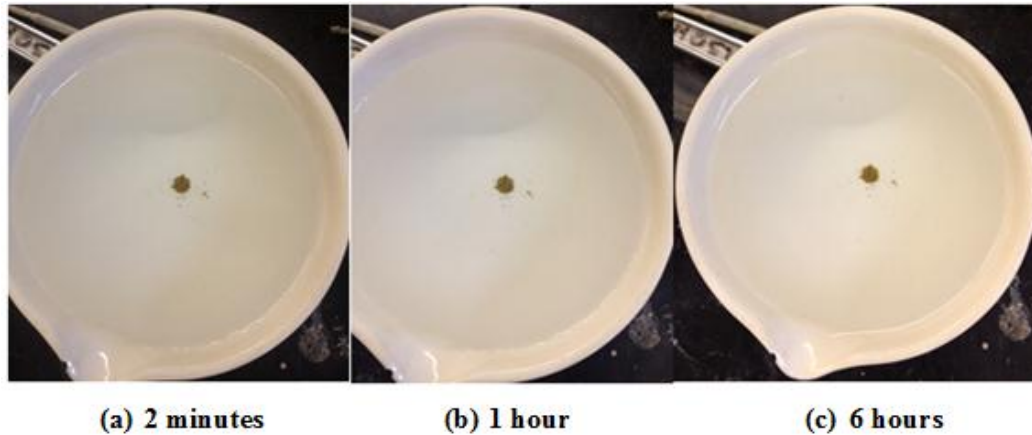


Figure 53. Crumb test for oxidized till at increasing times

Looking at the figures above, the soil was classified as Grade 1 Nondispersive at each recorded time. The crumb did slake upon initial placement in the water; however, the particles never interacted with the water nor did the liquid appear cloudy when

viewed from above. With a Grade 1 classification at all periods, the oxidized glacial till was classified as nondispersive per the crumb test.

Pinhole test

During the pinhole test, the turbidity was minimal and the water was completely clear from the top. A side view of the effluent is presented in Figure 54. The soil was tested under 2, 7, 15, and 40 inches of hydraulic head until the test was considered complete. After 40 inches of hydraulic head and 25 minutes, the turbidity was minutely discolored and had a flow rate of less than 3.0 mL/s. Once the test was complete, the sample was then extruded and the new diameter of the hole was observed from the top as well as after splitting the sample (shown in Figure 55 and Figure 56, respectively). Looking at the two, the hole size was approximately the diameter of the drill needle. Per the ASTM standard, the soil was then classified as ND1 Nondispersive.



Figure 54. Effluent from pinhole test for oxidized till



Figure 55. Aerial size of hole after pinhole test completion for oxidized till



Figure 56. Inner size of hole compared with drill needle for oxidized till

Double hydrometer test

The resulting particle size distribution curves (Figure 57) for the oxidized till using both sample in water only (blue line) and with a dispersant (green line) are shown below. The red line was used to determine particles finer than 5- μm for each respective test. The percent dispersion could then be calculated as a comparison of the percent of particles finer than 5- μm without a dispersion to the percent finer of 5- μm with a dispersant. These values are shown below as well as the calculated percent dispersion in Table 17. The percent dispersion was calculated using Equation 1, defined in Chapter 2. With calculated percent dispersion being 26%, the oxidized till was determined to be nondispersive (a dispersive soil is considered to have 30% dispersion or more).

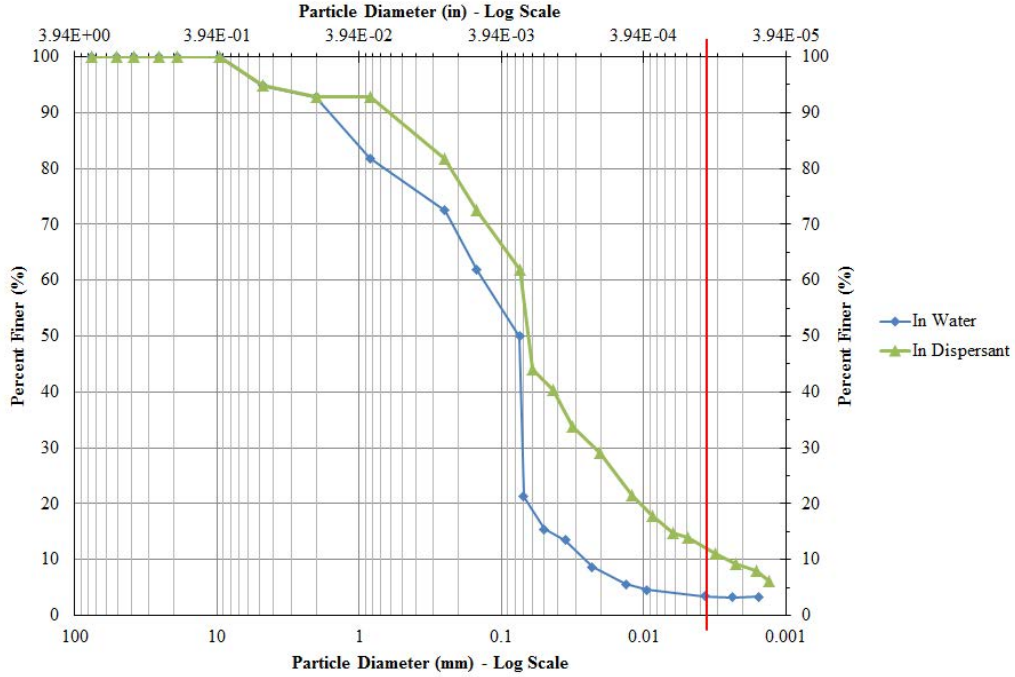


Figure 57. Double hydrometer particle size distributions for oxidized till

Table 17. Double hydrometer test results for oxidized till

Percent Finer than 5-μm in Water Solution	Percent Finer than 5-μm in Chemical Solution	Percent Dispersion
3.7%	14.0%	26%

Modified free swell index test

The modified free swell index of a soil is determined based on the amount of swelling in a graduated cylinder. After settling for a period of 24 hours, the final volume of the oxidized till was measured at 11 mL (shown in Figure 3). This volume was then used in the modified free swell index formulas (Equations 2 and 3 from Chapter 2) and the final index could be calculated (original mass, final volume, and swell index are shown in Table 18). Using those formulas, the modified free swell index was found to be 1.97. Per work done by Sivapullaiah et al. (1987), this garners a negligible swelling

potential. Related to dispersivity, there would then be a low likelihood of a dispersive behavior.



Figure 58. Final swell volume for modified free swell test for oxidized till

Table 18. Modified free swell Index results for oxidized till

Original Soil Mass (g)	Final Swell Volume (mL)	Modified Free Swell Index
10	11	2.0

SEM images

Figure 59 below presents images of an oxidized glacial till sample at increasing magnifications.

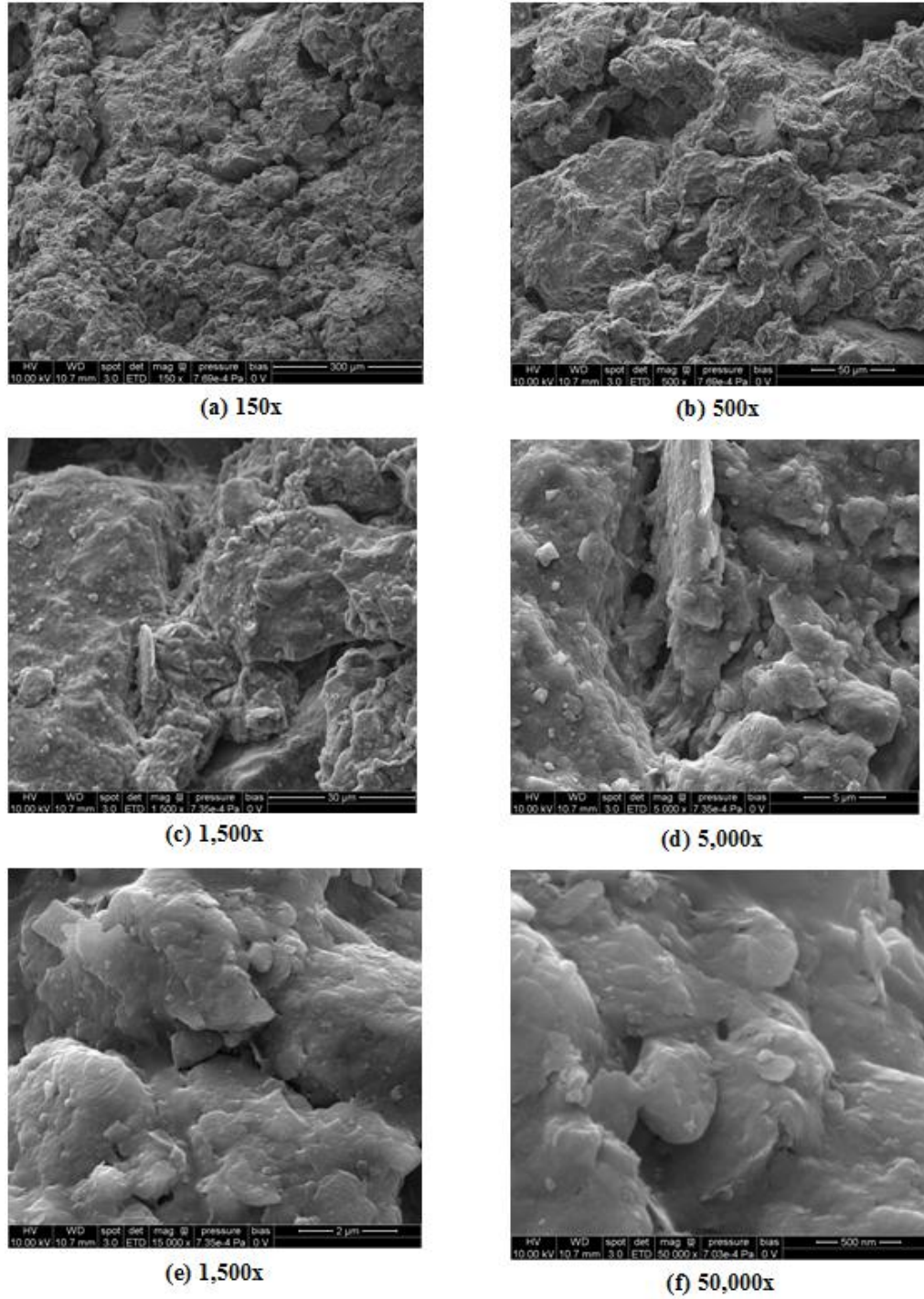


Figure 59. SEM images of oxidized till in order of increasing magnification

Ultimate sample classification

A summary table of the dispersivity classification by test is below for the oxidized till sample in Table 19. With agreement in each test, the oxidized glacial soil was classified as nondispersive.

Table 19. Summary table of dispersivity tests for oxidized glacial till

Test	Classification
Crumb Test	Nondispersive
Pinhole Test	Nondispersive
Double Hydrometer Test	Nondispersive
Modified Free Swell Index	Nondispersive

Alluvial top stratum

Four different dispersion classification tests were performed in the laboratory on the alluvial top stratum. After the pinhole test was performed, SEM images were also taken of the sample.

Crumb test

The following table shows the grade of dispersion at each time interval. Figure 60 and Table 20 present the corresponding pictures and readings for each of the increasing time intervals.

Table 20. Crumb test results for alluvial top stratum

Time Interval	Grade	Temperature (°C)
2 min	1	23.5
1 hour	1	23.5
6 hours	1	23.8



(a) 2 minutes

(b) 1 hour

(c) 6 hours

Figure 60. Crumb test for alluvial top stratum at increasing times

Referencing the figures above, the soil was classified as Grade 1 Nondispersive at all times. The crumb stayed intact throughout the entire test and had no reaction with the water. The alluvial top stratum was thus classified as nondispersive.

Pinhole test

Throughout the pinhole test, the effluent started as barely visible, however increased to a slightly dark discoloration, as shown below in Figure 61. The hydraulic head was raised from 2 to 7 to 15 inches before the test was considered complete. At this point (at 15 inches of head and 20 minutes), the flow was slightly dark and the flow rate was between 1.8 to 3.2 mL/s. It should be noted the sample was already distinctly dark and would thus be easier to see if any particles became even slightly erosive. Once complete, the sample was extruded and the hole diameter was observed from the top as well as after splitting the sample (shown in Figure 62 and Figure 63, respectively). Using the below images, the hole size appeared to be about the same diameter as the drill needle. Per the ASTM standard, the soil was then classified as ND4 Slightly to Moderately Dispersive.



Figure 61. Effluent from pinhole test for alluvial top stratum



Figure 62. Aerial size of hole after pinhole test completion for alluvial top stratum



Figure 63. Inner size of hole compared with drill needle for alluvial top stratum

Double hydrometer test

The particle size distribution curves (Figure 64) from the double hydrometer test for the oxidized till using both sample in water (blue line) and with a dispersant (green line) are shown below. The red line signifies particles finer than 5- μm . Percent dispersion was calculated similarly to above using Equation 1 from Chapter 2. The values used in the calculation and the resulting percent dispersion is shown below in Table 21. With calculated percent dispersion being 26% (less than 30% which is considered dispersive), the alluvial top stratum was classified as nondispersive.

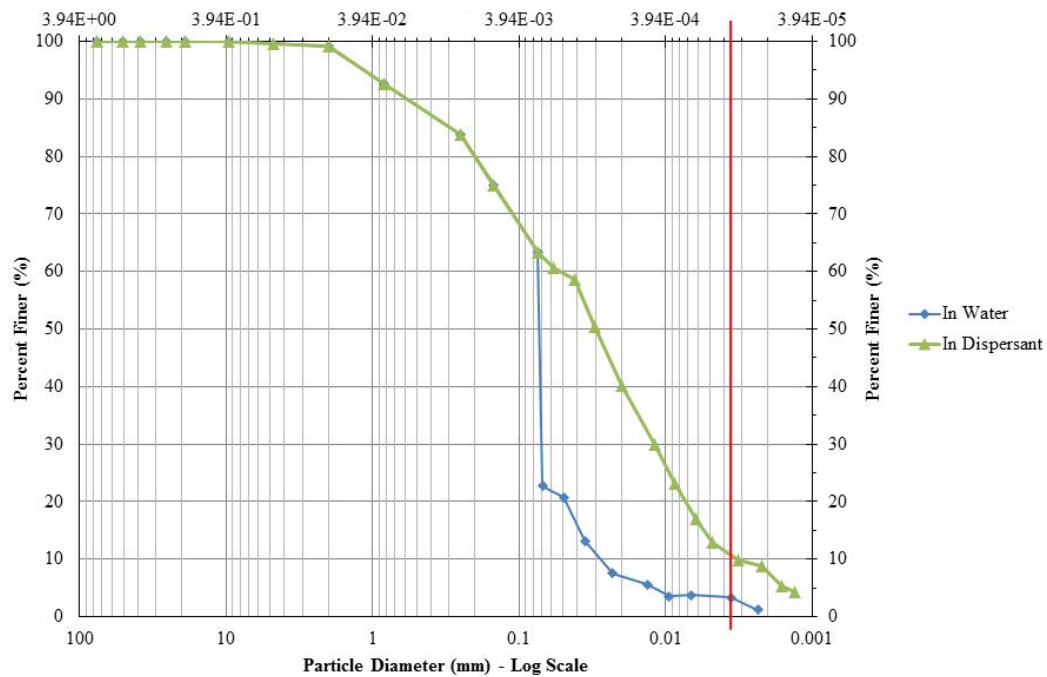


Figure 64. Double hydrometer particle size distributions for alluvial top stratum

Table 21. Double hydrometer test results for alluvial top stratum

Percent Finer than 5- μm in Water Solution	Percent Finer than 5- μm in Chemical Solution	Percent Dispersion
3.5%	13.5%	26%

Modified free swell index test

For this test, 10 grams of oven-dried alluvial top stratum were placed in a graduated cylinder filled with distilled water and allowed to settle for 24 hours. After settling for a period of 24 hours, the final volume of the alluvial top stratum was measured at 12.5 mL (shown in Figure 65). Using Equations 2 and 3 from Chapter 2, the modified free swell index was calculated (with all values shown in Table 22). With a modified free swell index of 2.4, the soil has a negligible swelling potential predicting a nondispersive soil.



Figure 65. Final swell volume for modified free swell test for alluvial top stratum

Table 22. Modified free swell index results for alluvial top stratum

Original Soil Mass (g)	Final Swell Volume (mL)	Modified Free Swell Index
10	12.5	2.4

SEM images

The following images in Figure 66 are presented for an alluvial top stratum sample at increasing magnifications.

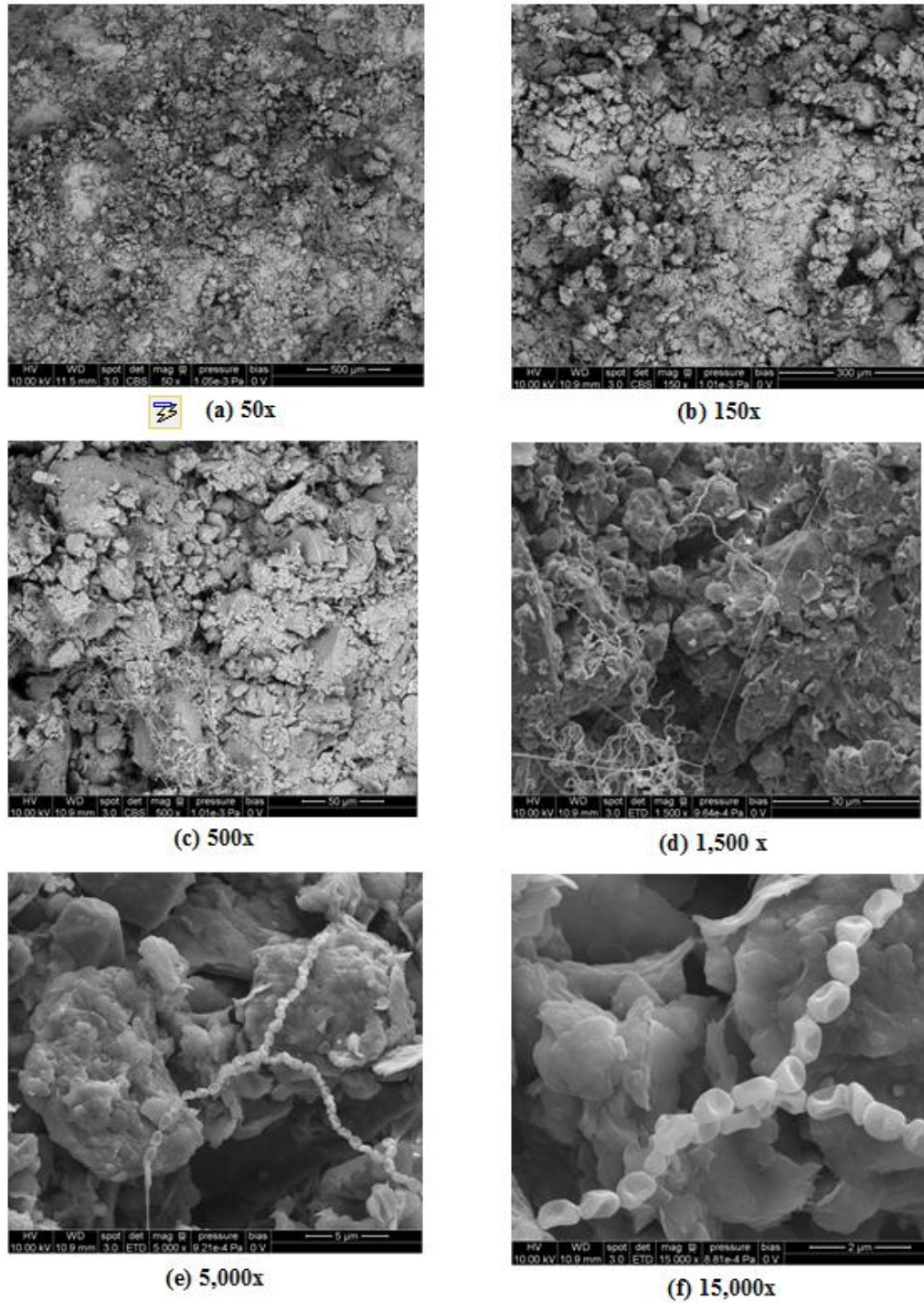


Figure 66. SEM images of alluvial top stratum in order of increasing magnification

Ultimate sample classification

Table 23 presents a summary of the dispersivity classification by test for the alluvial top stratum sample. There was some variance in test results; however, the soil was ultimately classified as a slightly dispersive sample. The percent dispersion calculated from the double hydrometer was 26% which is fairly close to the intermediate degree of dispersion (classified as 30 to 50%). Additionally, at times the crumb test may not provide a reliable resource as some dispersive samples may be classified as nondispersive. Considering the pinhole test is the most reliable, this test result held the most weight in the final determination of the alluvial top stratum showing slightly dispersive tendencies. However, it should be noted the ND4 classification from the pinhole test is the lowest dispersive classification without being completely nondispersive.

Table 23. Summary table of dispersivity tests for alluvial top stratum

Test	Classification
Crumb Test	Nondispersive
Pinhole Test	Slightly Dispersive
Double Hydrometer Test	Nondispersive
Modified Free Swell Index	Nondispersive

Western Iowa loess

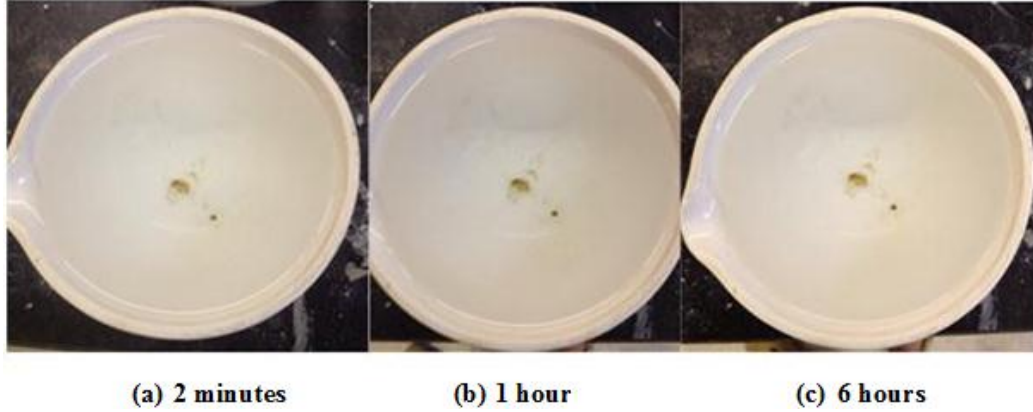
Four dispersion laboratory classification tests were performed on the Western Iowa loess. After the pinhole test, SEM images were also taken of a representative sample.

Crumb test

The following table, Table 24, shows the dispersion grade assigned to the crumb at each time interval. The images shown in Figure 60 are corresponding pictures for each of the readings at increasing time intervals.

Table 24. Crumb test results for Western Iowa loess

Time Interval	Grade	Temperature (°C)
2 min	1	23.8
1 hour	1	23.8
6 hours	1	23.8

**Figure 67. Crumb test for Western Iowa loess at increasing times**

Per the figures above, the soil was classified as Grade 1 Nondispersive at all times. The crumb crumbled with first contact with water; however, it did not interact with the water after that. The Western Iowa loess was thus classified as nondispersive.

Pinhole test

With the pinhole test, the Western Iowa loess was also found to be nondispersive. During the test, the effluent remained clear or barely visible throughout all hydraulic heads (final effluent shown in Figure 68). The test was considered complete after the head had reached its maximum at 40 inches after 25 minutes of run time. The flow rate was still less than 3.0mL/s and the turbidity was barely visible, as such the soil was classified as ND1 Nondispersive. The sample was also extruded after completion and the final flow path did not measure greater than the original drill diameter (shown in Figure 69 and Figure 70). This confirmed the above classification of ND1 Nondispersive.



Figure 68. Effluent from pinhole test for Western Iowa loess



Figure 69. Aerial size of hole after pinhole test completion for Western Iowa loess



Figure 70. Inner size of hole compared with drill needle for Western Iowa loess

Double hydrometer test

The double hydrometer test produced particle size distribution curves (Figure 71) for the Western Iowa loess for a sample in water (blue line) and in a dispersant (green line) are shown below. The red line delineates particles finer than 5- μm . Percent dispersion was calculated with values shown in Table 25 per Equation 1. The calculated percent dispersion being 27% (less than 30% which is considered dispersive), the oxidized till was classified as nondispersive.

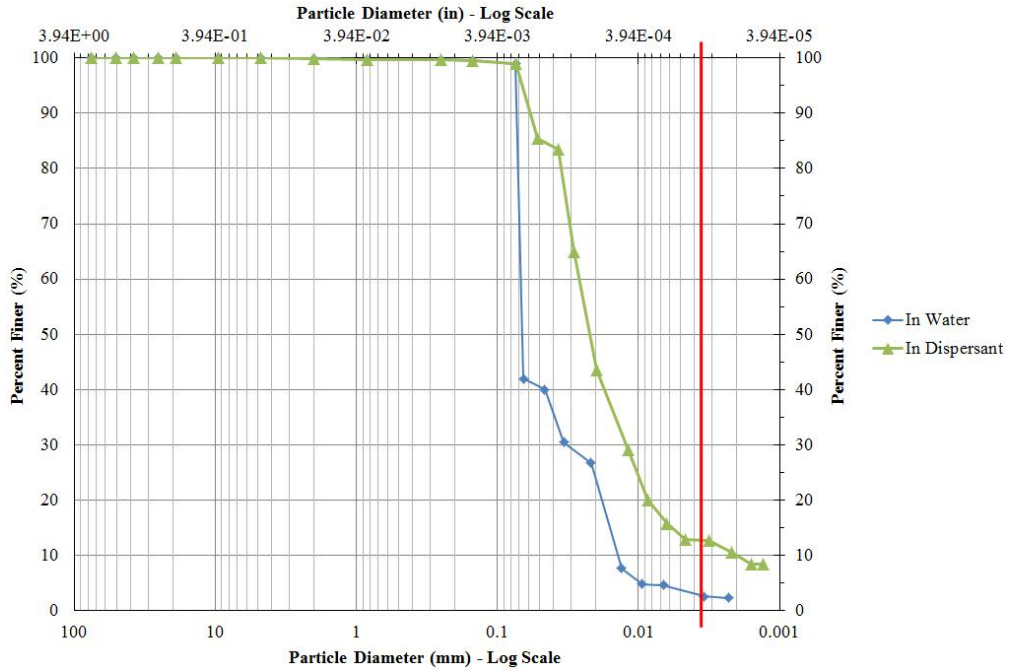


Figure 71. Double hydrometer particle size distributions for Western Iowa loess

Table 25. Double hydrometer test results for Western Iowa loess

Percent Finer than 5- μm in Water Solution	Percent Finer than 5- μm in Chemical Solution	Percent Dispersion
3.7%	13.5%	27%

Modified free swell index test

After 10 grams of oven-dried Western Iowa Loess were placed in a graduated cylinder filled with distilled water, the sample was allowed to sit and settle for 24 hours. After 24 hours, the final volume of the oxidized till was measured at 12 mL (shown in Figure 72). Using the values shown in Table 26 and Equations 2 and 3 from Chapter 2, the modified free swell index was calculated. With a modified free swell index of 2.4, the soil has a negligible swelling potential indicating a nondispersive soil.



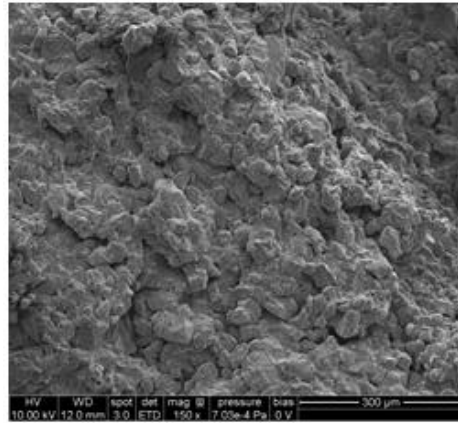
Figure 72. Final swell volume for modified free swell test for Western Iowa loess

Table 26. Modified free swell index results for Western Iowa loess

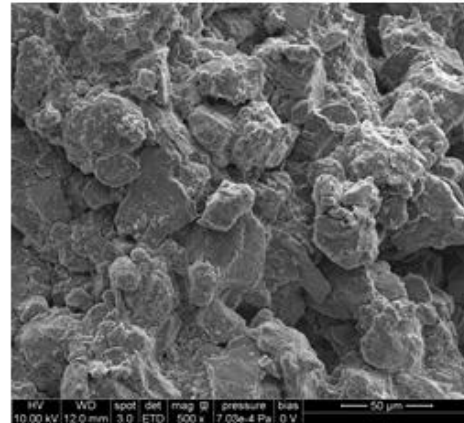
Original Soil Mass (g)	Final Swell Volume (mL)	Modified Free Swell Index
10	12.5	2.4

SEM images

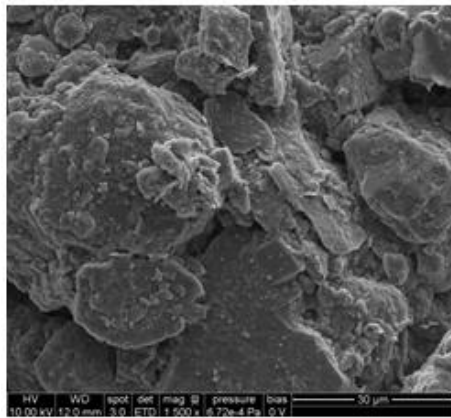
The following images in Figure 66 are presented for a Western Iowa loess sample at increasing magnifications.



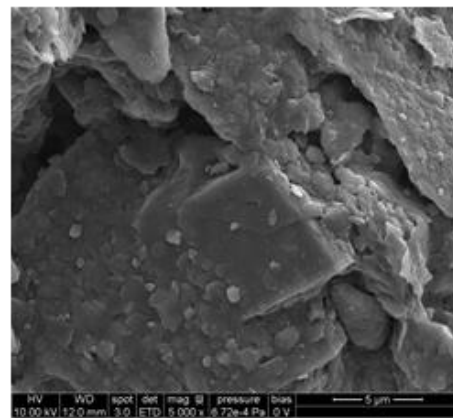
(a) 150x



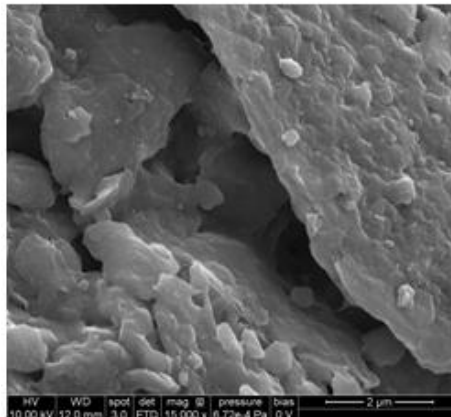
(b) 500x



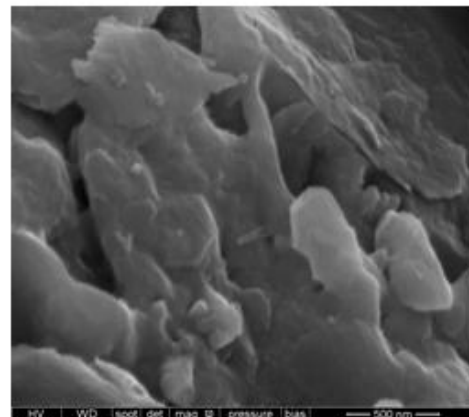
(c) 1,500x



(d) 5,000x



(e) 15,000x



(f) 50,000x

Figure 73. SEM images of Western Iowa loess in order of increasing magnification

Ultimate sample classification

A table summarizing the dispersivity classification by laboratory test is shown below in Table 27. With agreement in all tests, the Western Iowa loess was classified as nondispersive.

Table 27. Summary table of dispersivity tests for Western Iowa loess

Test	Classification
Crumb Test	Nondispersive
Pinhole Test	Nondispersive
Double Hydrometer Test	Nondispersive
Modified Free Swell Index	Nondispersive

Bentonite - untreated

Four dispersion laboratory classification tests were performed on an untreated bentonite sample. SEM imagery was also performed after the pinhole test was complete.

Crumb test

Table 28 below shows the dispersion grade assigned to the crumb at each time interval. The corresponding pictures at increasing time intervals for each reading are shown in Figure 74. Due to the light coloring of the soil, a glass container on a black surface was used in order to determine the appropriate dispersion grade at each reading.

Table 28. Crumb test results for untreated bentonite

Time Interval	Grade	Temperature (°C)
2 min	1	23.2
1 hour	3	23.2
6 hours	3	23

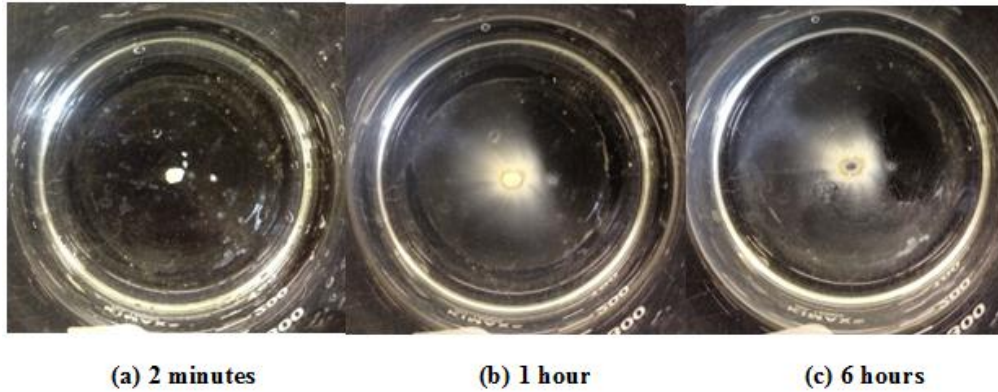


Figure 74. Crumb test for untreated bentonite at increasing times

Per the figures above, the soil was classified as Grade 3 Dispersive. At 1 hour, there appeared to be some interaction with water as a faint cloud can be seen around the crumb. The cloud spread a bit more at 6 hours and the grade increased accordingly, as the cloud surrounded the entirety of the sample. Per the ASTM standard, the untreated bentonite was classified as Grade 3 Moderately Dispersive.

Pinhole test

The untreated bentonite was classified as dispersive after the completion of the pinhole test. At the test onset, the effluent was clear and then quickly increased in discoloration culminating in dark turbidity as shown in Figure 75. The test ran only at a hydraulic head of 2 inches, after 10 minutes the effluent was distinctly dark and the flow rate was between 1.0 to 1.3 mL/s signifying a D2 Dispersive classification. The sample was then extruded and the final hole diameter was examined (Figure 76 and Figure 77, respectively). Upon aerial examination and direct comparison, the hole diameter appears to be 1.5 to 2 times larger than the initial drill. This increased hole size confirms the classification of the soil as D2 Dispersive.



Figure 75. Effluent from pinhole test for untreated bentonite



Figure 76. Aerial size of hole after pinhole test completion for untreated bentonite



Figure 77. Inner size of hole compared with drill needle for untreated bentonite

Double hydrometer test

The particle size curves from the double hydrometer test are shown below in Figure 78. The blue and green lines represent the test performed in water and in a dispersant, respectively. Using the values shown in Table 25, percent dispersion was calculated using Equation 1. The calculated percent dispersion was 66% which classifies the soil as being dispersive.

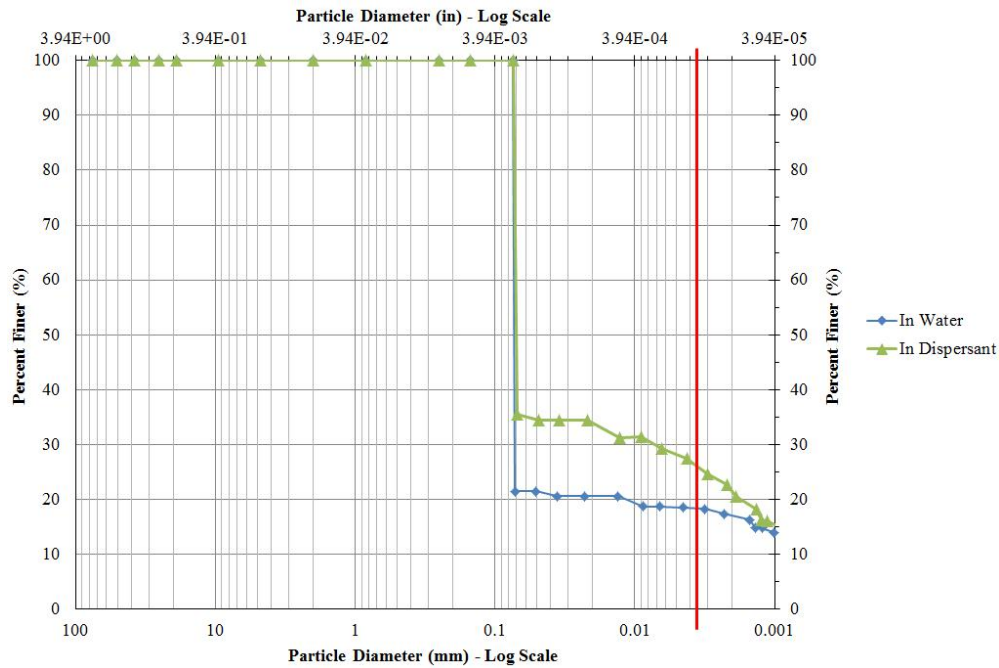


Figure 78. Double hydrometer particle size distributions for untreated bentonite

Table 29. Double hydrometer test results for untreated bentonite

Percent Finer than 5- μm in Water Solution	Percent Finer than 5- μm in Chemical Solution	Percent Dispersion
18.6%	28.1%	66%

Modified free swell index test

For the bentonite sample, only 3 grams of the soil was placed in the cylinder filled with distilled water (for a known expansive soil it was recommended to reduce the sample amount). After settling for 24 hours, the swollen bentonite volume was estimated at 14 mL (shown in Figure 72). Using the values shown in Table 26 and Equations 2 and 3 from Chapter 2, the modified free swell index was calculated to be 10.9. With a this high of an index number, the soil has a high swelling potential predicting a dispersive soil.



Figure 79. Final swell volume for modified free swell test for untreated bentonite

Table 30. Modified free swell index results for untreated bentonite

Original Soil Mass (g)	Final Swell Volume (mL)	Modified Free Swell Index
3	14	10.9

SEM images

The following images in Figure 66 are presented for a untreated bentonite sample at increasing magnifications.

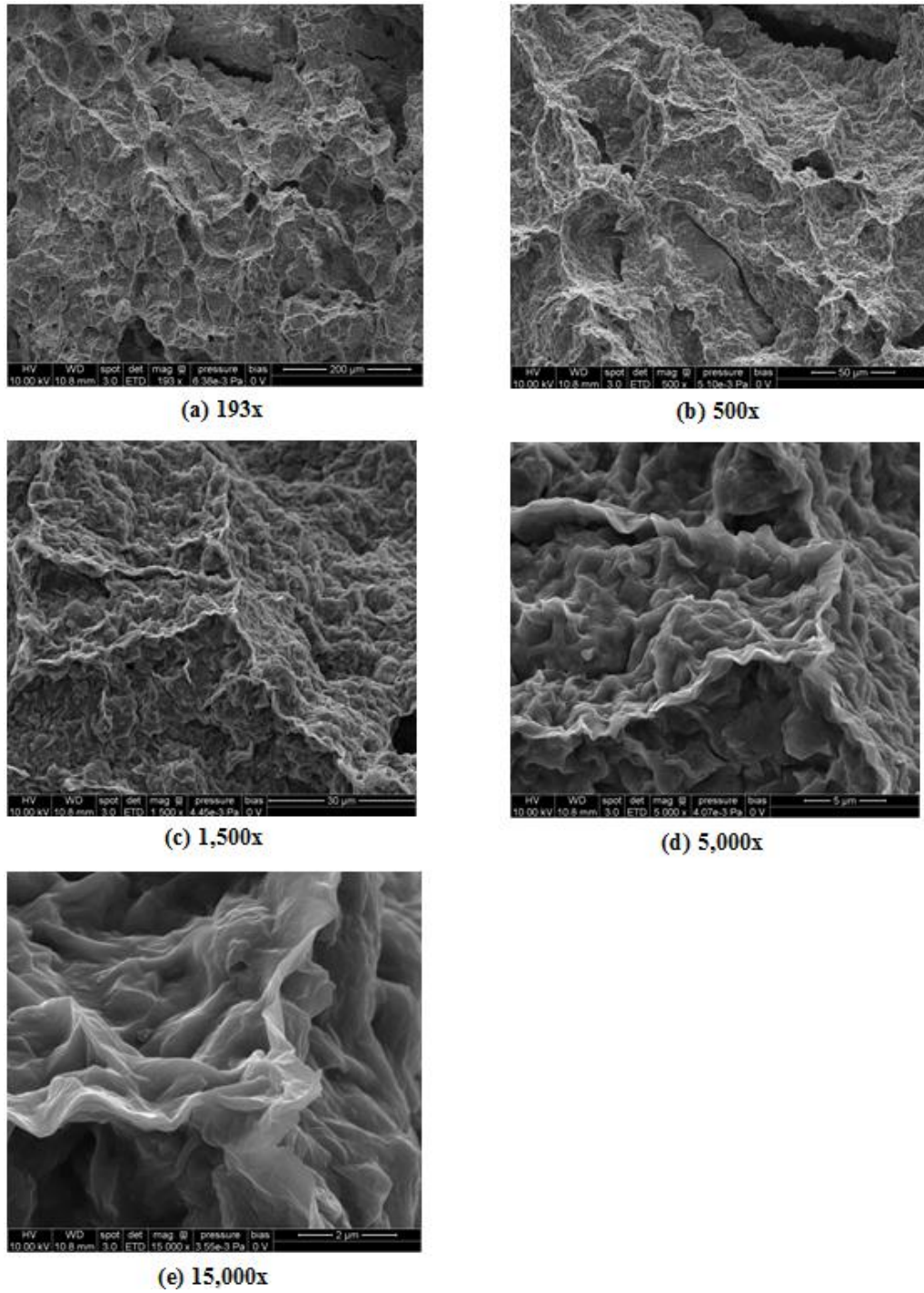


Figure 80. SEM images of untreated bentonite in order of increasing magnification

Ultimate sample classification

Table 31 summarizes the results from the dispersive classification tests. The tests all confirmed the dispersivity of the sample. As such, the untreated bentonite sample was classified as dispersive.

Table 31. Summary table of dispersivity tests for untreated bentonite

Test	Classification
Crumb Test	Dispersive
Pinhole Test	Dispersive
Double Hydrometer Test	Dispersive
Modified Free Swell Index	Dispersive

Bentonite – treated with 4% lime

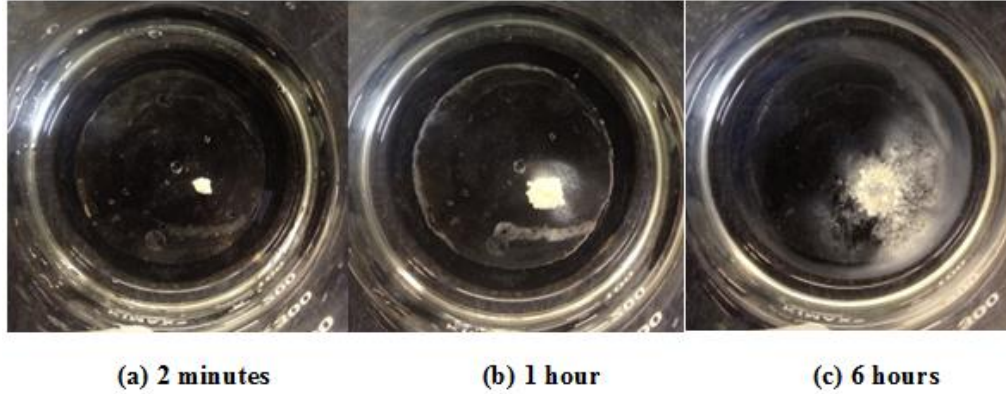
Three dispersion laboratory classification tests were performed on a bentonite sample treated with 4% lime by weight. The double hydrometer test was not performed due to a lack of sufficient sample. Because three other tests would be used to classify the soil, they were considered sufficient to make an educated classification. SEM images are also presented.

Crumb test

The following table shows the dispersion grade assigned to the treated bentonite crumb at each time reading. Figure 81 displays the corresponding pictures for each of the readings at increasing times. Because of the light hue of the soil, a glass container was used on a black surface in order to better view the turbidity from the sample.

Table 32. Crumb test results for treated bentonite

Time Interval	Grade	Temperature (°C)
2 min	1	24
1 hour	2	24
6 hours	2	23.5

**Figure 81. Crumb test for treated bentonite at increasing times**

Initially, the soil was classified as nondispersive as at first, the soil did not interact with the crumb at all. After 1 hour, the sample began to slake and a cloud formed. The cloud however, was very faint and confined to one area. At 6 hours, there seemed to be more interaction with the water but the resulting cloud did not surround the entirety of the crumb but rather seemed concentrated on one side. Based on these criteria, the soil was classified as Grade 2 Intermediate Dispersive.

Pinhole test

The treated bentonite was found to be nondispersive per the pinhole test. From the test beginning to its completion, the effluent was completely clear from the top and side (shown in Figure 82). The test ran for all hydraulic heads in the ASTM standard, in increasing order at 2, 7, 15, and 40 inches. After 20 minutes, the test was considered complete when the flow was nearly clear but the flow rate was greater than 3.0 mL/s. At

this point, the sample was extruded and the hole examined, as shown in Figure 83 and Figure 84. Looking at the figures, the final hole diameter appears to be approximately the same size as the original drill. As such, the bentonite treated with lime was classified as ND2 Nondispersive.



Figure 82. Effluent from pinhole test for treated bentonite



Figure 83. Aerial size of hole after pinhole test completion for treated bentonite



Figure 84. Inner size of hole compared with drill needle for treated bentonite

Modified free swell index test

For the treated bentonite sample, 5 grams of the soil was placed in the cylinder filled with distilled water (the sample was between 3 and 10 grams because it was unknown how the soil would react). After settling for 24 hours, the swollen treated bentonite volume was estimated at 27 mL (shown in Figure 85). The values shown in Table 33 show the values used in calculating the modified free swell index. At an index value of 14.2, this indicates a high swell potential and accordingly, a high likelihood of dispersivity.



Figure 85. Final swell volume for modified free swell test for treated bentonite

Table 33. Modified free swell index results for treated bentonite

Original Soil Mass (g)	Final Swell Volume (mL)	Modified Free Swell Index
5	27	14.2

SEM images

SEM images for a treated bentonite soil are shown below, in order of increasing magnifications, in Figure 86.

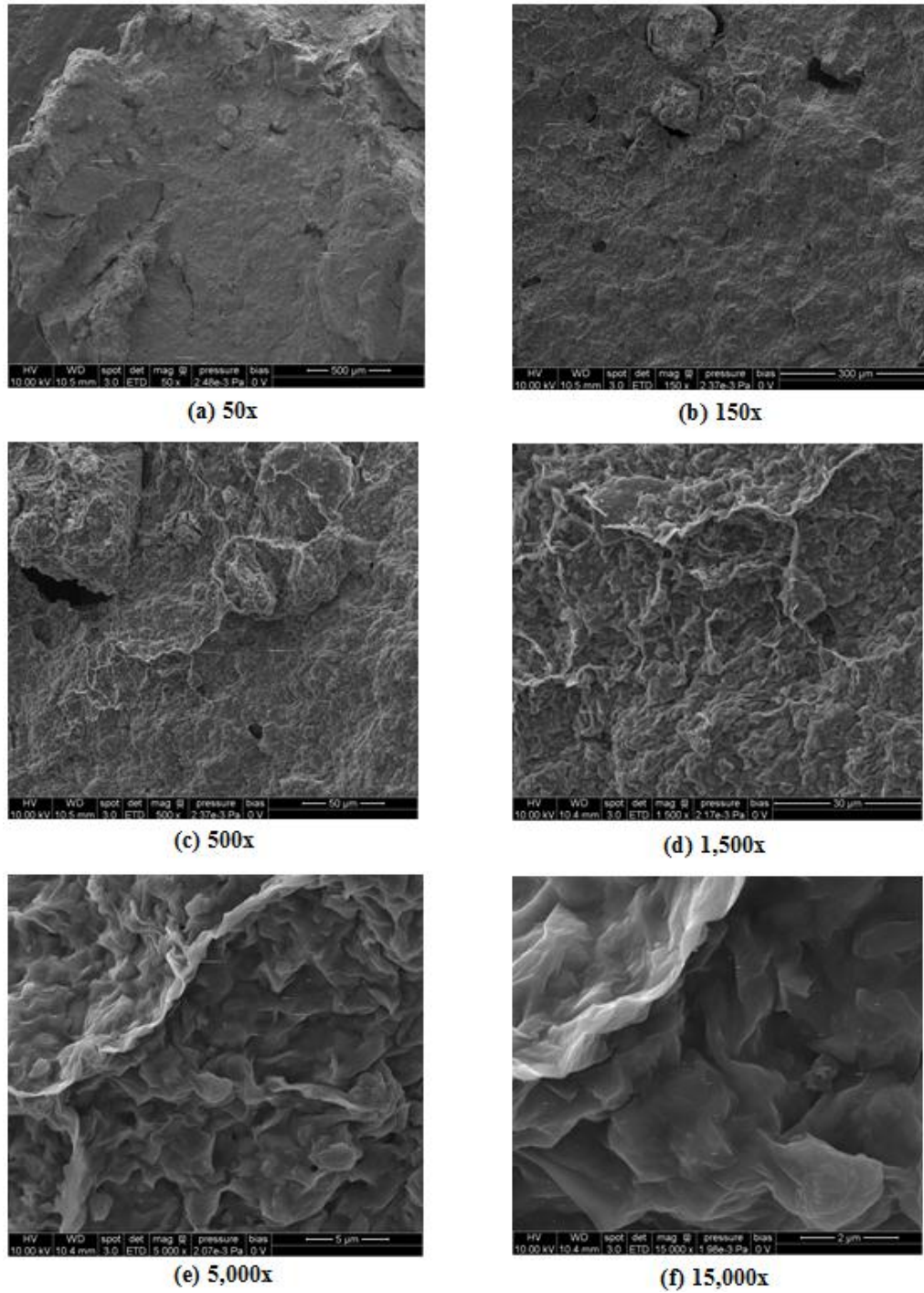


Figure 86. SEM images of treated bentonite in order of increasing magnification

Ultimate sample classification

Table 34 provides a summary of the dispersive classification tests. The tests showed somewhat variable results. The pinhole test is known as the most reliable test and would therefore likely hold the most influence over the final classification. Ultimately, the bentonite with 4% lime was classified as nondispersive due to the strong results from the pinhole test. It is interesting to note though that the lime may not have as large an effect on the sample when immersed in water (crumb test) or over-dried (modified free swell).

Table 34. Summary table of dispersivity tests for treated bentonite

Test	Classification
Crumb Test	Moderately Dispersive
Pinhole Test	Nondispersive
Modified Free Swell Index	Dispersive

Kaolinite

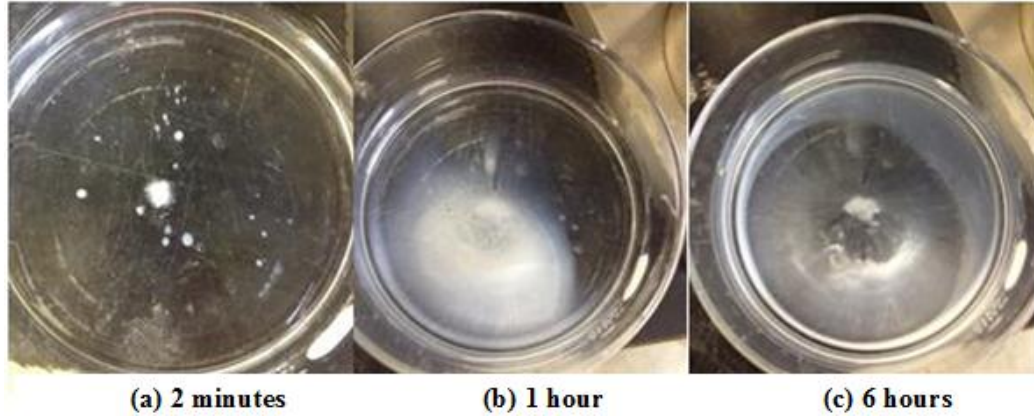
Four dispersion classification tests were conducted on the kaolinite sample. SEM images were also generated after the pinhole test. The following is a presentation of the results.

Crumb test

The following table shows the grade of dispersion at each time interval. Because the sample was white, a clear container was used on a black surface to better see the changes with time. Figure 87 and Table 35 are the corresponding pictures and grades for each of the readings at increasing time intervals.

Table 35. Crumb test results for kaolinite

Time Interval	Grade	Temperature (°C)
2 min	2	22.3
1 hour	3	22.2
6 hours	3	22.2

**Figure 87. Crumb test for kaolinite at increasing times**

Looking at the figures above, the soil was classified as Grade 3 Dispersive. The first reading was a transition grade and at the hour and 6-hour marks the sample appeared to stay somewhat constant. Although the last reading shows a fairly large cloud, it was not considered dense enough to be considered a higher (highly dispersive) grade. The sample was thus classified as Grade 3 Dispersive.

Pinhole test

During the pinhole test, the turbidity was slightly dark initially and only increased as the test progressed. The final turbidity is shown in Figure 88 below. Once the hydraulic head was raised to 7 inches and allowed to run for 5 additional minutes the effluent increased in discoloration and the flow rate increased as well. With a flow rate between 1.4 and 2.7 mL/s and a distinctly dark flow, the test was stopped and tentatively classified as ND3 Moderately Dispersive. The final specimen was then examined using

Figure 89 and Figure 90. From the figures, the hole appeared to be approximately 1.5 diameters of the initial drill. Accordingly, the initial grade was confirmed and the soil was classified as ND3 Moderately Dispersive.



Figure 88. Effluent from pinhole test for kaolinite



Figure 89. Aerial size of hole after pinhole test completion for kaolinite



Figure 90. Inner size of hole compared with drill needle for kaolinite

Double hydrometer test

The particle size distribution curves generated for the kaolinite are shown below in Figure 91 with the blue and green lines representing the analysis in water and dispersant, respectively. The percent dispersion was calculated using the values shown in Table 36. Using those values and Equation 1, the percent dispersion was calculated to be 47%. This value classifies the kaolinite as an intermediately dispersive soil.

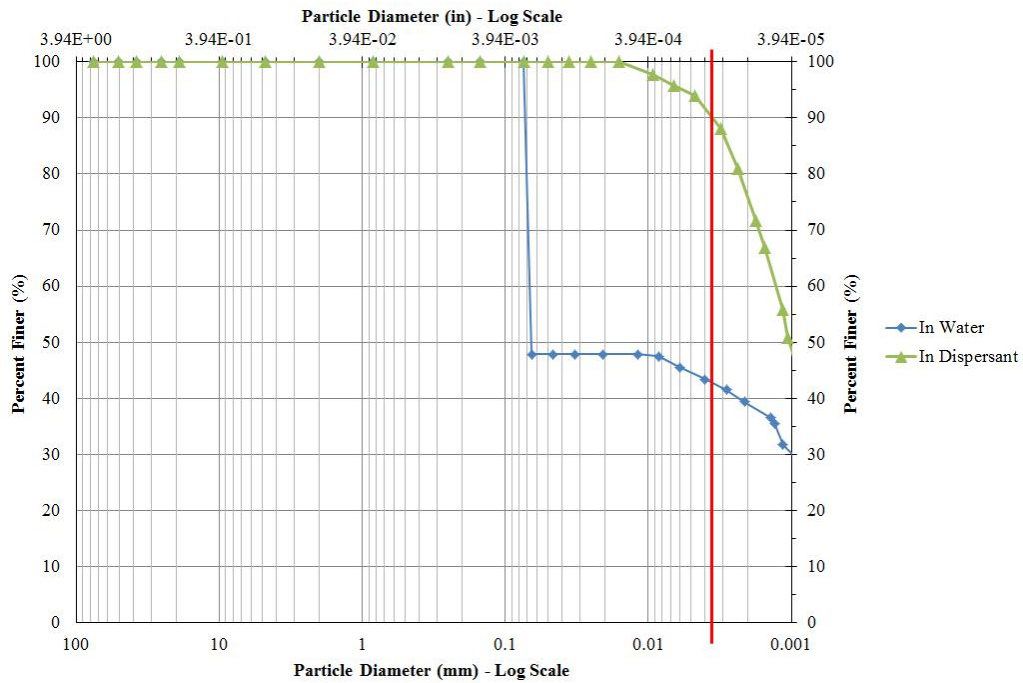


Figure 91. Double hydrometer particle size distributions for kaolinite

Table 36. Double hydrometer test results for kaolinite

Percent Finer than 5-μm in Water Solution	Percent Finer than 5-μm in Chemical Solution	Percent Dispersion
44.5%	94.3%	47%

Modified free swell index test

The modified free swell index was difficult to determine for the kaolinite. Because the particles are so small, the particles take a while to settle. Additionally, the particles are white and create a very milky effluent which makes the final reading difficult to approximate. Nonetheless, 5 grams of the soil was placed in a graduated cylinder and allowed to settle for 24 hours. After 24 hours, the final swell volume was measured at approximately 5 mL (shown in Figure 92). The swell index was then calculated using Equations 2 and 3 and the values shown in Table 37. The modified free swell index was thus found to be 1.7 indicating a negligible swelling behavior.

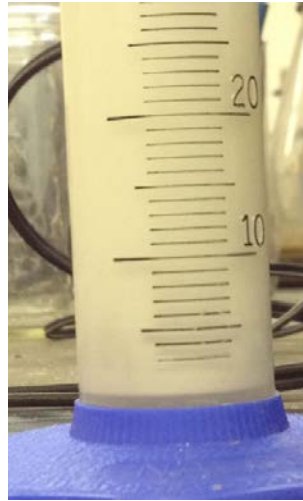
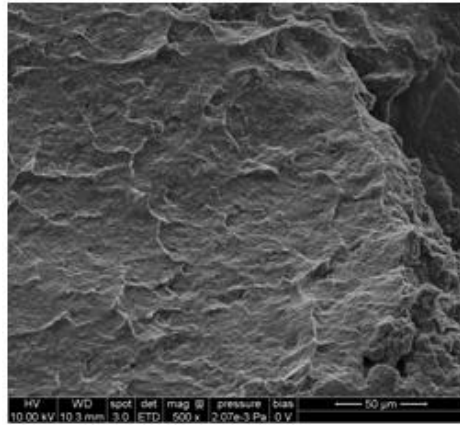
**Figure 92. Final swell volume for modified free swell test for kaolinite**

Table 37. Modified free swell index results for kaolinite

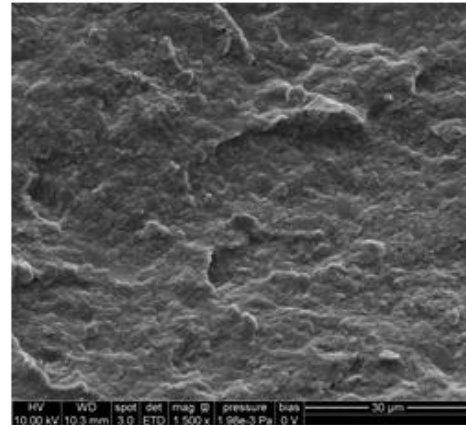
Original Soil Mass (g)	Final Swell Volume (mL)	Modified Free Swell Index
5	5	1.7

SEM images

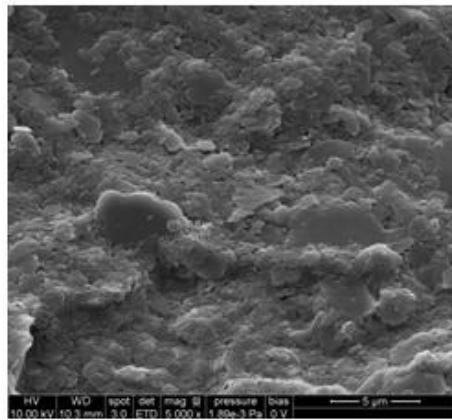
Figure 93 below presents images of a kaolinite sample at increasing magnifications.



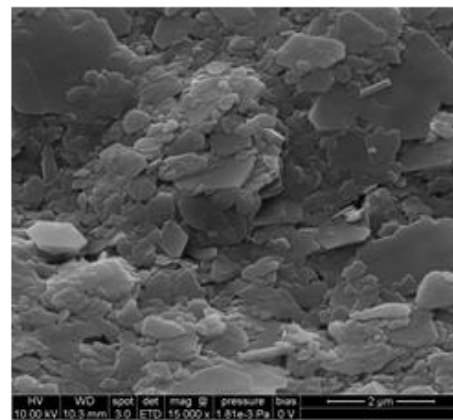
(a) 500x



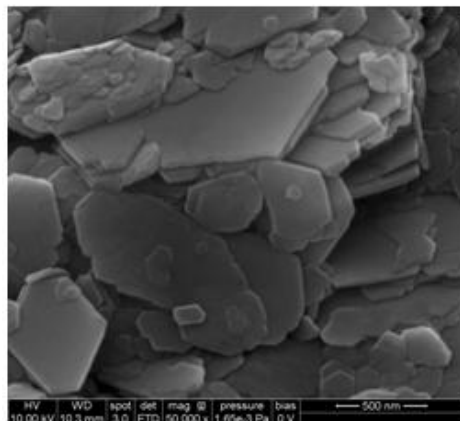
(b) 1,500x



(c) 5,000x



(d) 15,000x



(e) 50,000x

Figure 93. SEM images of kaolinite in order of increasing magnification

Ultimate sample classification

A summary table for the tests performed on kaolinite is presented in Table 38. With agreement in three of the four tests (the three being the primary tests performed in practice) and some difficulty in the one differing result (modified free swell), the kaolinite sample was classified as moderately dispersive.

Table 38. Summary table of dispersivity tests for kaolinite

Test	Classification
Crumb Test	Moderately Dispersive
Pinhole Test	Moderately Dispersive
Double Hydrometer Test	Moderately Dispersive
Modified Free Swell Index	Nondispersive

Santa Rosa clay

The results of four dispersion classification tests performed on the Santa Rosa clay sample are presented below. SEM images of the sample are also shown.

Crumb test

The following table shows the grade of dispersion for the Santa Rosa clay at increasing time recordings. Figure 94 shows corresponding pictures for each of the readings shown in Table 39.

Table 39. Crumb test results for Santa Rosa clay

Time Interval	Grade	Temperature (°C)
2 min	1	23
1 hour	1	23
6 hours	1	23



(a) 2 minutes

(b) 1 hour

(c) 6 hours

Figure 94. Crumb test for Santa Rosa clay at increasing times

Referencing the above figures, the soil was classified as Grade 1 Nondispersive. At all times, the sample appeared a bit crumbled but a lack of cloudiness indicated no interaction with the water. With consistent Grade 1 classifications, the soil was determined to be nondispersive per the crumb test.

Pinhole test

At the beginning of the pinhole test, the flow was distinctly slow and the hole had to be re-punched in order to ensure flow was occurring. Once flow began, the effluent was immediately determined to be moderately dark (Figure 95). With increasing the hydraulic head from 2 to 7 inches, the flow rate increased to a value between 1.4 and 2.7 mL/s. At this rate and with the discoloration of the discharge being distinctly dark, the test was stopped and the specimen was observed. Once extruded, the hole diameter was measured as approximately 2 times the initial drill diameter (seen in Figure 96 and Figure 97). With all the factors (high flow rate, dark turbidity, and increased hole diameter), the soil was classified as ND3 Moderately Dispersive.



Figure 95. Effluent from pinhole test for Santa Rosa clay



Figure 96. Aerial size of hole after pinhole test completion for Santa Rosa clay



Figure 97. Inner size of hole compared with drill needle for Santa Rosa clay

Double hydrometer test

The particle size distribution curves generated for the Santa Rosa clay (Figure 98) are shown below for a sample in water and in dispersant, blue and green lines, respectively. The percent dispersion was calculated using Table 40. Using those values and Equation 1, the percent dispersion was calculated to be 21% classifying the soil as

nondispersive. In the original HWS, Inc. report (1977) on the Santa Rosa clay, this test was also performed and this particular sample exhibited 31% dispersivity.

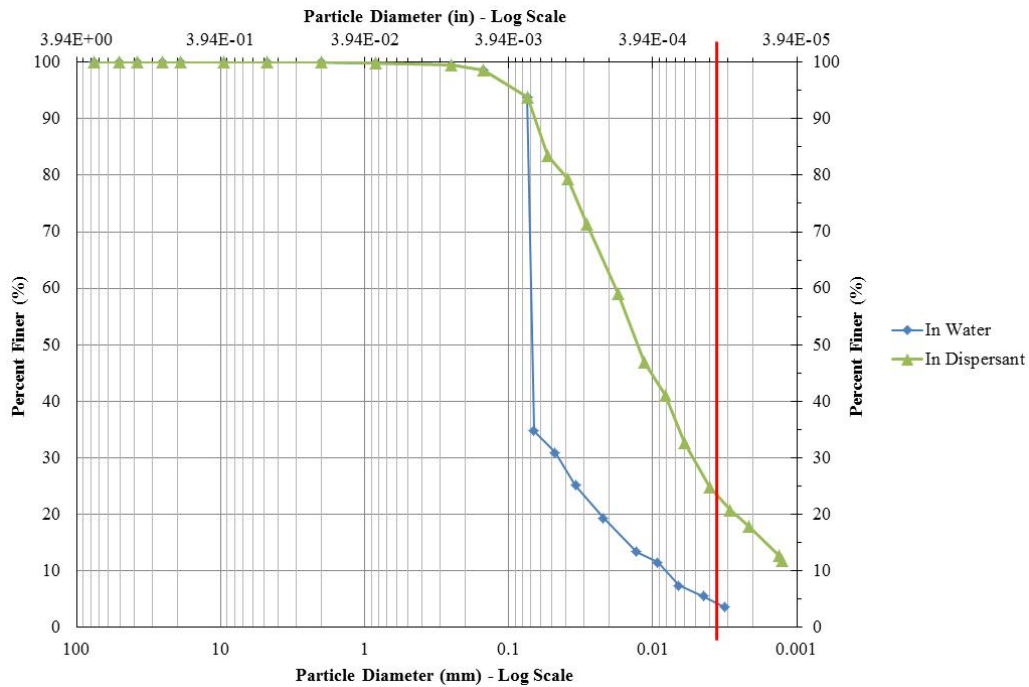


Figure 98. Double hydrometer particle size distributions for Santa Rosa clay

Table 40. Double hydrometer test results for Santa Rosa clay

Percent Finer than 5- μ m in Water Solution	Percent Finer than 5- μ m in Chemical Solution	Percent Dispersion
6.0%	28.8%	21%

Modified free swell index test

A 10 gram sample of Santa Rosa clay was placed in a graduated cylinder filled with distilled water. After settling for 24 hours, the swollen volume was approximated at 13 mL (shown in Figure 99). This value was then used to calculate the modified free swell index as shown in Table 41. This value was found to be the delineation between classifying the soil as having negligible and moderate swell potential. At 2.5, the Santa

Rosa clay was determined to have moderate swell potential which predicts moderately dispersive behavior.

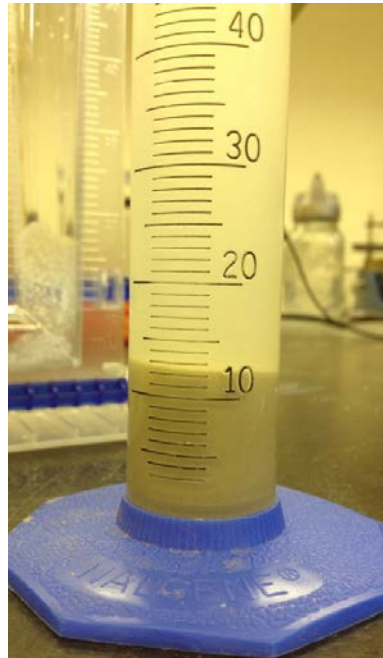


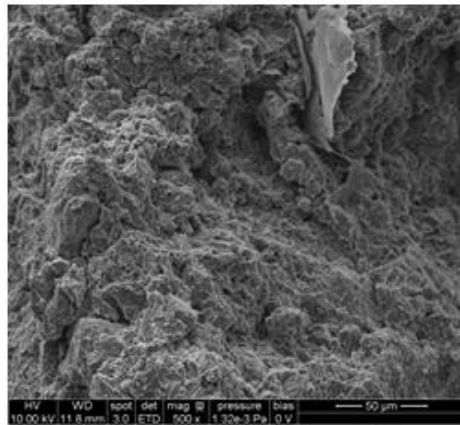
Figure 99. Final swell volume for modified free swell test for Santa Rosa clay

Table 41. Modified free swell Index results for Santa Rosa clay

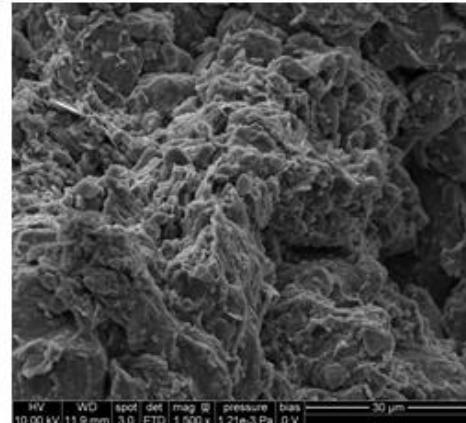
Original Soil Mass (g)	Final Swell Volume (mL)	Modified Free Swell Index
10	13	2.5

SEM images

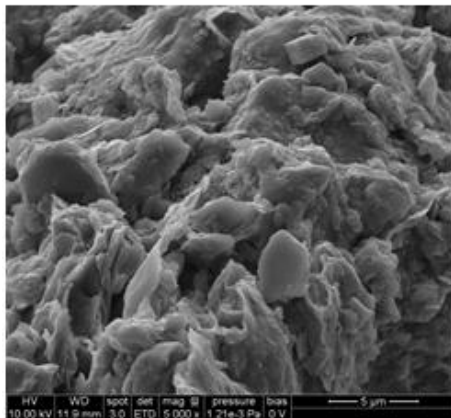
Figure 93 below presents SEM images of a Santa Rosa clay sample at increasing magnifications.



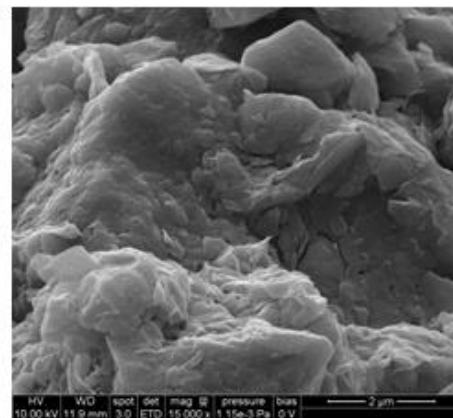
(a) 500x



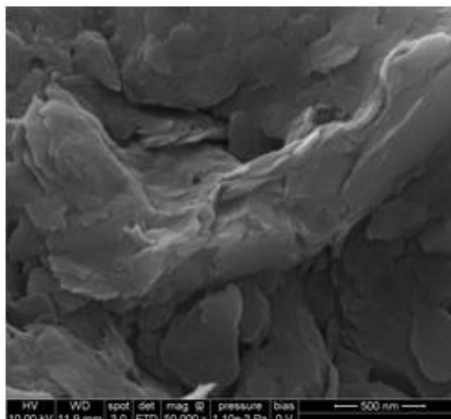
(b) 1,500x



(c) 5,000x



(d) 15,000x



(e) 50,000x

Figure 100. SEM images of Santa Rosa clay in order of increasing magnification

Ultimate sample classification

A summary table for all classification tests on the Santa Rosa clay is presented below in Table 42. As shown, the tests show some inconsistency. The pinhole test, which is the most reliable, found the test to be moderately dispersive. The crumb test indicated a nondispersive soil. However, this test is known to have limited success and has occasionally classified a dispersive soil as nondispersive. The modified free swell index found the soil to have intermediate swelling potential and, using above results on natural soil, this test seems to correlate well with predicting dispersivity.

The double hydrometer dispersivity percentage was 21%, well under the intermediate dispersive classification at 30%. It is interesting to note though that the report performed by HWS, Inc. (1977) found this sample to have a dispersion percentage of 31% indicating intermediate dispersivity; however, no other dispersion classification test was performed to confirm this classification. Although the test was performed over 30 years ago and the standard practices may have changed a bit, the original percent dispersivity was determined on a soil sample in a relatively undisturbed state, compared to its present condition. As such, when this test is considered in the classification, the Santa Rosa clay is moderately dispersive.

Table 42. Summary table of dispersivity tests for Santa Rosa clay

Test	Classification
Crumb Test	Nondispersive
Pinhole Test	Moderately Dispersive
Double Hydrometer Test (2013)	Nondispersive
Double Hydrometer Test (1977)	Moderately Dispersive
Modified Free Swell Index	Moderately Dispersive

Sodium illite - untreated

Dispersion classification tests results for an untreated sodium illite are presented below. SEM images of the sample are also shown.

Crumb test

The table below (Table 43) shows the grade of dispersion at each corresponding time interval for the untreated sodium illite. The images in Figure 101 present corresponding pictures for each of the readings with increasing time.

Table 43. Crumb test results for sodium illite

Time Interval	Grade	Temperature (°C)
2 min	1	22.3
1 hour	2	22.4
6 hours	3	22.3

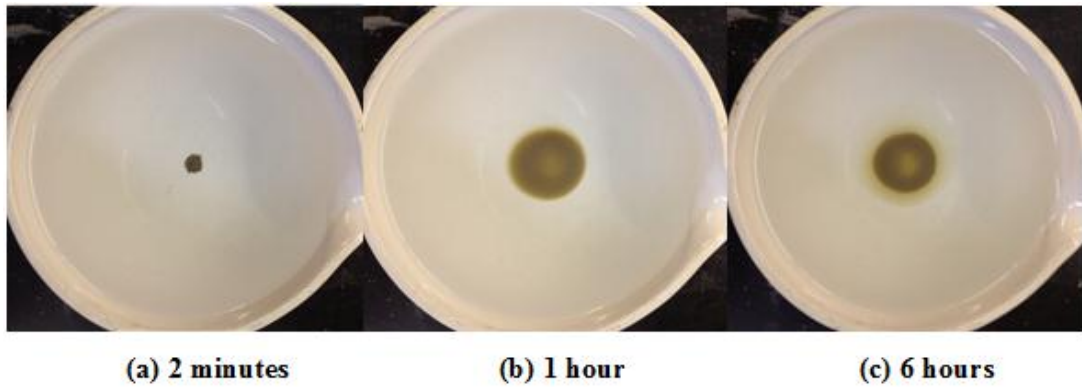


Figure 101. Crumb test for sodium illite at increasing times

Referencing the above figures, the soil was classified as Grade 1 Nondispersive initially with an increasing grade at the next reading. At 1 hour, a barely visible cloudy surface surrounded the soil sample. After 6 hours, the cloud became more pronounced and easier to see. It was thus assigned a higher grade. This classified the sample as Grade 3 Dispersive.

Pinhole test

Once water began flowing through the soil sample, the effluent became increasingly dark with time (shown in Figure 102). After running for 10 minutes under 2 inches hydraulic head, the flow rate was too slow to be classified as dispersive and the

head was raised 5 inches to 7 inches. At this increased head, the flow rate increased accordingly until after 15 minutes of total run time the test was stopped when the flow rate ran between 1.4 and 2.7 mL/s. With this high rate and dark effluent, the final specimen hole was examined as shown in Figure 103 and Figure 104. The specimen hole appeared quite eroded and had a diameter at least 1.5 diameters greater than the initial hole punch. Accordingly, the sample was classified as ND3 Moderately Dispersive.



Figure 102. Effluent from pinhole test for sodium illite



Figure 103. Aerial size of hole after pinhole test completion for sodium illite



Figure 104. Inner size of hole compared with drill needle for sodium illite

Double hydrometer test

Figure 105 below shows the complete particle size distribution generated from the double hydrometer test for the sodium illite sample. The blue and green line represent the distribution in water and dispersant, respectively. Table 44 shows the values obtained from the graph of particles smaller than 5- μm (marked by the red line). Using Equation 1, the percent dispersion was 39% indicating an intermediately dispersive soil.

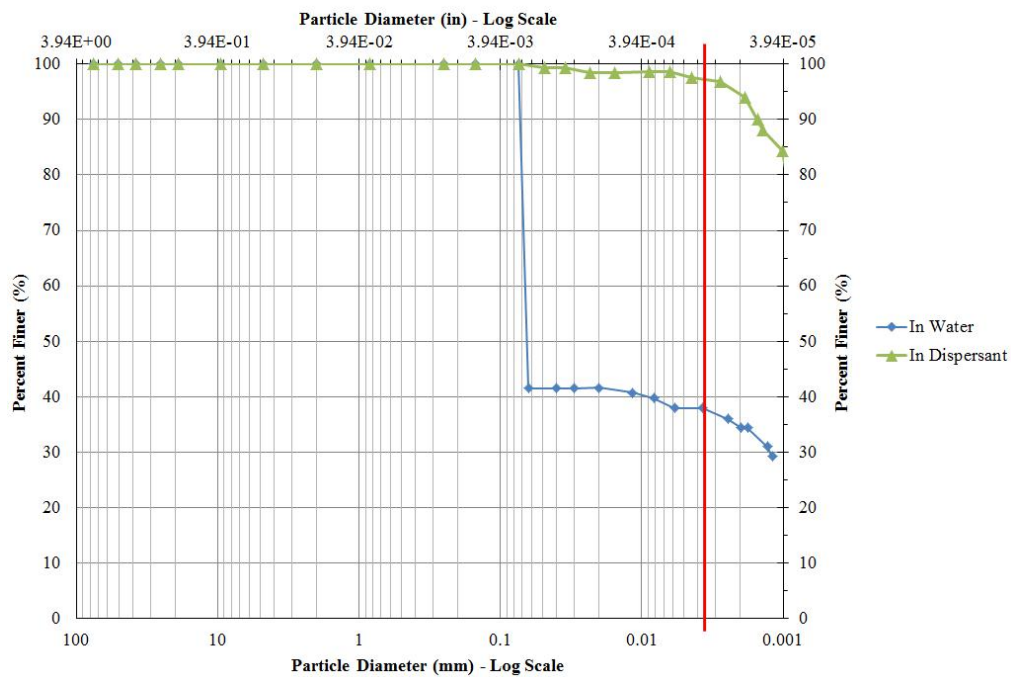


Figure 105. Double hydrometer particle size distributions for sodium illite

Table 44. Double hydrometer test results for sodium illite

Percent Finer than 5-μm in Water Solution	Percent Finer than 5-μm in Chemical Solution	Percent Dispersion
37.9%	97.8%	39%

Modified free swell index test

For the sodium illite free swell test, 5 grams of the sample was used (due to suspicions of the soil being highly expansive). The swollen volume after 24 hours was estimated at 19 mL (shown in Figure 106). This value was recorded in Table 45 and used to calculate the modified free swell index. With an index value of 9.7, the sodium illite was found to have moderate tendencies. It should be noted however, the boundary between moderate and high swell potential is 10.0. Using the value of 9.7, the sample was subject to moderate swelling and was classified as moderately dispersive.

**Figure 106. Final swell volume for modified free swell test for sodium illite**

Table 45. Modified free swell index results for sodium illite

Original Soil Mass (g)	Final Swell Volume (mL)	Modified Free Swell Index
5	19	9.7

SEM images

The sodium illite sample images are presented below in order of increasing magnitude in Figure 107 and Figure 108.

Unfortunately, the first images produced (in Figure 107) were determined to be not the most accurate depictions of the soil substructure. Because the soil was soaked in a sodium chloride solution, the SEM images only show the salt crystals that had formed on the sample. Once this was realized, the remaining soil sample was placed in dialysis tubing and set in a container of distilled water. The idea behind this is that the soil inside the dialysis tubing will try to reach equilibrium and the salt in the soil sample will diffuse outward into the water. The water is replenished often to instigate this movement across the membrane (Van Olphen, 1977).

To perform dialysis on the sample and clean the soil, the sample sat in the water solution for a week with the water being replaced often. After that time the soil was removed from the tube, dried, and then half was treated with lime. The images produced after this process are shown in Figure 108. Comparing the images, the salt crystals have been washed from the sample and the substructure shape can be seen much more easily.

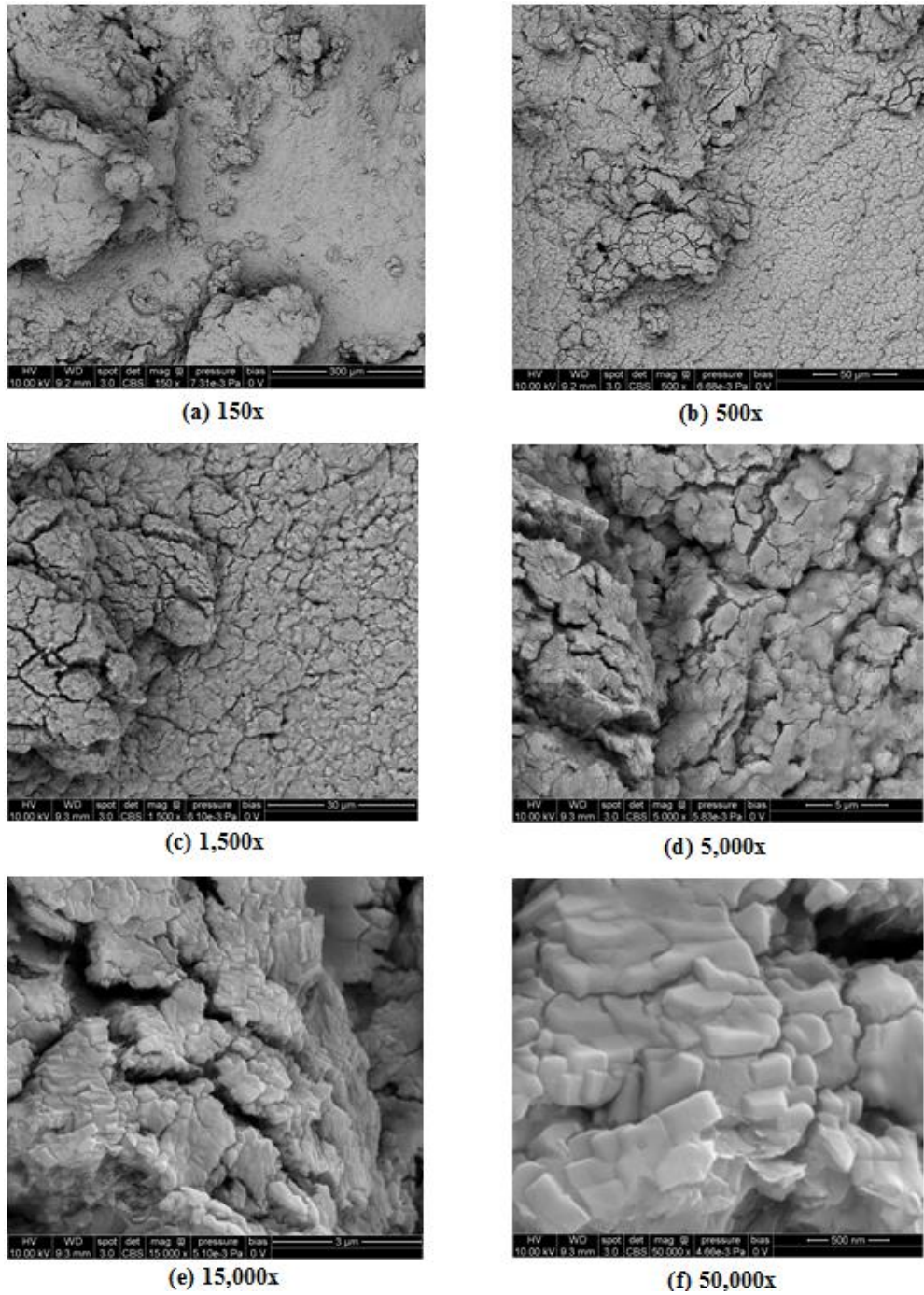


Figure 107. SEM images of sodium illite with salt by increasing magnification

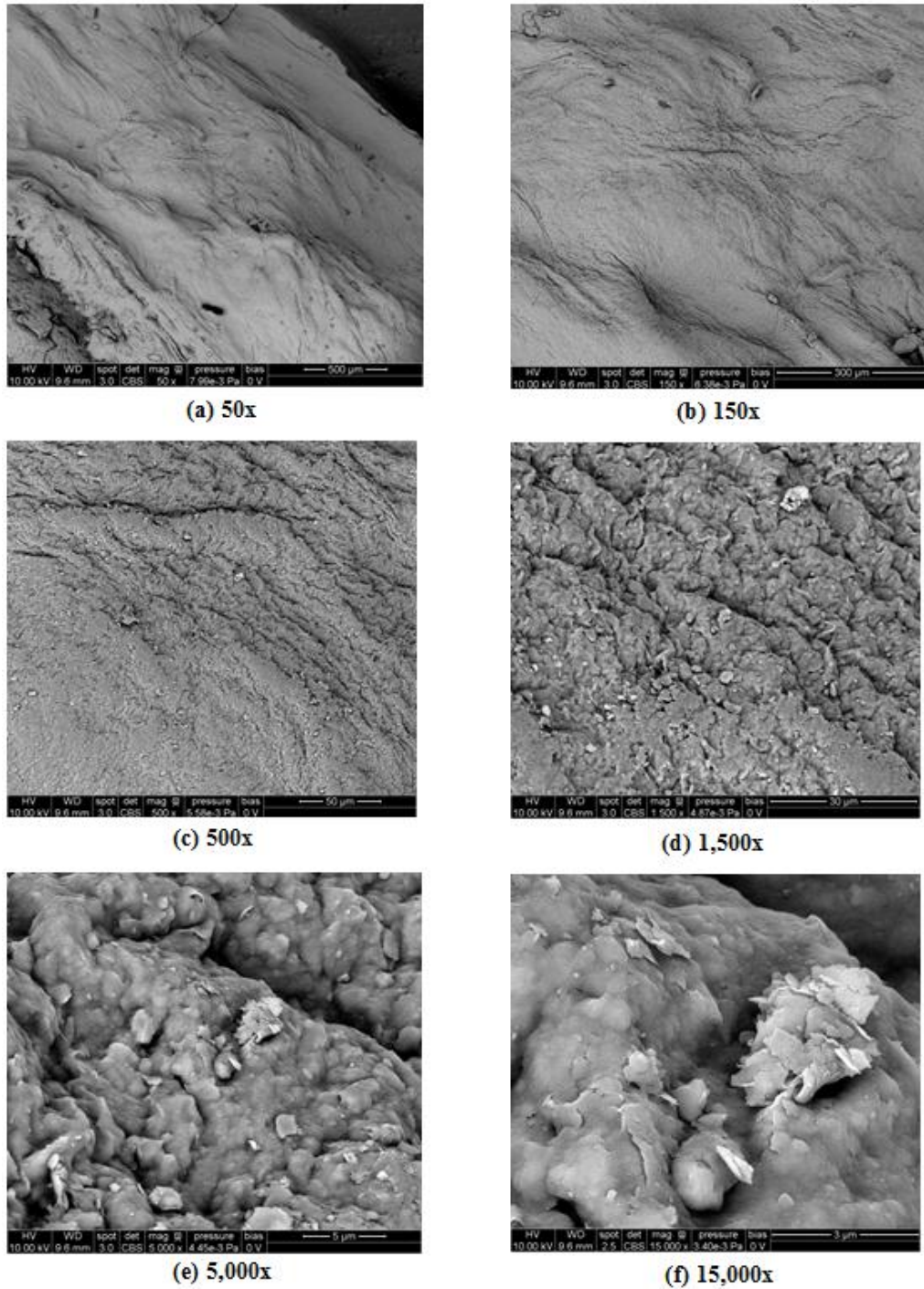


Figure 108. SEM images of sodium illite without salt by increasing magnification

Ultimate sample classification

Table 46 presents a summary of all the classification tests performed on the sodium illite. All the tests classified the sample as moderately dispersive; accordingly, the sodium illite was classified as such.

Table 46. Summary table of dispersivity tests for sodium illite

Test	Classification
Crumb Test	Moderately Dispersive
Pinhole Test	Moderately Dispersive
Double Hydrometer Test	Moderately Dispersive
Modified Free Swell Index	Moderately Dispersive

Sodium illite – treated with 4% lime

Three dispersion laboratory classification tests were performed on a sodium illite sample treated with 4% lime. The fourth test usually performed, the double hydrometer test, was not performed due to a lack of sufficient sample. Because three other reliable tests would be used to classify the soil, they were considered sufficient to make an adequate classification. SEM images of the treated sample are also presented.

Crumb test

Table 47 shows the dispersion grade for a treated sodium illite crumb and increasing time intervals. The corresponding images are shown in Figure 109.

Table 47. Crumb test results for treated sodium illite

Time Interval	Grade	Temperature (°C)
2 min	1	22.3
1 hour	1	22.4
6 hours	1	22.3

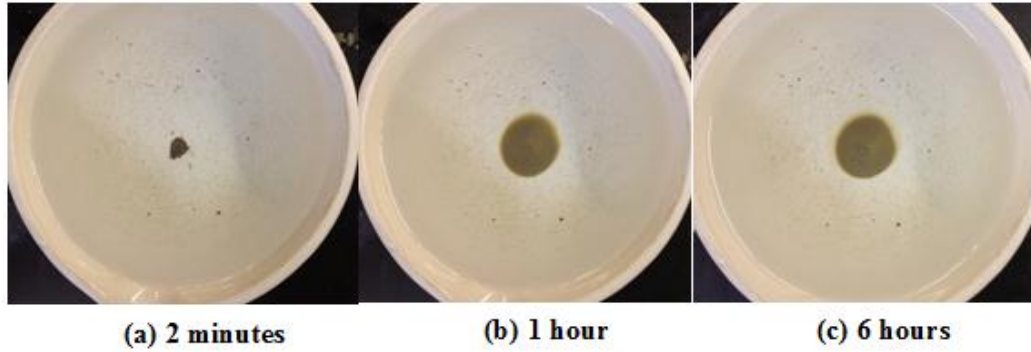


Figure 109. Crumb test for treated bentonite at increasing times

Per the figures above, the soil was classified as Grade 1 Nondispersive at all times. After 1 hour, the sample diffused quite a bit; however, no cloud appeared around the crumb. At 6 hours, a slight cloud is observed but as it is barely visible the sample kept its Grade 1 Nondispersive classification. With consistent grades, the treated sodium illite was classified as nondispersive.

Pinhole test

The treated sodium illite was classified as nondispersive from the pinhole test. The effluent from the test was barely visible throughout the entirety of the test (as seen in Figure 110). The test ran for all hydraulic heads as specified in the ASTM standard, in increasing order at 2, 7, 15, and 40 inches. After 25 minutes, the test was stopped when the flow exceeded 3.0 mL/s. The specimen was then extracted and the final hole diameter was observed (shown below in Figure 111 and Figure 112). Using the figures, the hole remained intact throughout the test and was about the same size as the initial drill. Under these criteria, the soil was classified as ND2 Nondispersive.



Figure 110. Effluent from pinhole test for treated sodium illite

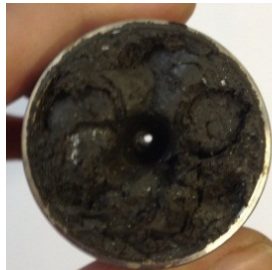


Figure 111. Aerial size of hole after pinhole test completion for treated sodium illite



Figure 112. Inner size of hole compared with drill needle for treated sodium illite

Modified free swell index test

For the treated sodium illite, 3 grams of the soil was used for the modified free swell index test. The sample was inserted in a cylinder filled with distilled water and allowed to settle for 24 hours. After this time period, the swollen volume (shown below

in Figure 113) was estimated at 9 mL. Comparing this value with the original mass, as displayed in Table 48, the modified free swell index was found to be 7.5 indicating both a moderate swell potential and moderate likelihood of dispersive behavior

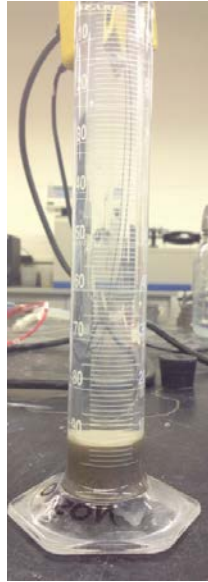


Figure 113. Final swell volume for modified free swell test for treated sodium illite

Table 48. Modified free swell index results for treated sodium illite

Original Soil Mass (g)	Final Swell Volume (mL)	Modified Free Swell Index
3	9	7.5

SEM images

The SEM images generated for a treated sodium illite soil are shown below, in order of increasing magnifications, in Figure 114.

As discussed in the previous section on the untreated bentonite, the first images taken (Figure 114) were not representative of the sample. As such, the soil was cleaned through dialysis and the images in Figure 115 were generated. In this images there are no longer salt crystals inundating the surface. The particle associations can be observed better and a more accurate comparison can be made using the soil structure.

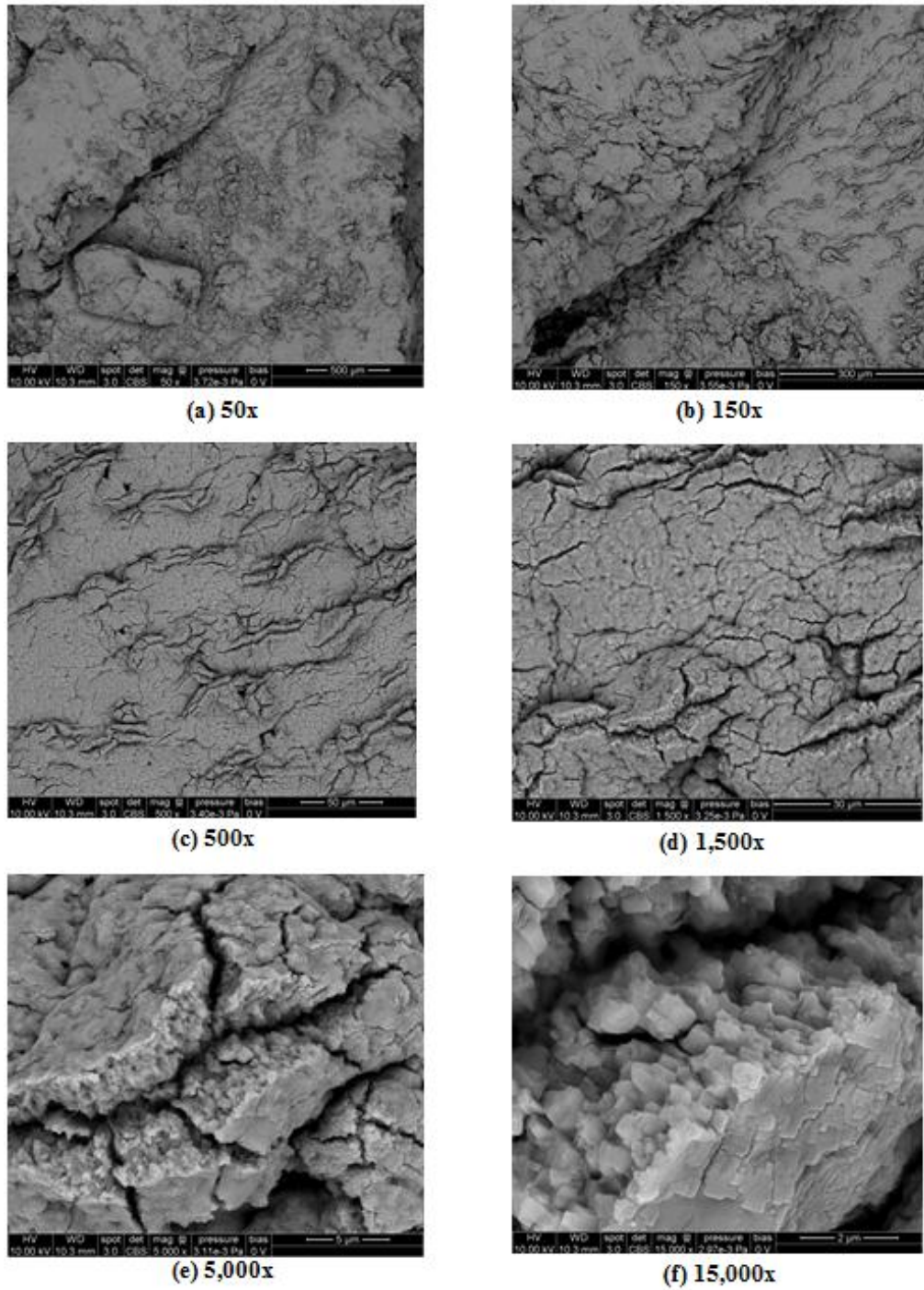
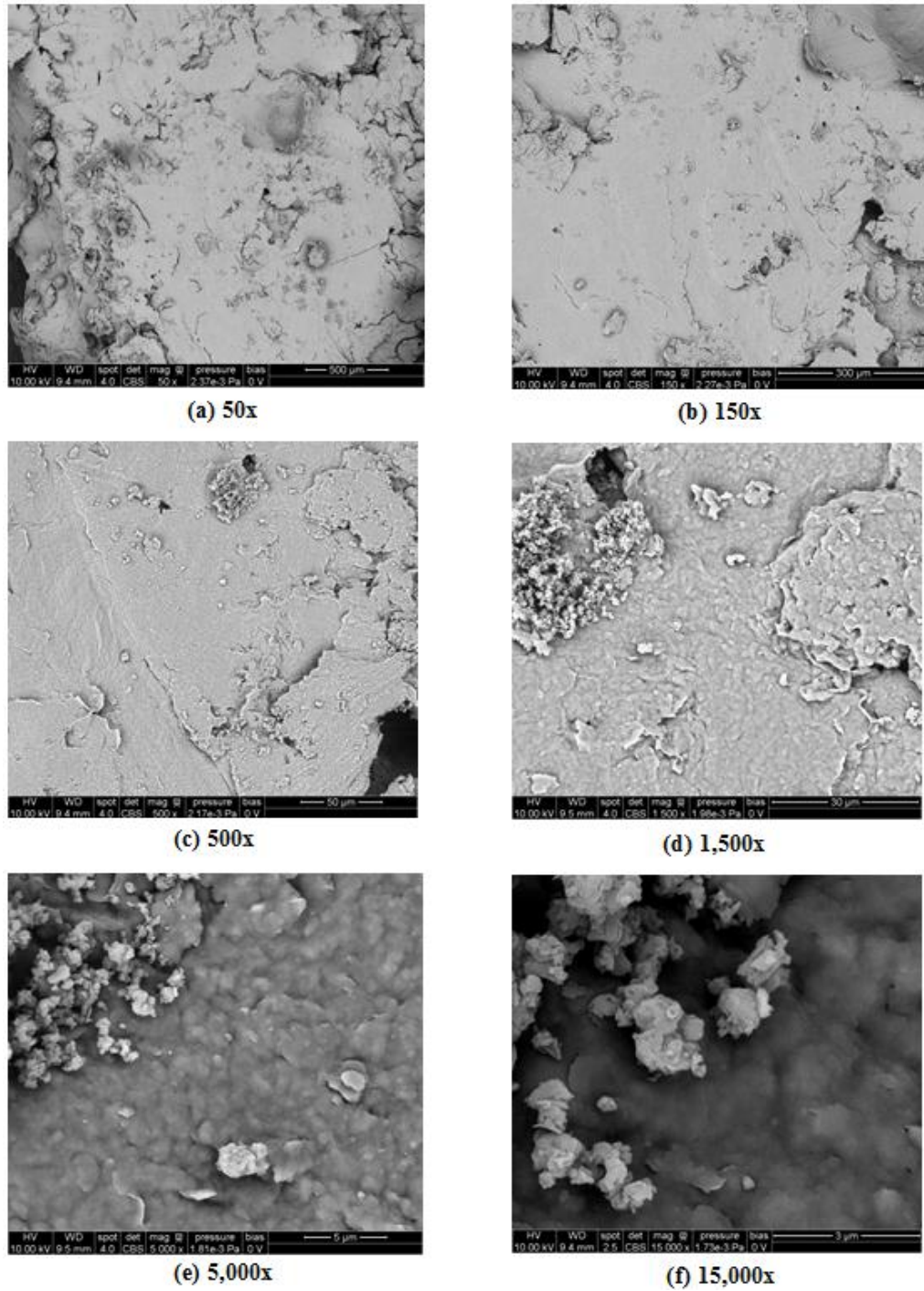


Figure 114. SEM images of treated sodium illite with salt; increasing magnification



Ultimate sample classification

Table 49 provides a summary of the dispersive classification tests performed on the treated sodium illite. The tests showed somewhat variable results. If the modified free swell index is ignored, the pinhole and crumb test provide a fairly sound classification. Using those two, the soil can be classified as nondispersive.

Table 49. Summary table of dispersivity tests for treated sodium illite

Test	Classification
Crumb Test	Nondispersive
Pinhole Test	Nondispersive
Modified Free Swell Index	Moderately Dispersive

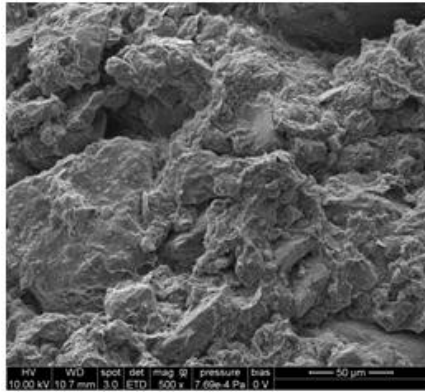
Discussion of SEM images by classification

This section provides a detailed comparison of the SEM images of the samples by their classification type. For the purpose of comparisons, the samples are all compared at a magnification of 500x. A magnification of 500x was chosen due to previous work performed by other researchers. Additionally, at this magnification the soil structure and larger interactions could best be seen and described. It should also be noted, the sodium illite images used are the cleaned samples after dialysis. The substructure on this images can be seen better.

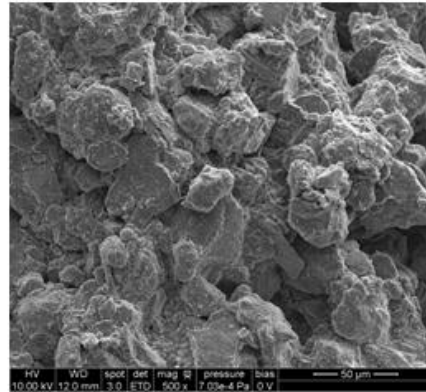
The samples were separated based on their final classification and are discussed in the following order of increased dispersivity: nondispersive, slightly to moderately dispersive, and dispersive.

Nondispersive soil images

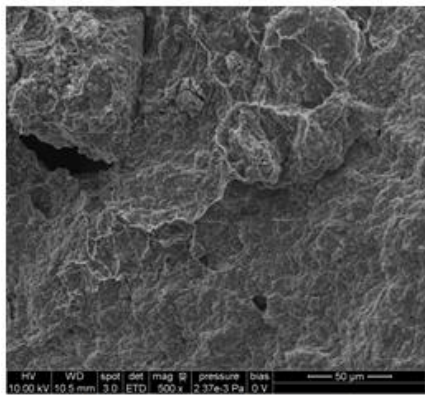
The soils classified as nondispersive included the oxidized glacial till, loess, bentonite treated with lime, and sodium illite treated with lime. The SEM images of these samples at 500x magnification are shown below in that same order in Figure 116.



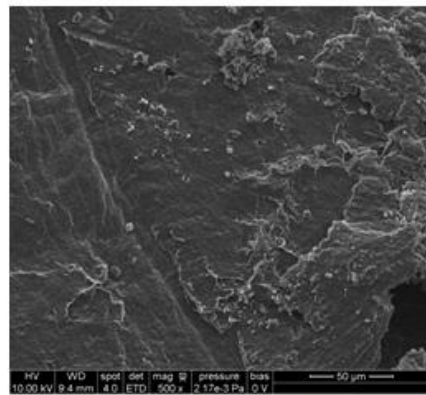
(a) Oxidized glacial till



(b) Western Iowa loess



(c) Bentonite with 4% lime



(d) Sodium Illite with 4% lime

Figure 116. SEM images of clays classified as nondispersive

As discussed earlier in Chapter 2, in a nondispersed clay SEM image, there should be no set particle orientation and a multitude of edges, planes, and cavities in every direction (Sides and Barden, 1971). All the above images seem to display these characteristics. One can pick out cavities easily in all of the images above. Additionally, although the surfaces appear rather rough, the particles are well aggregated in easy to spot masses. The flocs can be seen forming tight edge-to-face (EF) and edge-to-edge (EE) flocculations (originally defined in Chapter 2 in the Dispersive Clay Microstructure Using Scanning Electron Microscopy (SEM) section). This attraction between masses indicates a strong electrical force bonding them together. With such tight bonds,

dispersion is inhibited as the particles are able to maintain their shape through the introduction of water in the system.

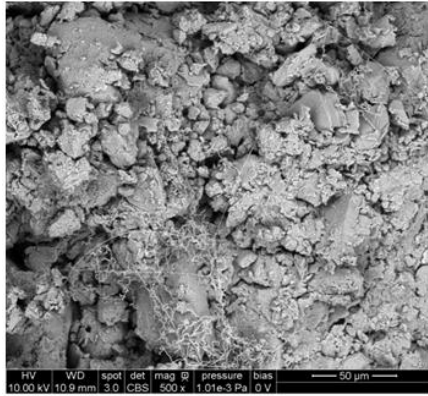
Bentonite, shown in figure (c), is not known to be nondispersive; however, with the addition of lime it begins to lose its dispersive tendencies. As discussed above, there are several large flocs indicating strong interparticle bonding. Within these bonds, EF and EE associations are held tightly together and oppose dispersion. Although there are not as many large masses as images (a) and (b), this image is drastically different than the untreated bentonite specimen. The structure has a definitive topography compared to the shapeless topography of pre-treated specimen.

Sodium illite was originally classified as a moderately dispersive clay. However, when treated with lime, the additive interacts with the soil's chemical composition and flocculation of particles is promoted. Looking at the soil surface, definite masses can be identified and the associations seem to be very closely joined. Similar to figures (a) and (b), which are naturally nondispersive, the surface is shows several small flocs. The flocs of the treated illite are not as large as the other nondispersive samples, but they are located throughout the entirety of the image and are very tight. With the promotion of more, smaller floc, stronger bonding occurs in the sample and the moderate dispersive tendencies of the untreated sodium illite are minimized.

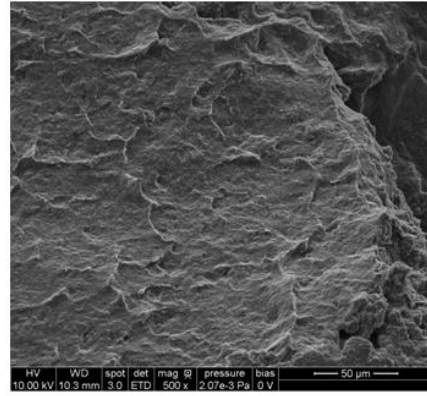
For a more detailed discussion on the effects of lime on the soil structures of bentonite and sodium illite, Figure 119 and Figure 121 respectively, refer to the section entitled SEM Comparison of Untreated to Treated Soil.

Moderately dispersive soil images

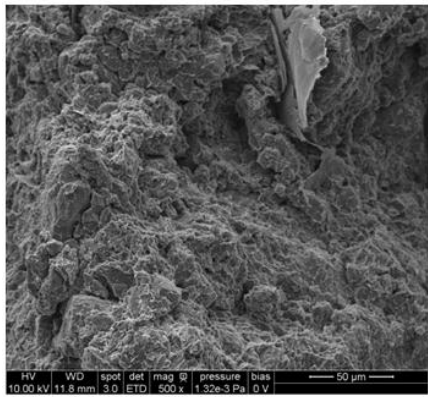
The soils classified as moderately dispersive were the alluvial top stratum, kaolinite, Santa Rosa clay, and sodium illite. The SEM images of these samples at 500x magnification are shown below in that same order in Figure 117.



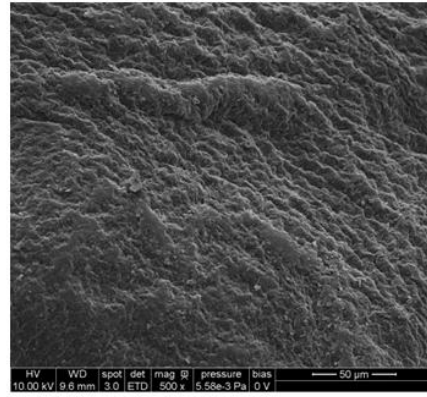
(a) Alluvial top stratum



(b) Kaolinite



(c) Santa Rosa clay



(d) Sodium illite

Figure 117. SEM images of clays classified as moderately dispersive

In comparison to the nondispersive SEM images, these images appear to have less definitive shapes. With the exception of figure (a), the masses present on the surfaces are much less pronounced. Rather than forming a multitude of attached associations, the flocs seem separate and deflocculated. Additionally, there appear to be more face-to-face (FF) associations separating the larger more flocculated EE and EF associations. Although the EE and EF associations are flocculated, they seem dispersed from one another. Meaning, although there are defined associations, the plates don't appear to be aggregated together. They seem fairly spread out which may indicate weaker bonds. Relating this to its classification as a moderately dispersive soil, although

the associations are able to withstand some water flow, under increased flows the bonds may prove too weak and succumb to dispersion.

The image of the alluvial top stratum is an interesting one. Although it was classified as slightly dispersive (a step below moderate but not completely nondispersive), some dispersive tendencies were seen. In the SEM image there are well pronounced shapes; however, the flocs are much smaller than the shapes exhibited in the nondispersive soil SEM images. In fact, although there are more flocs present they seem to be less connected and more aggregated within their separate masses. This disconnection between flocs could be indicative of weak bonding forces which would promote dispersive behavior in the sample. It is also interesting to note that, although there are no definite geologic origins of a dispersive clay, alluvial deposits have been known to exhibit some dispersive behavior (. This sample's in-situ geology and formation could also promote some dispersivity.

Kaolinite is known to be nondispersive so it is intriguing that it was classified as moderate. Looking at the surface though, the associations seem to be fairly flat and mostly FF. They appear to be rather aggregated associations but not very pronounced. Although there may be tight bonding between some of the particles (based in large part to the mineral's chemical composition), they seem somewhat disassociated from one another and do not form a complete network of associations. This deflocculation of associations may be indicative of weak bonds in those areas. When water comes in contact with such bonds, some dispersion could occur.

The Santa Rosa clay sample has characteristics reminiscent of a dispersive bentonite (seen in Figure 118). Flakes can be seen in the image and the surficial topography of the sample appears to be somewhat sinuous and film-like with platy peak masses predominating the structure rather than large round flocs (seen in the nondispersive images). The few round flocs present are indicative of flocculated associations located throughout the image in EF and EE orientations. These associations help the soil maintain its structure. The dispersed wave-like associations appear to have more FF connections with weaker bonds holding them together. With a mixture of these

associations that promote opposite behavior, some dispersiveness is bound to occur when water is introduced.

The last moderately dispersive sample, untreated sodium illite, shows very few large masses. Additionally, the surface topography seems similar to that of the Santa Rosa clay. Although not as pronounced, the associations seem almost wave-like and loosely connected. Flat, FF associations seem to dominate the majority of the image. While the large flocs maintain the shape of the substructure when water is introduced, the weaker FF associations do just the opposite. Because of their dispersed structure, the bonds between these associations are weak and cannot withstand the addition of water into the system. With a majority of weak bonds, it is understandable that sodium illite exhibits some dispersive behavior.

Dispersive soil

The untreated bentonite was the only soil classified as a dispersive soil. The 500x magnification image is presented below in Figure 118 as a comparison to the above discussed samples.

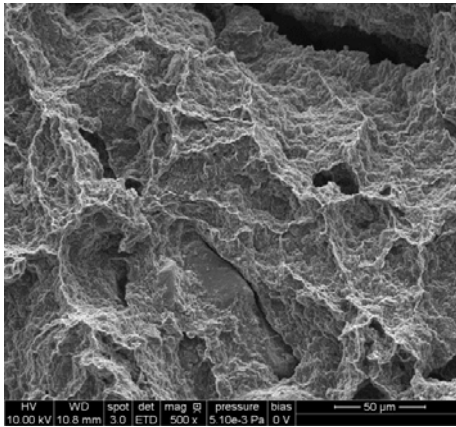


Figure 118. SEM images of clay classified as dispersive (bentonite)

In comparison to the nondispersive and moderately dispersive images, the untreated bentonite seems to have almost no stable structure. The flakes are dispersed and deflocculated from one another with a majority of only edges being shown. Its overall appearance is film-like with particle associations being not tight formations but

rather winding and loose. These weak bonds are characteristic of a bentonite and are fairly easy to see in the above image. Due to this lack of structure and weak bonding system, dispersive tendencies are promoted. The particles in the soil are free to disperse and leave their associations once water is introduced to the system.

SEM comparison of treated Soils to untreated

Bentonite

Two comparisons of bentonite are shown below. Figure 119 presents the SEM images produced specifically for this study and Figure 120 which was previously presented in Chapter 2 (Figure 18) from research performed by Bhuvaneshwari et al. (2007). In the (a) image of both figures, the particles are very clearly dispersed. There are no explicit floc formations but rather a web of dispersed particles that seem barely connected. The particle associations seem to only be composed of FF orientations with some EE at the peaks of associations. With such weak forces holding the particles together, dispersive behavior is likely.

In the accompanying (b) figure of the treated soil, masses can now be seen on the surface. There are still some FF associations but they are much less prominent and dispersed. These associations now appear aggregated together indicating tighter bonds with one another. Additionally, the new presence of flocculated masses inhibits dispersive behavior. In the previous image there was a complete lack of well-defined shapes and now, through pozzolanic and ion exchange reactions with the lime, stronger bonds prevail and the soil loses its dispersive tendencies.

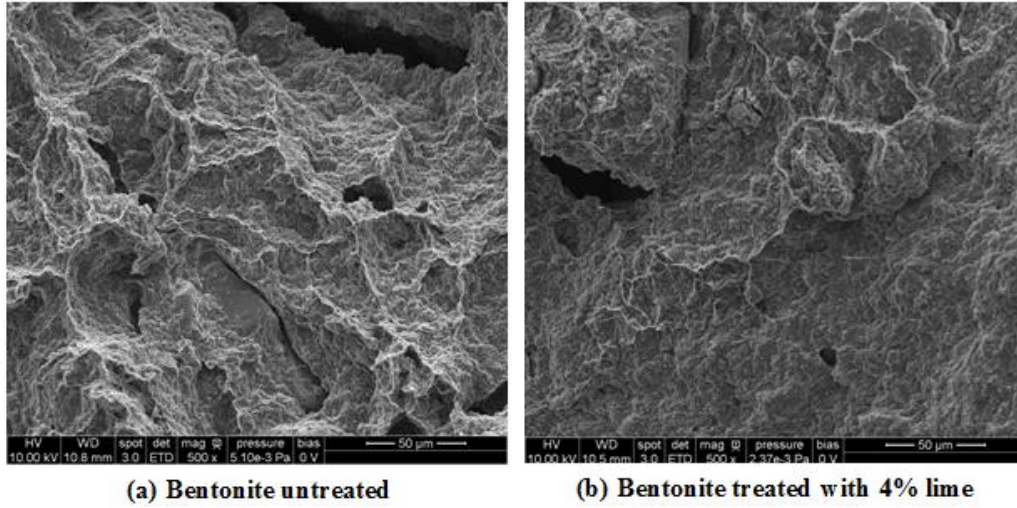


Figure 119. SEM images of bentonite with and without 500x magnification

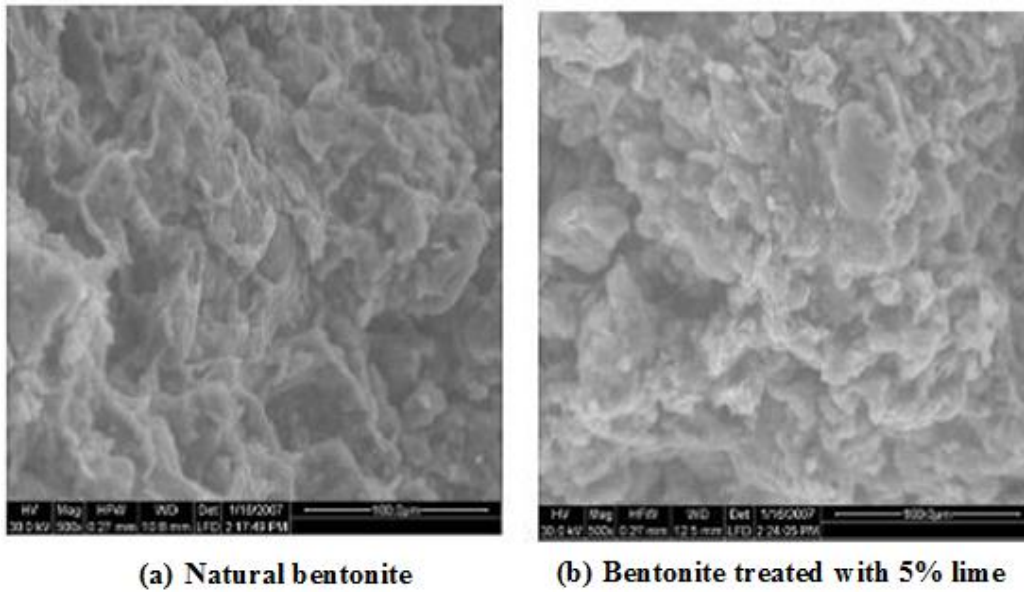


Figure 120. SEM images of bentonite with and without treatment (after Bhuvaneshwari et al., 2007)

Sodium illite

Two comparisons of illite are shown below. Figure 121 (at 500x magnification) and Figure 122 (at 1,500x magnification) present the SEM images produced specifically

for this study and Figure 123 shows a dispersed and flocculated illite image produced by Sides and Barden (1971). For the purpose of this discussion, the dispersed image will be considered an untreated sample and the flocculated image will be considered treated with an additive. For the comparison of the illite used in this study, the images analyzed were supplemented with images further magnified as the structure of the lime treated sample was not as informative as it could have been.

Using both images, one can see a distinct improvement in the treated sodium illite (b) as compared to (a). In the (a) images of all figures, the sodium illite shows a dominance of FF associations (more so in the vertical image). However, there are minimal flocculated masses in all images. Additionally, the soil structure in Figure 122a, shows a predominance of flakey particles and surficial topography of the sample appears to be somewhat sinuous and film-like. There are some rounded flocs but they seem small and dispersed rather than large and aggregated with one another. Few flocculated masses indicate a majority of weak interparticle bond forces in the soil sample. Weak forces cannot withstand the introduction of water into the system and thus, the soil is susceptible to dispersive behavior.

In the (b) images of treated illite, there are several more well-defined shapes on the soil surface. They are still fairly small flocculations, but they are tightly aggregated and are located throughout the surface. In the (a) image, the flocs are small and spread out, which meant if water were to come into contact with the sample, weak bonds would prevail and the structure would be susceptible to erosion. In (b) with more tight bonds throughout, there is an increased likelihood of a strong bond protecting the surface when water is introduced. The lime promotes an increase in masses on the surface which help combat dispersive behavior.

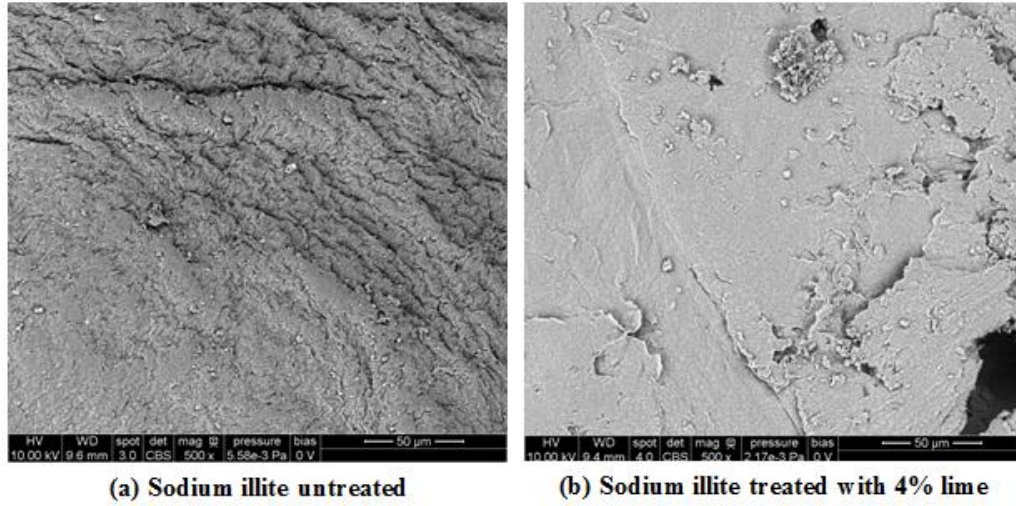


Figure 121. SEM images of treated and untreated illite at 500x magnification

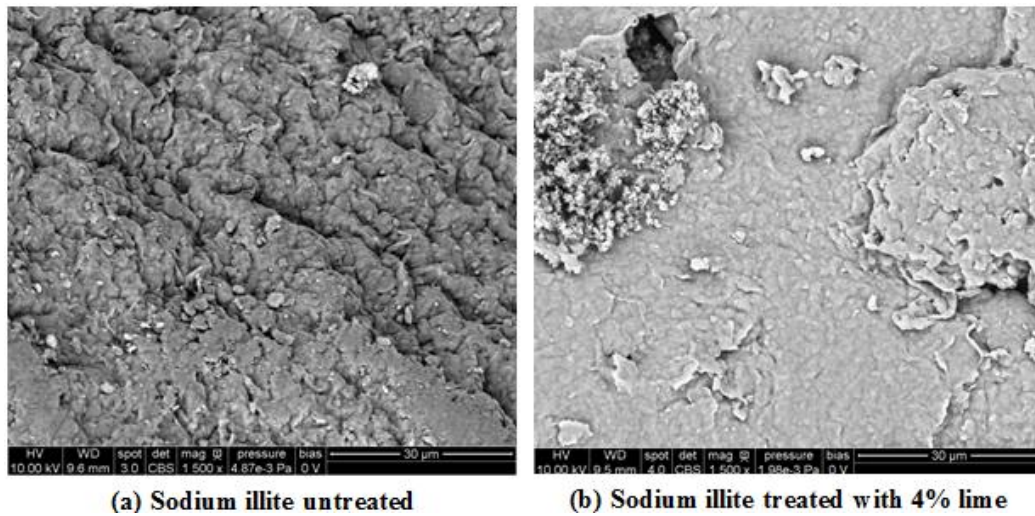
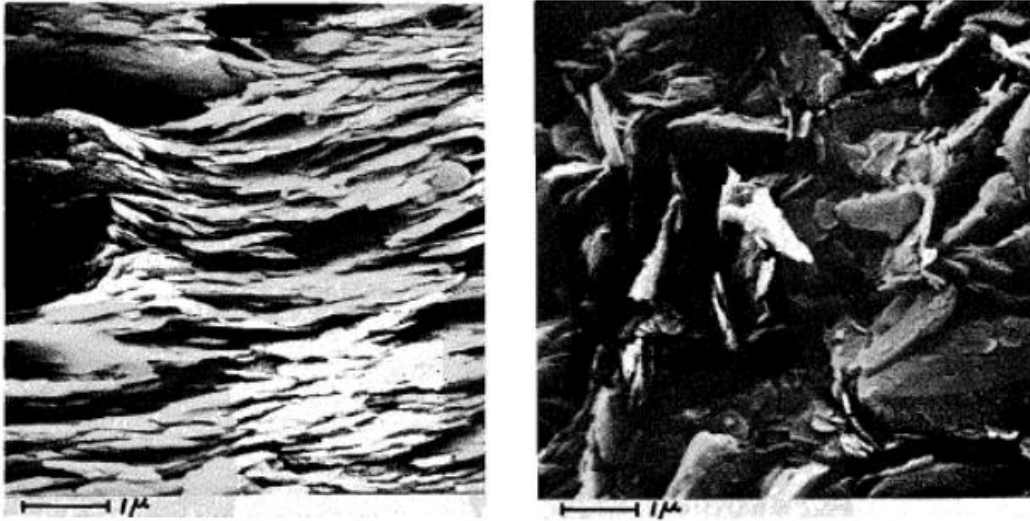


Figure 122. SEM images of untreated and treated illite at 1,500x magnification



(a) Illite dispersed (vertical section)

(b) Illite flocculated (vertical section)

Figure 123. SEM images of dispersed and flocculated illite
(after Sides and Barden, 1971)

CHAPTER 6. CONCLUSIONS AND RECOMMENDATIONS

This chapter presents a synopsis of the results from this study and lessons learned throughout the process. It will present an overview of the technical merit and scientific value obtained from this research. The conclusions are organized by dispersive clay properties, dispersive clay identification test methods, and dispersive clay microstructure observation using SEM technology. This chapter also includes recommendations for further research and practices.

Conclusions

Conclusions are categorized by dispersive clay properties, identification test methods, treatment effects, and microstructure observation using SEM technology.

Dispersive clay properties

Little is known conclusively on the properties specific to dispersive clays. There has been speculation that certain geologic areas may promote dispersive behavior over other locations. Additionally, others have stated the importance of mineralogical makeup of a clay in predicting dispersive tendencies. These two variables were examined and the following three conclusions were made;

- In accordance with Sherard et al. (1977), the alluvial sample was found to exhibit some dispersive tendencies, though was not classified as completely dispersive,
- Using laboratory tests, the bentonite and illite were classified as dispersive and moderately dispersive, respectively, this matches with the generally accepted knowledge of their structures, and
- Using laboratory tests, the kaolinite sample was classified as moderately dispersive, differing from its most accepted classification as nondispersive.

Dispersive clay identification test methods

There are various chemical and physical tests that can be used to identify dispersive clay. However, none of the tests are 100% accurate and more than one should be performed in order to make a well-informed classification. In this study, the physical tests were examined and compared. Of the physical tests, the pinhole test is generally accepted to be the most reliable and the other tests were compared to those results. Through performing the crumb test, pinhole test, double hydrometer test, and modified free swell index test, the following four conclusions were made;

- With the exception of the double hydrometer and free swell test, classifications are very subjective, grades are determined many times based on arbitrary discoloration adjectives without access to a direct comparison chart,
- The crumb test agreed well with the pinhole test a majority of the time, however it provided contrasting classifications when lime was present,
- The double hydrometer test agreed fairly well with the pinhole test in all but two classifications of untreated samples,
- There was some difficulty in performing the modified free swell index test with too fine of soil, specifically the kaolinite particles did not settle within the specified time period and the resulting index value was calculated with great uncertainty, and
- The modified free swell index generally predicted dispersive behavior well based on the amount of swelling; however, the soil treated with lime showed no reduction in swelling and provided curious results given the pinhole test classification.

Dispersive clay treatment effects

To combat dispersive tendencies, a chemical additive can be added to a soil. In this study, two samples were treated with 4% lime by weight, cured, and then classified using physical classification test methods. The following three conclusions were made;

- Adding 4% lime by weight to a sample is sufficient to change a dispersive and moderately dispersive sample to nondispersive,
- Lime does not reduce the swelling potential of a soil per the modified free swell index test, and
- The introduction of lime promotes flocculating of the soil structure at a microscopic level.

Dispersive clay microstructure observation using SEM technology

Several studies have been undertaken using SEM technology to observe the microstructural differences between flocculated and dispersed soil samples. However, these studies focus on specific, pure soil types such as kaolinite, illite, and bentonite. No one has classified seemingly random soils (such as oxidized glacial till, alluvial top stratum, Western Iowa loess, and Santa Rosa clay) and compared their substructures to pure dispersed or nondispersed soils. Additionally, one dispersed and one moderately dispersed soil were treated with lime and viewed using SEM imagery. In undertaking this task, the following five conclusions were made;

- Nondispersive samples showed a rather rough soil surface with a plethora of large masses arranged in edge-to-face (EF) and edge-to-edge (EE) associations,
- Moderately dispersive samples showed some large flocs in EF and EE associations, however the flocs were seemingly separate and dispersed from one another rather than located on the entirety of the image,
- Moderately dispersive samples showed some face-to-face (FF) associations which separated the stronger EF and EE flocs and may promote some dispersive properties,
- Dispersive sample surfaces consist of loose wave-like flakes with no definitive mass structures, and

- Lime promotes flocculation within a soil sample; small masses form over the entirety of the surface and create stronger bonds with other particles inhibiting dispersion.

Recommendations for future research

Future research on dispersive clays should focus on the following;

- Testing of alluvial soil in various environments to determine if there is in fact a direct correlation between dispersive behavior and soil transported via streams,
- A comparison of classifications on a sample in an undisturbed and remolded state. All the soils used in this study were in the remolded state; however, the double hydrometer test was performed on the Santa Rosa sample in a remolded state for this study and previously in 1977 at an in-situ state, it would be interesting to see if this would have an effect on other soil samples;
- The creation of a comprehensive illustrative turbidity classification chart, which would ensure grades could be assigned consistently regardless of the technician,
- The inclusion of chemical tests in the analysis to make a better comparison of all the available classification tests,
- The microstructural effects using other chemical additives, specifically gypsum as little to no research was found explicitly relating its effects on dispersivity, and
- A preliminary classification analysis using only SEM imagery then subsequent classification using accepted tests, in this study the soil was already classified using the pinhole test so some bias likely existed when describing the soil substructure.

Recommendations for future practices

Physical classification tests and SEM images have provided insight into the behavior and substructure of a dispersive clay. A recommendation would be to perform as many tests on a potentially dispersive clay as possible (physical and chemical) and, if equipment is available, take careful note of the amount of flocs present on the surface. Several large flocs are indicative of nondispersive behavior while small dispersed flocs and particles oriented in face-to-face associations imply some dispersive tendencies.

REFERENCES

- Arulanandan, K., and R. T. Heinzen. "Factors Influencing Erosion in Dispersive Clays and Methods of Identification." *Dispersive Clays, Related Piping, and Erosion in Geotechnical Projects, ASTM STP 623* (1977): 202-17. Print.
- ASTM Standard D 698, 2007, "Standard Test Methods for Particle Size Analysis of Soils," ASTM International, West Conshohocken, PA, 2012, DOI: 10.1520/D0422-63R07, www.astm.org.
- ASTM Standard D 698, 2012, "Standard Test Methods for Laboratory Compaction Characteristics of Soil Using Standard Effort (12,400 ft-lb/ft³ (600 kN-m/m³)),," ASTM International, West Conshohocken, PA, 2012, DOI: 10.1520/D0698-12, www.astm.org.
- ASTM Standard D 4221, 201, "Standard Test Methods for Dispersive Characteristics of Clay Soil by Double Hydrometer," ASTM International, West Conshohocken, PA, 2012, DOI: 10.1520/D4221-11, www.astm.org.
- ASTM Standard D 4647, 1987 (2006), "Standard Test Methods for Identification and Classification of Dispersive Clay Soils by the Pinhole Test," ASTM International, West Conshohocken, PA, 2006, DOI: 10.1520/D4647_D4647M-13, www.astm.org.
- ASTM Standard D 6572, 2006, "Standard Test Methods for Determining Dispersive Characteristics of Clayey Soils by the Crumb Test," ASTM International, West Conshohocken, PA, 2006, DOI: 10.1520/D6572-12, www.astm.org.
- Bell, F. G., and R. R. Maud. "Dispersive Soils: A Review from a South African Perspective." *Quarterly Journal of Engineering Geology and Hydrogeology* 27.3 (1994): 195-210. Print.
- Bell, F. G. "Lime Stabilization of Clay Minerals and Soils." *Engineering Geology* 42.4 (1996): 223-37. *ScienceDirect*. Elsevier B.V., 1996. Web. 29 May 2013.
- Bhuvaneshwari, S., et al. "Stabilization and microstructural modification of dispersive clayey soils." *1st International Conference on Soil and Rock Engineering, Srilankan Geotechnical Society, Columbo, Srilanka*. 2007.
- Bowles, Joseph E. *Foundation Analysis and Design*. New York: McGraw-Hill, 1997. Print.
- Chorom, M., P. Rengasamy, and R.S. Murray. "Clay Dispersion as Influenced by PH and Net Particle Charge of Sodic Soils." *Australian Journal of Soil Research* 32.6 (1994): 1243-252. Print.

- Decker, R. S., and L. P. Dunnigan. "Development and Use of the Soil Conservation Service Dispersion." *Dispersive Clays, Related Piping, and Erosion in Geotechnical Projects, ASTM STP 623* (1977): 94-109. Print.
- Dispersive Clay Studies for Los Esteros Lake Project Santa Rosa, New Mexico*. Rep. Lincoln: Hoskins-Western-Sonderegger, 1977. Print.
- Emerson, W. W. "A Classification of Soil Aggregates Based on Their Coherence in Water." *Australian Journal of Soil Research* 5.1 (1967): 47-57. Print.
- Fell, Robin, Patrick MacGregor, David Stapledon, and Graeme Bell. *Geotechnical Engineering of Dams*. Leiden: A.A. Balkema, 2005. Print.
- Fernando, Jayantha. "Effect of Water Quality on the Dispersive Characteristics of Soils Found in the Morwell Area, Victoria, Australia." *Geotechnical and Geological Engineering* 28.6 (2010): 835-50. Print.
- Indraratna, B., P. Nutalaya, and N. Kuganenthira. "Stabilization of a Dispersive Soil by Blending with Fly Ash." *Quarterly Journal of Engineering Geology and Hydrogeology* 24.3 (1991): 275-90. *Quarterly Journal of Engineering Geology*. The Geological Societ, 1991. Web. 18 Sept. 2012.
- Indraratna, B. "Utilization of Lime, Slag and Fly Ash for Improvement of a Colluvial Soil in New South Wales, Australia." *Geotechnical and Geological Engineering* 14 (1996): 169-91. Print.
- "Introduction to Energy Dispersive X-ray Spectrometry (EDS)." *Central Facility for Advanced Microscopy and Microanalysis*. University of California Riverside, 2 Feb. 2011. Web. 3 June 2013. <<http://micron.ucr.edu/public/manuals/EDS-intro.pdf>>.
- Jury, William A., and Robert Horton. *Soil Physics*. 6th ed. Hoboken: J. Wiley & Sons, 2004. Print.
- Kavak, Aydin, and Gökhan Baykal. "Long-term Behavior of Lime-Stabilized Kaolinite Clay." *Environmental Earth Sciences* 66.7 (2012): 1943-955. Springer Link, Aug. 2012. Web. 31 May 2013.
- Knodel, Paul C. *Characteristics and Problems of Dispersive Clay Soils*. Rep. Denver: US Department of the Interior, 1991. *Characteristics and Problems of Dispersive Clay Soils*. Bureau of Reclamation, Oct. 1991. Web.

- McDaniel, Thomas N., and Rey S. Decker. "Dispersive Soil Problem at Los Esteros Dam." *Journal of the Geotechnical Engineering Division* 105.9 (1979): 1017-030. Print.
- "Mineralogy Database." *Mineralogy Database*. David Barthelmy, 2007. Web. 5 June 2013. <<http://webmineral.com/>>.
- Mitchell, James K., and Kenichi Soga. *Fundamentals of Soil Behavior*. 3rd ed. Hoboken: J. Wiley & Sons, 2005. Print.
- Nickel, Stephen H. "Consolidation of Flocculated Illite." Thesis. University of Nebraska-Lincoln, 1972. Print.
- Ouhadi, VR., and A.R. Goodarzi. "Assessment of the Stability of a Dispersive Soil Treated by Alum." *Engineering Geology* 85.1-2 (2006): 91-101. Elsevier. Web. 18 Sept. 2012.
- "Pelco Conductive Graphite Isopropanol Based Product No. 16053." *Pelco Technical Notes*. Ted Pella, Inc., 9 Aug. 2012. Web. 5 June 2013. <http://www.tedpella.com/technote_html/16053%20TN.pdf>.
- "Q150T Turbo-Pumped Sputter Coater/Carbon Coater." *Quorum Technologies*. Quorum Technologies Limited Company, 27 Feb. 2012. Web. 5 June 2013. <www.quorumtech.com>.
- "Quanta 250 FEG." *Quanta Scanning Electron Microscopes (SEM)*. FEI, 2013. Web. 7 June 2013. <<http://www.fei.com/products/scanning-electron-microscopes/quanta.aspx>>.
- Ranjan, Gopal, and A. S. R. Rao. *Basic and Applied Soil Mechanics*. New Delhi: New Age International (P) Limited, 2005. Print.
- Reed, S. J. B. *Electron Microprobe Analysis and Scanning Electron Microscopy in Geology*. Cambridge: Cambridge UP, 1996. Print.
- Ritter, Dale F., R. Craig Kochel, and Jerry R. Miller. *Process Geomorphology*. 5th ed. Long Grove: Waveland, 2011. Print.
- Sherard, J. L., and R. S. Decker. *Dispersive Clays, Related Piping, and Erosion in Geotechnical Projects*. Philadelphia, PA: American Society for Testing and Materials, 1977. Print.

- Sherard, J. L., L. P. Dunnigan, and R. S. Decker. "Some Engineering Problems with Dispersive Clays." *Dispersive Clays, Related Piping, and Erosion in Geotechnical Projects, ASTM STP 623* (1977): 3-12. Print.
- Sherard, James L., Lorn P. Dunnigan, Rey S. Decker, and Edgar F. Steele. "Pinhole Test for Identifying Dispersive Soils." *Journal of the Geotechnical Engineering Division* 102.1 (1976): 69-85. Print.
- Sides, Geoffrey, and Laing Barden. "The Microstructure of Dispersed and Flocculated Samples of Kaolinite, Illite, and Montmorillonite." *Canadian Geotechnical Journal* 8.3 (1971): 391-99. *NRC Research Press*. Canadian Science Publishing. Web. 30 May 2013.
- Sivapullaiah, Puvvadi V., Thallak G. Sitharam, and Kanakapura S. Subba Rao. "Modified Free Swell Index for Clays." *Geotechnical Testing Journal* 10.2 (1987): 80-85. *ASTM Standards and Engineering Digital Library*. ASTM. Web. 25 Apr. 2013.
- "Soil Stabilization." *Soil Stabilization*. National Lime Association, n.d. Web. 30 May 2013.
- Van Olphen, H. *An Introduction to Clay Colloid Chemistry*. 2nd ed. N.p.: John Wiley & Sons, 1977. Print.
- Velasco-Molina, Hugo Alejo, Allen R. Swoboda, and Curtis L. Godfry. "Dispersion of Soils of Different Mineralogy in Relation to Sodium Adsorption Ratio and Electrolyte Concentration." *Soil Sciences* 3.1 (1971): 282-87. Print.
- White, David. "Scanning Electron Microscopy Lecture." *CE 565 Fundamentals of Geomaterials Behavior*. 26 March 2012. Print
- Wischnitzer, Saul. *Introduction to Electron Microscopy*. 2nd ed. New York: Pergamon, 1970. Print.
- Yilmaz, Gulgun. "The Effects of Temperature on the Characteristics of Kaolinite and Bentonite." *Scientific Research and Essays* 6.9 (2011): 1928-939. *Scientific Research and Essays*. AcademicJournals, 4 May 2011. Web. 29 May 2013.

APPENDIX. TEST RESULTS

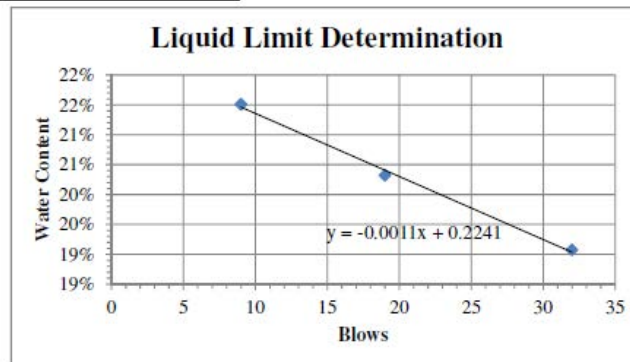
Oxidized glacial till

ATTERBERG LIMIT RESULTS

Soil: Oxidized Glacial Till

Liquid Limit					
can (g)	wet (g)	dry (g)	water (g)	w%	blows
11.15	17.83	16.76	1.07	19%	32
10.97	19.91	18.4	1.51	20%	19
11.03	17.47	16.33	1.14	22%	9

	blows	w%
LL	25	20%



Plastic Limit				
can (g)	wet (g)	dry (g)	water (g)	w%
11.08	13.31	13.05	0.26	13%
10.98	12.73	12.53	0.2	13%
			PL	13%

Plasticity Index	7%
------------------	----

Figure 124. Atterberg limits for oxidized glacial till

Date	Time of Reading	Elapsed Time, t (min)	Temperature (°C)	Actual Hydrometer Reading, R _a	Corrected Hydrometer Reading, R _c	% Finer	Hydrometer Correction only for Meniscus, R	L (cm)	L/t	K	D (mm)
5/9/2013	10:03:00 AM	0	-	-	-	-	-	-	-	-	-
5/9/2013	10:03:30 AM	0.5	24.3	29	23.6	44.11	30	11.5	23.0	0.01263	0.060562
5/9/2013	10:04:00 AM	1	24.3	27	21.6	40.37	28	11.9	11.9	0.01263	0.043562
5/9/2013	10:05:00 AM	2	24.3	23.5	18.1	33.82	25	12.5	6.23	0.01263	0.031507
5/9/2013	10:08:00 AM	5	24.3	21	15.6	29.15	22	12.9	2.58	0.01263	0.020284
5/9/2013	10:18:00 AM	15	24.2	17	11.6	21.61	18	13.5	0.900	0.01264	0.011993
5/9/2013	10:33:00 AM	30	24.0	15	9.5	17.76	16	13.8	0.460	0.01267	0.008593
5/9/2013	11:03:00 AM	60	23.8	13.5	7.9	14.85	15	14.1	0.235	0.01285	0.006229
5/9/2013	12:03:00 PM	97	23.8	13	7.4	13.91	14	14.2	0.1464	0.01285	0.004917
5/9/2013	2:03:00 PM	240	23.8	11.5	5.9	11.11	13	14.4	0.06000	0.01285	0.003148
5/9/2013	6:03:00 PM	480	23.8	10.5	4.9	9.24	12	14.6	0.03042	0.01285	0.002241
5/10/2013	2:03:00 AM	967	23.1	10	4.2	7.91	11	14.7	0.01520	0.01296	0.001597
5/10/2013	10:03:00 AM	1446	23.1	9	3.2	6.04	10	14.8	0.01024	0.01296	0.001311

$R_c = R_a - \text{Zero Correction} + C_T$; C_T from Table 6-3 of Bowles.

$$\% \text{ Finer} = \frac{R_c a}{W_s}$$

$$D = K \sqrt{\frac{L}{t}}$$

Hydrometer Analysis Parameters	
Hydrometer Number	152H
G _s of Solids	2.70
a	0.99
Dispersing Agent	125 mL of Sodium Hexametaphosphate
Weight of Soil, W _s	52.94865004 grams
Zero Correction	6.5
Meniscus Correction	1.0

Figure 126. Hydrometer analysis in a dispersant for oxidized glacial till

Particle Size Distribution in Dispersant

Sieve #	Particle Diameter (mm)	Percent Finer (%)	Particle Diameter (in)
	76.2	100	3.00000
	50.8	100	2.00000
	38.1	100	1.50000
	25.4	100	1.00000
	19.05	100	0.75000
	9.53	100.00	0.37520
4	4.76	94.89	0.18740
10	2.00	92.82	0.07874
40	0.841	92.82	0.03311
60	0.250	81.79	0.00984
100	0.1490	72.51	0.00587
200	0.0740	61.84	0.00291
	0.0606	44.11	0.00238
	0.0436	40.37	0.00172
	0.0315	33.82	0.00124
	0.0203	29.15	0.00080
	0.0120	21.61	0.00047
	0.0086	17.76	0.00034
	0.0062	14.85	0.00025
	0.0049	13.91	0.00019
	0.0031	11.11	0.00012
	0.0022	9.24	0.00009
	0.0016	7.91	0.00006
	0.0013	6.04	0.00005

Figure 127. Particle size distribution in a dispersant for oxidized glacial till

Date	Time of Reading	Elapsed Time, t (min)	Temperature (°C)	Actual Hydrometer Reading, R _a	Corrected Hydrometer Reading, R _c	% Finer	Hydrometer Correction only for Meniscus, R	L (cm)	L/t	K	D (mm)
5/20/2013	3:31:00 PM	0	-	-	-	-	-	-	-	-	-
5/20/2013	3:31:30 PM	0.5	23.8	10	10.9	21.29	11	14.7	29.4	0.01285	0.069675
5/20/2013	3:32:00 PM	1	23.8	7	7.9	15.45	8	15.2	15.2	0.01285	0.050099
5/20/2013	3:33:00 PM	2	23.8	6	6.9	13.51	7	15.3	7.65	0.01285	0.035541
5/20/2013	3:36:00 PM	5	23.8	3.5	4.4	8.64	5	15.8	3.16	0.01285	0.022843
5/20/2013	3:46:00 PM	15	23.5	2	2.9	5.55	3	16.0	1.067	0.01290	0.013318
5/20/2013	4:01:00 PM	30	23.5	1.5	2.4	4.57	3	16.1	0.535	0.01290	0.009432
5/20/2013	4:31:00 PM	196	23.2	1	1.8	3.43	2	16.1	0.082	0.01294	0.003709
5/20/2013	7:21:00 PM	489	22.8	1	1.6	3.19	2	16.1	0.0329	0.01300	0.002359
5/20/2013	12:21:00 PM	1117	23.0	1	1.7	3.31	2	16.1	0.01441	0.01297	0.001557

$R_c = R_a - \text{Zero Correction} + C_T$; C_T from Table 6-3 of Bowles.

$$\% \text{ Finer} = \frac{R_c \alpha}{W_s}$$

$$D = K \sqrt{L/t}$$

Hydrometer Analysis Parameters	
Hydrometer Number	152H
G _s of Solids	2.70
α	0.99
Dispersing Agent	Distilled Water
Weight of Soil, W _s	50.86986778 grams
Zero Correction	0
Meniscus Correction	1.0

Figure 128. Hydrometer analysis in water for oxidized glacial till

Particle Size Distribution in Distilled Water

Sieve #	Particle Diameter (mm)	Percent Finer (%)	Particle Diameter (in)
	76.2	100	3.00000
	50.8	100	2.00000
	38.1	100	1.50000
	25.4	100	1.00000
	19.05	100	0.75000
	9.53	100	0.37520
4	4.76	94.89	0.18740
10	2.00	92.82	0.07874
40	0.841	81.79	0.03311
60	0.250	72.51	0.00984
100	0.1490	61.84	0.00587
200	0.0740	49.94	0.00291
	0.0697	21.29	0.00274
	0.0501	15.45	0.00197
	0.0355	13.51	0.00140
	0.0228	8.64	0.00090
	0.0133	5.55	0.00052
	0.0094	4.57	0.00037
	0.0037	3.43	0.00015
	0.0024	3.19	0.00009
	0.0016	3.31	0.00006

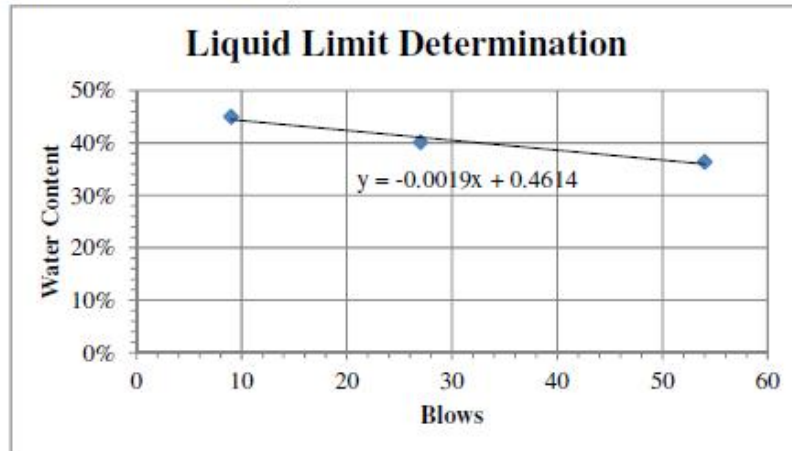
Figure 129. Particle size distribution in water for oxidized glacial till

Alluvial top stratum
ATTERBERG LIMIT RESULTS

Soil: Alluvial Top Stratum

Liquid Limit					
can (g)	wet (g)	dry (g)	water (g)	w%	blows
11.09	15.29	14.17	1.12	36%	54
11.1	15.78	14.44	1.34	40%	27
10.99	20.3	17.41	2.89	45%	9

	blows	w%
LL	25	41%



Plastic Limit				
can (g)	wet (g)	dry (g)	water (g)	w%
10.93	12.56	12.23	0.33	25%
10.92	11.93	11.72	0.21	26%
		PL		26%

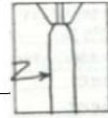
Plasticity Index 16%

Figure 130. Atterberg limit results for alluvial top stratum

PINHOLE TEST DATA

Sample No. Alluvial Top Stratum
 Compaction Characteristics: compacted using Harvard miniature
 Water Content: 18%
 Distilled Water Added: Yes No
 Curing Time: 24 hr
 State: remolded using Harvard mini compaction
 Project: Velasco Thesis Site No. _____

Specimen after test

Final hole:
see picture

Date 21-May
 Page _____
 By EV

Flow started on _____ trial

Clock Time		Head (in)	Flow		Flow Rate ml/sec	Turbidity from Side							Completely Clear from Top	Remarks
minutes	seconds		ml	sec		Very Dark	Dark	Moderately Dark	Slightly Dark	Barely Visible	Clear			
0	17	2	10	17	0.588						X			
1	52	2	20	112	0.105						X			
3	20	2	50	200	0.341				X					
4	50	2	100	290	0.556				X					
7	20	2	150	440	0.333				X					
10	0	7	200	600	0.313				X					
11	30	7	250	690	0.556				X					
13	0	7	300	780	0.556				X					
14	20	7	350	860	0.625				X					
15	20	7	400	920	0.833				X					
16	40	15	500	1000	1.250				X					
17	30	15	550	1050	1.000				X					
18	30	15	600	1110	0.833				X					
19	23	15	700	1163	1.887				X					
20	0	15	800	1200	2.703				X					
														Under 15 in head and 20 min, flow is slightly dark, flow rate is between 1.8 and 3.2 mL/s --> is classified as ND 4

Figure 131. Pinhole test data for alluvial top stratum

Date	Time of Reading	Elapsed Time, t (min)	Temperature (°C)	Actual Hydrometer Reading, R_a	Corrected Hydrometer Reading, R_c	% Finer	Hydrometer Correction only for Meniscus, R	L (cm)	L/t	K	D (mm)
5/9/2013	10:03:00 AM	0	-	-	-	-	-	-	-	-	-
5/9/2013	10:03:30 AM	0.5	24.3	35	29.6	60.62	36	10.3	20.6	0.01278	0.057982
5/9/2013	10:04:00 AM	1	24.3	34	28.6	58.57	35	10.7	10.7	0.01278	0.041788
5/9/2013	10:05:00 AM	2	24.3	30	24.6	50.38	31	11.4	5.70	0.01278	0.030500
5/9/2013	10:08:00 AM	5	24.3	25	19.6	40.14	26	12.2	2.44	0.01278	0.019955
5/9/2013	10:18:00 AM	15	24.2	20	14.6	29.83	21	13.0	0.867	0.01279	0.011907
5/9/2013	10:33:00 AM	30	23.2	17	11.3	23.07	18	13.5	0.450	0.01294	0.008680
5/9/2013	11:03:00 AM	60	23.2	14	8.3	16.92	15	14.0	0.233	0.01294	0.006251
5/9/2013	11:46:00 AM	103	23.2	12	6.3	12.83	13	14.3	0.1388	0.01294	0.004822
5/9/2013	2:03:00 PM	240	23.4	10.5	4.8	9.88	12	14.6	0.06083	0.01291	0.003184
5/9/2013	6:24:00 PM	504	23.4	10	4.3	8.85	11	14.7	0.02917	0.01291	0.002205
5/10/2013	2:16:00 AM	973	22.8	8.5	2.6	5.41	10	14.9	0.01531	0.01300	0.001609
5/10/2013	10:17:00 AM	1454	22.8	8	2.1	4.38	9	15.0	0.01032	0.01300	0.001320

$R_c = R_a - \text{Zero Correction} + C_T$; C_T from Table 6-3 of Bowles.

$$\% \text{ Finer} = \frac{R_c \cdot a}{W_s}$$

$$D = K \sqrt{L/t}$$

Hydrometer Analysis Parameters	
Hydrometer Number	152H
G_s of Solids	2.70
a	0.99
Dispersing Agent	125 mL of Sodium Hexametaphosphate
Weight of Soil, W_s	48.32118271 grams
Zero Correction	6.5
Meniscus Correction	1.0

Figure 132. Particle size analysis in a dispersant for alluvial top stratum

Particle Size Distribution in Dispersant

Sieve #	Particle Diameter (mm)	Percent Finer (%)	Particle Diameter (in)
	76.2	100	3.00000
	50.8	100	2.00000
	38.1	100	1.50000
	25.4	100	1.00000
	19.05	100	0.75000
	9.53	100	0.37520
4	4.76	99.69	0.18740
10	2.00	99.13	0.07874
40	0.841	92.74	0.03311
60	0.250	83.78	0.00984
100	0.1490	75.08	0.00587
200	0.0740	63.33	0.00291
	0.0580	60.62	0.00228
	0.0418	58.57	0.00165
	0.0305	50.38	0.00120
	0.0200	40.14	0.00079
	0.0119	29.83	0.00047
	0.0087	23.07	0.00034
	0.0063	16.92	0.00025
	0.0048	12.83	0.00019
	0.0032	9.88	0.00013
	0.0022	8.85	0.00009
	0.0016	5.41	0.00006
	0.0013	4.38	0.00005

Figure 133. Particle size distribution in a dispersant for alluvial top stratum

Date	Time of Reading	Elapsed Time, t (min)	Temperature (°C)	Actual Hydrometer Reading, R_a	Corrected Hydrometer Reading, R_c	% Finer	Hydrometer Correction only for Meniscus, R	L (cm)	L/t	K	D (mm)
5/20/2013	3:31:00 PM	0	-	-	-	-	-	-	-	-	-
5/20/2013	3:31:30 PM	0.5	23.8	11	11.9	22.65	12	14.5	29.0	0.01285	0.069199
5/20/2013	3:32:00 PM	1	23.8	10	10.9	20.75	11	14.7	14.7	0.01285	0.049268
5/20/2013	3:33:00 PM	2	23.8	6	6.9	13.16	7	15.3	7.65	0.01285	0.035541
5/20/2013	3:36:00 PM	5	23.8	3	3.9	7.47	4	15.8	3.16	0.01285	0.022843
5/20/2013	3:46:00 PM	15	23.8	2	2.9	5.58	3	16.0	1.067	0.01285	0.013271
5/20/2013	4:01:00 PM	30	23.5	1	1.9	3.51	2	16.1	0.537	0.01290	0.009447
5/20/2013	4:31:00 PM	60	23.8	1	1.9	3.68	2	16.1	0.268	0.01285	0.006656
5/20/2013	8:01:00 PM	210	23.2	1	1.8	3.34	2	16.1	0.0767	0.01294	0.003583
5/21/2013	12:21:00 AM	506	22.8	0	0.6	1.21	1	16.3	0.03221	0.01300	0.002333
5/21/2013	10:26:00 AM	1135	23.0	0	0.7	1.33	1	16.3	0.01436	0.01297	0.001554

$R_c = R_a - \text{Zero Correction} + C_T$; C_T from Table 6-3 of Bowles.

$$\% \text{ Finer} = \frac{R_c a}{W_t}$$

$$D = K \sqrt{L/t}$$

Hydrometer Analysis Parameters	
Hydrometer Number	152H
G_s of Solids	2.70
a	0.99
Dispersing Agent	Distilled Water
Weight of Soil, W_s	52.19012116 grams
Zero Correction	0
Meniscus Correction	1.0

Figure 134. Particle size analysis in water for alluvial top stratum

Particle Size Distribution in Distilled Water

Sieve #	Particle Diameter (mm)	Percent Finer (%)	Particle Diameter (in)
	76.2	100	3.00000
	50.8	100	2.00000
	38.1	100	1.50000
	25.4	100	1.00000
	19.05	100	0.75000
	9.53	100	0.37520
4	4.76	99.69	0.18740
10	2.00	99.13	0.07874
40	0.841	92.74	0.03311
60	0.250	83.78	0.00984
100	0.1490	75.08	0.00587
200	0.0740	63.33	0.00291
	0.0692	22.65	0.00272
	0.0493	20.75	0.00194
	0.0355	13.16	0.00140
	0.0228	7.47	0.00090
	0.0133	5.58	0.00052
	0.0094	3.51	0.00037
	0.0067	3.68	0.00026
	0.0036	3.34	0.00014
	0.0023	1.21	0.00009

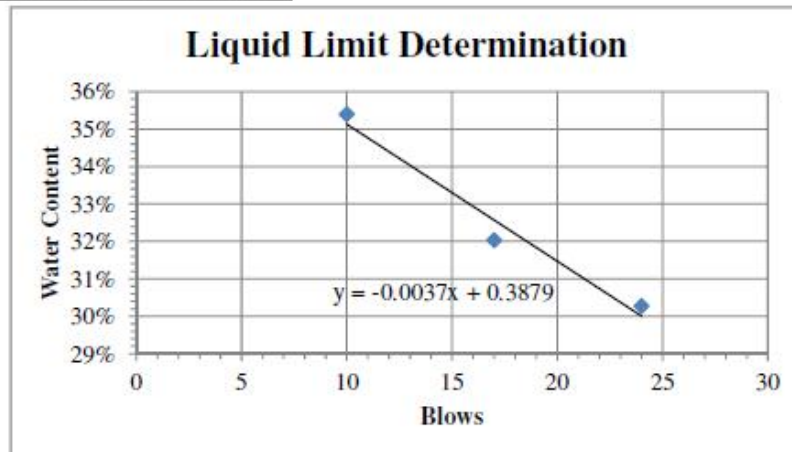
Figure 135. Particle size distribution in water for alluvial top stratum

Western Iowa loess
ATTERBERG LIMIT RESULTS

Soil: Western Iowa Loess

Liquid Limit					
can (g)	wet (g)	dry (g)	water (g)	w%	blows
11.13	17.8	16.25	1.55	30%	24
11.09	20.2	17.99	2.21	32%	17
11.05	21.53	18.79	2.74	35%	10

	blows	w%
LL	25	30%



Plastic Limit				
can (g)	wet (g)	dry (g)	water (g)	w%
11.06	12.88	12.51	0.37	26%
11.06	12.86	12.5	0.36	25%
		PL		25%

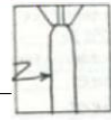
Plasticity Index	4%
------------------	----

Figure 136. Atterberg test results for Western Iowa loess

PINHOLE TEST DATA

Sample No. Loess
 Compaction Characteristics: compacted using Harvard miniature
 Water Content: 17%
 Distilled Water Added: Yes X No _____
 Curing Time: _____
 State: remolded using Harvard mini compaction
 Project: Velasco Thesis Site No. _____

Specimen after test



Date 24-May
 Page _____
 By EV

Final hole:
see picture

Flow started on _____ trial

Clock Time		Head (in)	Flow		Flow Rate	Turbidity from Side						Completely Clear from Top	Remarks
minutes	seconds		ml	sec	ml/sec	Very Dark	Dark	Moderately Dark	Slightly Dark	Barely Visible	Clear		
0	45	2	25	45	0.556						X		
1	110	2	50	110	0.385						X		
4	240	2	100	240	0.385						X		
5	300	2	140	300	0.667						X		
6	360	2	160	360	0.333						X		
7	420	2	195	420	0.583						X		
8	480	2	220	480	0.417						X		
9	540	2	255	540	0.583						X		
10	600	2	285	600	0.500						X		
11	660	7	320	660	0.583						X		
12	720	7	370	720	0.833						X		
14	840	7	410	840	0.333						X		
15	900	7	455	900	0.750						X		
16	960	15	500	960	0.750						X		
17	1020	15	595	1020	1.583						X		
18	1080	15	690	1080	1.583						X		
19	1140	15	840	1140	2.500						X		
20	1200	15	925	1200	1.417						X		
21	1260	40	1150	1260	3.750						X		
23	1380	40	1350	1380	1.667						X		
24	1440	40	1500	1440	2.500						X		
25	1500	40	1650	1500	2.500						X		
													Under 40 in head and 25 min, flow is trace dark, flow rate is less than 3.0 mL/s and hole diameter is not much greater than needle diameter -> is classified as ND 1

Figure 137. Pinhole data form for Western Iowa loess

Date	Time of Reading	Elapsed Time, t (min)	Temperature (°C)	Actual Hydrometer Reading, R_a	Corrected Hydrometer Reading, R_c	% Finer	Hydrometer Correction only for Meniscus, R	L (cm)	L/t	K	D (mm)
5/9/2013	10:03:00 AM	0	-	-	-	-	-	-	-	-	-
5/9/2013	10:03:30 AM	0.5	24.8	47	41.7	85.45	48	8.4	16.8	0.01270	0.052055
5/9/2013	10:04:00 AM	1	24.8	46	40.7	83.40	47	8.6	8.6	0.01270	0.037244
5/9/2013	10:05:00 AM	2	24.8	37	31.7	64.98	38	10.2	5.10	0.01270	0.028681
5/9/2013	10:08:00 AM	5	24.8	26.5	21.2	43.48	28	12.0	2.39	0.01270	0.019634
5/9/2013	10:18:00 AM	15	24.8	19.5	14.2	29.15	21	13.1	0.873	0.01270	0.011868
5/9/2013	10:33:00 AM	30	24.8	15	9.7	19.94	16	13.8	0.460	0.01270	0.008614
5/9/2013	11:03:00 AM	60	23.1	13.5	7.7	15.82	15	14.1	0.235	0.01296	0.006280
5/9/2013	12:03:00 PM	112	23.2	12	6.3	12.82	13	14.3	0.1277	0.01294	0.004624
5/9/2013	2:03:00 PM	240	23.0	12	6.2	12.69	13	14.3	0.05958	0.01297	0.003166
5/9/2013	6:03:00 PM	513	23.0	11	5.2	10.65	12	14.5	0.02827	0.01297	0.002181
5/10/2013	2:03:00 AM	982	22.8	10	4.1	8.48	11	14.7	0.01497	0.01300	0.001591
5/10/2013	10:03:00 AM	1462	22.8	10	4.1	8.48	11	14.7	0.01005	0.01300	0.001304

$R_c = R_a - \text{Zero Correction} + C_T$; C_T from Table 6-3 of Bowles.

$$\% \text{ Finer} = \frac{R_c \alpha}{W_s}$$

$$D = K \sqrt{L/t}$$

Hydrometer Analysis Parameters	
Hydrometer Number	152H
G_s of Solids	2.70
α	0.99
Dispersing Agent	125 mL of Sodium Hexametaphosphate
Weight of Soil, W_s	48.35865083 grams
Zero Correction	6.5
Meniscus Correction	1.0

Figure 138. Particle size analysis in a dispersant for Western Iowa loess

Particle Size Distribution in Dispersant

Sieve #	Particle Diameter (mm)	Percent Finer (%)	Particle Diameter (in)
	76.2	100	3.00000
	50.8	100	2.00000
	38.1	100	1.50000
	25.4	100	1.00000
	19.05	100	0.75000
	9.53	100	0.37520
4	4.76	100	0.18740
10	2.00	99.90	0.07874
40	0.841	99.73	0.03311
60	0.250	99.73	0.00984
100	0.1490	99.56	0.00587
200	0.0740	98.92	0.00291
	0.0521	85.45	0.00205
	0.0372	83.40	0.00147
	0.0287	64.98	0.00113
	0.0196	43.48	0.00077
	0.0119	29.15	0.00047
	0.0086	19.94	0.00034
	0.0063	15.82	0.00025
	0.0046	12.82	0.00018
	0.0032	12.69	0.00012
	0.0022	10.65	0.00009
	0.0016	8.48	0.00006
	0.0013	8.48	0.00005

Figure 139. Particle size distribution in a dispersant for Western Iowa loess

Date	Time of Reading	Elapsed Time, t (min)	Temperature (°C)	Actual Hydrometer Reading, R_a	Corrected Hydrometer Reading, R_c	% Finer	Hydrometer Correction only for Meniscus, R	L (cm)	L/t	K	D (mm)
5/20/2013	3:31:00 PM	0	-	-	-	-	-	-	-	-	-
5/21/2013	3:31:30 PM	0.5	23.8	21	21.9	41.97	22	12.9	25.8	0.01285	0.065270
5/22/2013	3:32:00 PM	1	23.8	20	20.9	40.06	21	13.0	13.0	0.01285	0.046331
5/23/2013	3:33:00 PM	2	23.8	15	15.9	30.49	16	13.8	6.90	0.01285	0.033754
5/24/2013	3:36:00 PM	5	24.0	13	14.0	26.78	14	14.2	2.84	0.01282	0.021605
5/25/2013	3:46:00 PM	15	24.0	3	4.0	7.65	4	15.8	1.053	0.01282	0.013157
5/26/2013	4:01:00 PM	30	24.0	1.5	2.5	4.78	3	16.1	0.535	0.01282	0.009377
5/27/2013	4:31:00 PM	60	23.8	1.5	2.4	4.67	3	16.1	0.268	0.01285	0.006646
5/28/2013	7:21:00 PM	230	23.5	0.5	1.4	2.58	2	16.2	0.0704	0.01290	0.003422
5/29/2013	12:21:00 PM	523	23.0	0.5	1.2	2.30	2	16.2	0.03098	0.01297	0.002283
2/17/2010	10:42:00 AM	1151	23.0	0.5	1.2	2.30	2	16.2	0.01407	0.01297	0.001539

$R_c = R_a - \text{Zero Correction} + C_T$; C_T from Table 6-3 of Bowles.

$$\% \text{ Finer} = \frac{R_c a}{W_s}$$

$$D = K \sqrt{L/t}$$

Hydrometer Analysis Parameters	
Hydrometer Number	152H
G_s of Solids	2.70
a	0.99
Dispersing Agent	Distilled Water
Weight of Soil, W_s	51.75097276 grams
Zero Correction	0
Meniscus Correction	1.0

Figure 140. Particle size analysis in water for Western Iowa loess

Particle Size Distribution in Distilled Water

Sieve #	Particle Diameter (mm)	Percent Finer (%)	Particle Diameter (in)
	76.2	100	3.00000
	50.8	100	2.00000
	38.1	100	1.50000
	25.4	100	1.00000
	19.05	100	0.75000
	9.53	100	0.37520
4	4.76	100	0.18740
10	2.00	99.90	0.07874
40	0.841	99.73	0.03311
60	0.250	99.73	0.00984
100	0.1490	99.56	0.00587
200	0.0740	98.92	0.00291
	0.0653	41.97	0.00257
	0.0463	40.06	0.00182
	0.0338	30.49	0.00133
	0.0216	26.78	0.00085
	0.0132	7.65	0.00052
	0.0094	4.78	0.00037
	0.0066	4.67	0.00026
	0.0034	2.58	0.00013
	0.0023	2.30	0.00009

Figure 141. Particle size distribution in water for Western Iowa loess

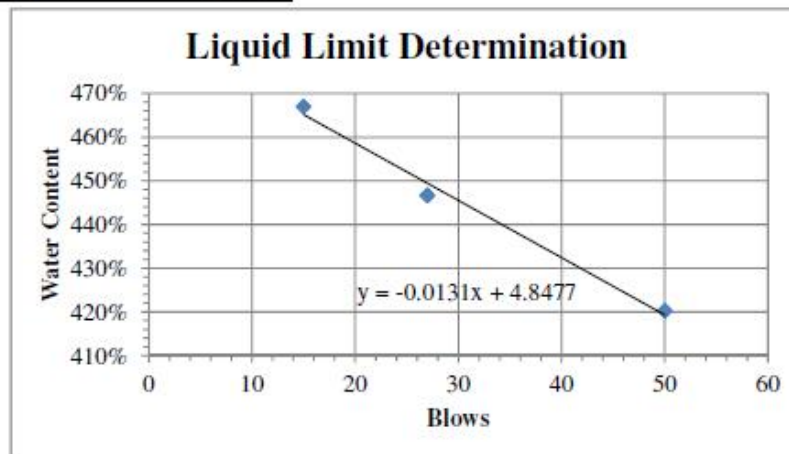
Bentonite

ATTERBERG LIMIT RESULTS

Soil: Bentonite

Liquid Limit					
can (g)	wet (g)	dry (g)	water (g)	w%	blows
10.99	15.36	11.83	3.53	420%	50
10.92	17.37	12.1	5.27	447%	27
11.09	17.44	12.21	5.23	467%	15

	blows	w%
LL	25	452%



Plastic Limit				
can (g)	wet (g)	dry (g)	water (g)	w%
11.09	12.36	11.94	0.42	49%
11.14	12	11.71	0.29	51%
			PL	50%

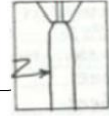
Plasticity Index	402%
-------------------------	-------------

Figure 142. Atterberg limit results for bentonite

PINHOLE TEST DATA

Sample No. Bentonite
 Compaction Characteristics: compacted using Harvard miniature
 Water Content: optimum at 46.7%
 Distilled Water Added: Yes No
 Curing Time: 24 hr
 State: remolded using Harvard mini compaction
 Project: Velasco Thesis Site No. _____

Specimen after test



Date 22-May
 Page _____
 By EV

Final hole:
see picture

Flow started on _____ trial

Clock Time		Head (in)	Flow		Flow Rate (ml/sec)	Turbidity from Side						Completely Clear from Top	Remarks
minutes	seconds		ml	sec		Very Dark	Dark	Moderately Dark	Slightly Dark	Barely Visible	Clear		
0	41	2	25	41	0.610						X		
2	145	2	50	145	0.240				X				
4	260	2	100	260	0.435				X				
5	300	2	125	300	0.625				X				
6	360	2	150	360	0.417				X				
7	420	2	200	420	0.833			X					
7	450	2	235	450	1.167			X					
8	480	2	280	480	1.500		X						
9	540	2	340	540	1.000		X						
10	600	7	420	600	1.333		X						Under 2 in head and 10 min, flow is distinctly dark, flow rate is between 1 and 1.3 mL/s and hole diameter is greater than 1.5-2 needle diameters -> is classified as D 2

Figure 143. Pinhole test results for bentonite

Date	Time of Reading	Elapsed Time, t (min)	Temperature (°C)	Actual Hydrometer Reading, R_a	Corrected Hydrometer Reading, R_c	% Finer	Hydrometer Correction only for Meniscus, R	L (cm)	L/t	K	D (mm)
5/20/2013	11:00:00 AM	0	-	-	-	-	-	-	-	-	-
5/20/2013	11:00:30 AM	0.5	22.0	22.5	16.4	35.58	24	12.6	25.2	0.01374	0.068974
5/20/2013	11:01:00 AM	1	22.0	22	15.9	34.50	23	12.7	12.7	0.01374	0.048965
5/20/2013	11:02:00 AM	2	22.0	22	15.9	34.50	23	12.7	6.35	0.01374	0.034624
5/20/2013	11:05:00 AM	5	22.0	22	15.9	34.50	23	12.7	2.54	0.01374	0.021898
5/20/2013	11:15:00 AM	15	22.1	20.5	14.4	31.31	22	13.0	0.863	0.01372	0.012752
5/20/2013	11:35:00 AM	30	22.2	20.5	14.5	31.37	22	13.0	0.432	0.01371	0.009006
5/20/2013	12:00:00 PM	60	22.2	19.5	13.5	29.20	21	13.1	0.218	0.01371	0.006405
5/20/2013	1:11:00 PM	135	23.0	18.5	12.7	27.55	20	13.3	0.0981	0.01358	0.004254
5/20/2013	3:30:00 PM	270	23.5	17	11.4	24.62	18	13.5	0.0500	0.01350	0.003019
5/20/2013	7:23:00 PM	525	23.8	16	10.4	22.65	17	13.7	0.0261	0.01345	0.002173
5/21/2013	6:48:00 AM	710	23.8	15	9.4	20.48	16	13.8	0.0194	0.01345	0.001875
5/21/2013	11:10:00 AM	1398	23.8	14	8.4	18.31	15	14.0	0.0100	0.01345	0.001346
5/21/2013	4:50:00 PM	1674	24.0	13	7.5	16.27	14	14.2	0.00848	0.01342	0.001236
5/21/2013	6:28:00 PM	1998	23.8	13	7.4	16.14	14	14.2	0.00711	0.01345	0.001134
5/22/2013	10:55:00 AM	2820	24.0	12.5	7.0	15.19	14	14.3	0.00505	0.01342	0.000954
5/22/2013	3:18:00 PM	3085	24.0	12	6.5	14.10	13	14.3	0.00464	0.01342	0.000914
		3348	23.5	12	6.4	13.78	13	14.3	0.00427	0.01350	0.000882

$R_c = R_a - \text{Zero Correction} + C_T$; C_T from Table 6-3 of Bowles.

$$\% \text{ Finer} = \frac{R_c \alpha}{W_s}$$

$$D = K \sqrt{L/t}$$

Hydrometer Analysis Parameters	
Hydrometer Number	152H
G_s of Solids	2.55
α	1.02
Dispersing Agent	125 mL of Sodium Hexametaphosphate
Weight of Soil, W_s	47.01492537 grams
Zero Correction	6.5
Meniscus Correction	1.0

Figure 144. Particle size analysis in a dispersant for bentonite

Particle Size Distribution in Dispersant

Sieve #	Particle Diameter (mm)	Percent Finer (%)	Particle Diameter (in)
	76.2	100	3.00000
	50.8	100	2.00000
	38.1	100	1.50000
	25.4	100	1.00000
	19.05	100	0.75000
	9.53	100	0.37520
4	4.76	100	0.18740
10	2.00	100	0.07874
40	0.841	100	0.03311
60	0.250	100	0.00984
100	0.1490	100	0.00587
200	0.0740	100.0	0.00291
	0.0690	35.6	0.00272
	0.0490	34.5	0.00193
	0.0346	34.5	0.00136
	0.0219	34.5	0.00086
	0.0128	31.3	0.00050
	0.0090	31.4	0.00035
	0.0064	29.2	0.00025
	0.0043	27.6	0.00017
	0.0030	24.6	0.00012
	0.0022	22.6	0.00009
	0.0019	20.5	0.00007
	0.0013	18.3	0.00005
	0.0012	16.3	0.00005
	0.0011	16.1	0.00004
	0.0010	15.2	0.00004
	0.0009	14.1	0.00004
	0.0009	13.8	0.00003

Figure 145. Particle size distribution in a dispersant for bentonite

Date	Time of Reading	Elapsed Time, t (min)	Temperature (°C)	Actual Hydrometer Reading, R_a	Corrected Hydrometer Reading, R_c	% Finer	Hydrometer Correction only for Meniscus, R	L (cm)	L/t	K	D (mm)
5/20/2013	11:00:00 AM	0	-	-	-	-	-	-	-	-	-
5/20/2013	11:00:30 AM	0.5	23.8	10.5	11.4	21.51	12	14.6	29.2	0.01329	0.071826
5/20/2013	11:01:00 AM	1	23.8	10.5	11.4	21.51	12	14.6	14.6	0.01329	0.050789
5/20/2013	11:02:00 AM	2	23.8	10	10.9	20.57	11	14.7	7.4	0.01329	0.036036
5/20/2013	11:05:00 AM	5	23.8	10	10.9	20.57	11	14.7	2.9	0.01329	0.022791
5/20/2013	11:15:00 AM	15	23.8	10	10.9	20.57	11	14.7	1.0	0.01329	0.013158
5/20/2013	11:35:00 AM	35	23.8	9	9.9	18.69	10	14.8	0.4	0.01329	0.008643
5/20/2013	12:00:00 PM	60	23.8	9	9.9	18.69	10	14.8	0.2	0.01329	0.006602
5/20/2013	1:11:00 PM	131	23.5	9	9.9	18.52	10	14.8	0.1	0.01334	0.004484
5/20/2013	3:30:00 PM	270	23.0	9	9.7	18.24	10	14.8	0.1	0.01342	0.003142
5/20/2013	7:23:00 PM	503	23.2	8.5	9.3	17.41	10	14.9	0.0	0.01339	0.002304
5/21/2013	6:48:00 AM	1188	23.0	8	8.7	16.36	9	15.0	0.0	0.01342	0.001508
5/21/2013	11:10:00 AM	1450	23.5	7	7.9	14.76	8	15.2	0.0	0.01334	0.001366
5/21/2013	4:50:00 PM	1790	23.5	7	7.9	14.76	8	15.2	0.0	0.01334	0.001229
5/21/2013	6:28:00 PM	2608	23.8	6.5	7.4	13.99	8	15.3	0.0	0.01329	0.001016
5/22/2013	10:55:00 AM	2875	23.5	6	6.9	12.88	7	15.3	0.0	0.01334	0.000973
5/22/2013	3:18:00 PM	3138	23.0	6	6.7	12.60	7	15.3	0.0	0.01342	0.000937

$R_c = R_a - \text{Zero Correction} + C_T$; C_T from Table 6-3 of Bowles.

$$\% \text{ Finer} = \frac{R_c \cdot a}{W_s}$$

$$D = K \sqrt{L/t}$$

Hydrometer Analysis Parameters	
Hydrometer Number	152H
G_s of Solids	2.55
a	1
Dispersing Agent	Distilled Water
Weight of Soil, W_s	53.17460317 grams
Zero Correction	0
Meniscus Correction	1.0

Figure 146. Particle size analysis in water for bentonite

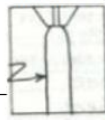
Particle Size Distribution in Distilled Water

Sieve #	Particle Diameter (mm)	Percent Finer (%)	Particle Diameter (in)
	76.2	100	3.00000
	50.8	100	2.00000
	38.1	100	1.50000
	25.4	100	1.00000
	19.05	100	0.75000
	9.53	100	0.37520
4	4.76	100	0.18740
10	2.00	100	0.07874
40	0.841	100	0.03311
60	0.250	100	0.00984
100	0.1490	100	0.00587
200	0.0740	100.0	0.00291
	0.0718	21.5	0.00283
	0.0508	21.5	0.00200
	0.0360	20.6	0.00142
	0.0228	20.6	0.00090
	0.0132	20.6	0.00052
	0.0086	18.7	0.00034
	0.0066	18.7	0.00026
	0.0045	18.5	0.00018
	0.0031	18.2	0.00012
	0.0023	17.4	0.00009
	0.0015	16.4	0.00006
	0.0014	14.8	0.00005
	0.0012	14.8	0.00005
	0.0010	14.0	0.00004
	0.0010	12.9	0.00004
	0.0009	12.6	0.00004

Figure 147. Particle size distribution in water for bentonite

PINHOLE TEST DATA

Sample No. Bentonite
 Compaction Characteristics: compacted using Harvard miniature
 Water Content: _____
 Distilled Water Added: Yes No _____
 Curing Time: 48 hr
 State: remolded using Harvard mini compaction
 Project: Velasco Thesis Site No. _____

Specimen after test
 Date 6-Jun
 Page _____
 By EV
 Final hole: see picture 
 Flow started on _____ trial

Clock Time		Head (in)	Flow		Flow Rate (ml/sec)	Turbidity from Side						Completely Clear from Top	Remarks
minutes	seconds		ml	sec		Very Dark	Dark	Moderately Dark	Slightly Dark	Barely Visible	Clear		
2	160	2	25	160	0.156						X	X	
5	300	2	50	300	0.179						X	X	
8	500	2	80	500	0.150						X	X	
10	600	2	100	600	0.200						X	X	
12	720	7	155	720	0.458						X	X	
13	810	7	210	810	0.611						X	X	
15	900	7	280	900	0.778						X	X	
17	1020	15	450	1020	1.417						X	X	
17	1050	15	515	1050	2.167						X	X	
18	1110	15	660	1110	2.417						X	X	
19	1140	15	810	1140	5.000						X		
19	1170	15	975	1170	5.500						X		
20	1200	15	1150	1200	5.833						X		
													Under 40 in head and 15 min, flow is nearly clear, flow rate is greater than 3.0 mL/s and hole diameter is less than 1.5-2 needle diameters --> is classified as ND2

Figure 148. Pinhole test data form for bentonite with 4% lime

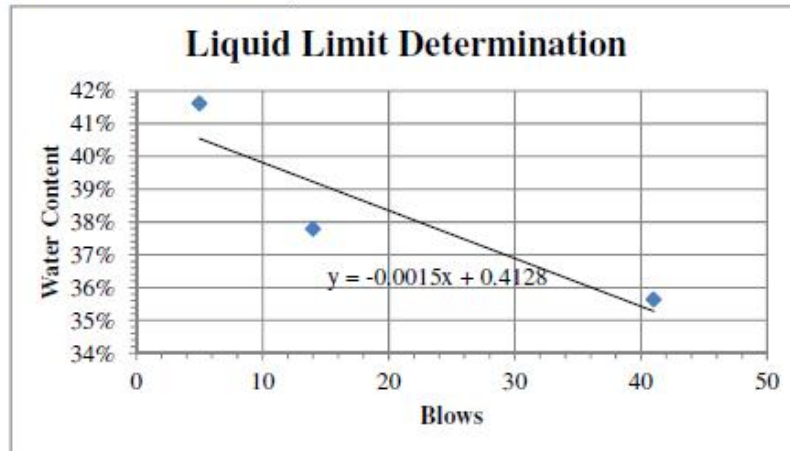
Kaolinite

ATTERBERG LIMIT RESULTS

Soil: Kaolinite

Liquid Limit					
can (g)	wet (g)	dry (g)	water (g)	w%	blows
11.1	16.34	14.8	1.54	42%	5
10.95	18.06	16.11	1.95	38%	14
10.98	18.25	16.34	1.91	36%	41

	blows	w%
LL	25	38%



Plastic Limit				
can (g)	wet (g)	dry (g)	water (g)	w%
11.02	11.92	11.72	0.2	29%
11.12	11.41	11.34	0.07	32%
		PL		30%

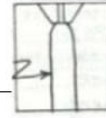
Plasticity Index	7%
------------------	----

Figure 149. Atterberg limit results for kaolinite

PINHOLE TEST DATA

Sample No. Kaolin
 Compaction Characteristics: compacted using Harvard miniature
 Water Content: optimum at 26%
 Distilled Water Added: Yes No
 Curing Time: 24 hr
 State: remolded using Harvard mini compaction
 Project: Velasco Thesis Site No. _____

Specimen after test



Final hole: see picture

Date 22-May
 Page _____
 By EV

Flow started on _____ trial

Clock Time		Head (in)	Flow		Flow Rate ml/sec	Turbidity from Side						Completely Clear from Top	Remarks
minutes	seconds		ml	sec		Very Dark	Dark	Moderately Dark	Slightly Dark	Barely Visible	Clear		
1	105	2	25	105	0.238				X				
2	160	2	50	160	0.455				X				
3	228	2	100	228	0.735				X				
5	300	2	150	300	0.694				X				
6	360	2	205	360	0.917				X				
8	480	2	295	480	0.750				X				
9	540	2	330	540	0.583				X				
10	600	7	375	600	0.750			X					
11	660	7	420	660	0.750			X					
12	750	7	580	750	1.778			X					
13	780	7	615	780	1.167			X					
14	840	7	715	840	1.667			X					
15	900	7	820	900	1.750			X					Under 7 in head and 15 min, flow is distinctly dark, flow rate is between 1.4 and 2.7 mL/s and hole diameter is greater than 1.5-2 needle diameters --> is classified as ND3

Figure 150. Pinhole test data form for kaolinite

Date	Time of Reading	Elapsed Time, t (min)	Temperature (°C)	Actual Hydrometer Reading, R_a	Corrected Hydrometer Reading, R_c	% Finer	Hydrometer Correction only for Meniscus, R	L (cm)	L/t	K	D (mm)
5/23/2013	10:00:00 AM	0	-	-	-	-	-	-	-	-	-
5/23/2013	10:00:30 AM	0.5	22.8	55	49.1	99.99	56	7.3	14.6	0.01320	0.050437
5/23/2013	10:01:00 AM	1	22.8	55	49.1	99.99	56	7.3	7.3	0.01320	0.035664
5/23/2013	10:02:00 AM	2	22.8	55	49.1	99.99	56	7.3	3.65	0.01320	0.025219
5/23/2013	10:05:00 AM	5	22.8	55	49.1	99.99	56	7.3	1.46	0.01320	0.015950
5/23/2013	10:15:00 AM	15	22.5	54	48.1	97.77	55	7.4	0.493	0.01325	0.009303
5/23/2013	10:30:00 AM	30	22.5	53	47.1	95.74	54	7.6	0.253	0.01325	0.006667
5/23/2013	11:00:00 AM	60	23.0	52	46.2	94.01	53	7.8	0.130	0.01317	0.004749
5/23/2013	12:26:00 PM	146	23.2	49	43.3	88.03	50	8.3	0.0568	0.01314	0.003133
5/23/2013	2:30:00 PM	270	23.2	45.5	39.8	80.90	47	8.9	0.0328	0.01314	0.002379
5/23/2013	6:45:00 PM	525	23.2	41	35.3	71.75	42	9.6	0.0183	0.01314	0.001777
5/23/2013	10:02:00 PM	722	23.5	38.5	32.9	66.84	40	10.0	0.0139	0.01309	0.001541
5/24/2013	9:28:00 AM	1408	23.8	33	27.4	55.83	34	10.9	0.0077	0.01304	0.001148
5/24/2013	2:05:00 PM	1685	24.0	30.5	25.0	50.87	32	11.3	0.00671	0.01301	0.001065
5/24/2013	7:29:00 PM	2009	23.8	29.5	23.9	48.71	31	11.5	0.00570	0.01304	0.000985
5/25/2013	9:10:00 AM	2830	24.0	26	20.5	41.71	27	12.0	0.00424	0.01301	0.000847
5/25/2013	1:35:00 PM	3095	24.0	24	18.5	37.64	25	12.4	0.00401	0.01301	0.000823
5/25/2013	6:00:00 PM	3360	23.2	24	18.3	37.16	25	12.4	0.00369	0.01314	0.000798

$R_c = R_a - \text{Zero Correction} + C_T$; C_T from Table 6-3 of Bowles.

$$\% \text{ Finer} = \frac{R_c a}{W_s}$$

$$D = K \sqrt{L/t}$$

Hydrometer Analysis Parameters	
Hydrometer Number	152H
G_s of Solids	2.65
a	1
Dispersing Agent	125 mL of Sodium Hexametaphosphate
Weight of Soil, W_s	49.14500684 grams
Zero Correction	6.5
Meniscus Correction	1.0

Figure 151. Particle size analysis in a dispersant for kaolinite

Particle Size Distribution in Dispersant

Sieve #	Particle Diameter (mm)	Percent Finer (%)	Particle Diameter (in)
	76.2	100	3.00000
	50.8	100	2.00000
	38.1	100	1.50000
	25.4	100	1.00000
	19.05	100	0.75000
	9.53	100	0.37520
4	4.76	100	0.18740
10	2.00	100	0.07874
40	0.841	100	0.03311
60	0.250	100	0.00984
100	0.1490	100	0.00587
200	0.0740	100.0	0.00291
	0.0504	100.0	0.00199
	0.0357	100.0	0.00140
	0.0252	100.0	0.00099
	0.0159	100.0	0.00063
	0.0093	97.8	0.00037
	0.0067	95.7	0.00026
	0.0047	94.0	0.00019
	0.0031	88.0	0.00012
	0.0024	80.9	0.00009
	0.0018	71.7	0.00007
	0.0015	66.8	0.00006
	0.0011	55.8	0.00005
	0.0011	50.9	0.00004
	0.0010	48.7	0.00004
	0.0008	41.7	0.00003
	0.0008	37.6	0.00003
	0.0008	37.2	0.00003

Figure 152. Particle size distribution in a dispersant for kaolinite

Date	Time of Reading	Elapsed Time, t (min)	Temperature (°C)	Actual Hydrometer Reading, R_a	Corrected Hydrometer Reading, R_c	% Finer	Hydrometer Correction only for Meniscus, R	L (cm)	L/t	K	D (mm)
5/23/2013	10:00:00 AM	0	-	-	-	-	-	-	-	-	-
5/23/2013	10:00:30 AM	0.5	23.8	23	23.9	47.88	24	12.5	25.0	0.01304	0.065210
5/23/2013	10:01:00 AM	1	23.8	23	23.9	47.88	24	12.5	12.5	0.01304	0.046110
5/23/2013	10:02:00 AM	2	23.8	23	23.9	47.88	24	12.5	6.3	0.01304	0.032605
5/23/2013	10:05:00 AM	5	23.8	23	23.9	47.88	24	12.5	2.5	0.01304	0.020621
5/23/2013	10:15:00 AM	15	23.8	23	23.9	47.88	24	12.5	0.8	0.01304	0.011906
5/23/2013	10:30:00 AM	30	23.2	23	23.8	47.52	24	12.5	0.4	0.01314	0.008481
5/23/2013	11:00:00 AM	60	23.2	22	22.8	45.52	23	12.7	0.2	0.01314	0.006044
5/23/2013	12:20:00 PM	140	23.0	21	21.7	43.40	22	12.9	0.1	0.01317	0.003998
5/23/2013	2:40:00 PM	280	23.2	20	20.8	41.52	21	13.0	0.0	0.01314	0.002831
5/23/2013	6:32:00 PM	512	23.0	19	19.7	39.40	20	13.2	0.0	0.01317	0.002115
5/24/2013	6:00:00 AM	1200	23.2	17.5	18.3	36.52	19	13.4	0.0	0.01314	0.001388
5/24/2013	10:20:00 AM	1460	23.2	17	17.8	35.52	18	14.5	0.0	0.01314	0.001309
5/24/2013	4:00:00 PM	1800	23.5	15	15.9	31.70	16	13.8	0.0	0.01309	0.001146
5/24/2013	5:38:00 PM	2618	23.5	14	14.9	29.70	15	14.0	0.0	0.01309	0.000957
5/25/2013	10:24:00 AM	2885	23.5	13	13.9	27.70	14	14.2	0.0	0.01309	0.000918
5/25/2013	2:30:00 PM	3150	23.2	13	13.8	27.52	14	14.2	0.0	0.01314	0.000882

$R_c = R_a - \text{Zero Correction} + C_T$; C_T from Table 6-3 of Bowles.

$$\% \text{ Finer} = \frac{R_c \cdot a}{W_s}$$

$$D = K \sqrt{L/t}$$

Hydrometer Analysis Parameters	
Hydrometer Number	152H
G_s of Solids	2.65
σ	1
Dispersing Agent	Distilled Water
Weight of Soil, W_s	50 grams
Zero Correction	0
Meniscus Correction	1.0

Figure 153. Particle size analysis in water for kaolinite

Particle Size Distribution in Distilled Water

Sieve #	Particle Diameter (mm)	Percent Finer (%)	Particle Diameter (in)
	76.2	100	3.00000
	50.8	100	2.00000
	38.1	100	1.50000
	25.4	100	1.00000
	19.05	100	0.75000
	9.53	100	0.37520
4	4.76	100	0.18740
10	2.00	100	0.07874
40	0.841	100	0.03311
60	0.250	100	0.00984
100	0.1490	100	0.00587
200	0.0740	100.0	0.00291
	0.0652	47.9	0.00257
	0.0461	47.9	0.00182
	0.0326	47.9	0.00128
	0.0206	47.9	0.00081
	0.0119	47.9	0.00047
	0.0085	47.5	0.00033
	0.0060	45.5	0.00024
	0.0040	43.4	0.00016
	0.0028	41.5	0.00011
	0.0021	39.4	0.00008
	0.0014	36.5	0.00005
	0.0013	35.5	0.00005
	0.0011	31.7	0.00005
	0.0010	29.7	0.00004
	0.0009	27.7	0.00004
	0.0009	27.5	0.00003

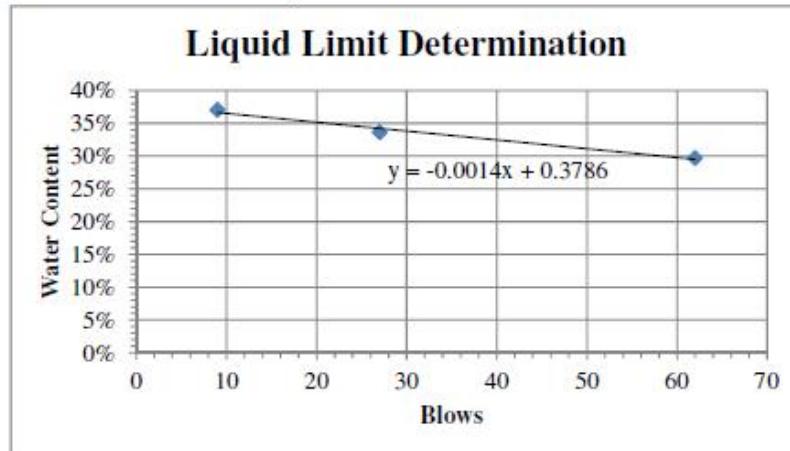
Figure 154. Particle size distribution in water for kaolinite

Santa Rosa clay
ATTERBERG LIMIT RESULTS

Soil: Santa Rosa Clay

Liquid Limit					
can (g)	wet (g)	dry (g)	water (g)	w%	blows
11.04	17.33	15.89	1.44	30%	62
11.02	17.22	15.66	1.56	34%	27
11.03	21.02	18.32	2.7	37%	9

	blows	w%
LL	25	34%



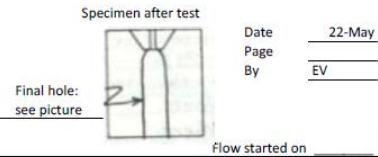
Plastic Limit				
can (g)	wet (g)	dry (g)	water (g)	w%
11.13	14.26	13.75	0.51	19%
10.97	13.42	13.03	0.39	19%
		PL		19%

Plasticity Index	15%
------------------	-----

Figure 155. Atterberg limit results for Santa Rosa clay

PINHOLE TEST DATA

Sample No. Santa Rosa Clay
 Compaction Characteristics: compacted using Harvard miniature
 Water Content: optimum at 16%
 Distilled Water Added: Yes X No
 Curing Time: 24 hr
 State: remolded using Harvard mini compaction
 Project: Velasco Thesis Site No.



Clock Time		Head (in)	Flow		Flow Rate (ml/sec)	Turbidity from Side					Completely Clear from Top	Remarks	
minutes	seconds		ml	sec		Very Dark	Dark	Moderately Dark	Slightly Dark	Barely Visible			Clear
2	129	2	25	129	0.194			X				repunch hole to instigate flow	
5	0	2	50	300	0.146			X					
10	0	7	90	600	0.133			X					
11	30	7	125	690	0.389			X					
12	0	7	150	720	0.833			X					
13	0	7	200	780	0.833			X					
14	0	7	260	840	1.000			X					
15	0	7	350	900	1.500			X					
													Under 7 in head and 15 min, flow is distinctly dark, flow rate is between 1.4 and 2.7 mL/s and hole diameter is greater than 1.5-2 needle diameters -> is classified as ND 3

Figure 156. Pinhole test data form for Santa Rosa clay

Date	Time of Reading	Elapsed Time, t (min)	Temperature (°C)	Actual Hydrometer Reading, R _a	Corrected Hydrometer Reading, R _c	% Finer	Hydrometer Correction only for Meniscus, R	L (cm)	L/t	K	D (mm)
5/9/2013	10:03:00 AM	0	-	-	-	-	-	-	-	-	-
5/9/2013	10:03:30 AM	0.5	22.8	47	42.6	86.50	48	8.6	17.2	0.01300	0.053915
5/9/2013	10:04:00 AM	1	22.8	45	40.6	82.44	46	8.9	8.9	0.01300	0.038783
5/9/2013	10:05:00 AM	2	22.8	41	36.6	74.33	42	9.6	4.80	0.01300	0.028482
5/9/2013	10:08:00 AM	6	22.8	35	30.6	62.16	36	10.6	1.77	0.01300	0.017279
5/9/2013	10:18:00 AM	15	22.8	29	24.6	49.98	30	11.5	0.767	0.01300	0.011383
5/9/2013	10:33:00 AM	30	23.0	26	21.7	44.02	27	12.0	0.400	0.01297	0.008203
5/9/2013	11:03:00 AM	60	22.8	22	17.6	35.78	23	12.7	0.212	0.01300	0.005981
5/9/2013	11:46:00 AM	137	23.2	18	13.8	27.91	19	13.3	0.0971	0.01294	0.004032
5/9/2013	2:03:00 PM	270	23.2	16	11.8	23.86	17	13.7	0.05074	0.01294	0.002915
5/9/2013	6:24:00 PM	503	23.5	14.5	10.4	21.00	16	13.9	0.02763	0.01290	0.002144
5/10/2013	2:16:00 AM	1375	23.3	12	7.8	15.80	13	14.3	0.01040	0.01293	0.001318
5/10/2013	10:17:00 AM	1496	23.5	11.5	7.4	14.91	13	14.4	0.00963	0.01290	0.001265

$R_c = R_a - \text{Zero Correction} + C_T$; C_T from Table 6-3 of Bowles.

$$\% \text{ Finer} = \frac{R_c \cdot a}{W_s}$$

$$D = K \sqrt{L/t}$$

Hydrometer Analysis Parameters	
Hydrometer Number	152H
G _s of Solids	2.70
a	0.99
Dispersing Agent	125 mL of Sodium Hexametaphosphate
Weight of Soil, W _s	48.80239521 grams
Zero Correction	5
Meniscus Correction	1.0

Figure 157. Particle size analysis in a dispersant for Santa Rosa clay

Particle Size Distribution in Dispersant

Sieve #	Particle Diameter (mm)	Percent Finer (%)	Particle Diameter (in)
	76.2	100	3.00000
	50.8	100	2.00000
	38.1	100	1.50000
	25.4	100	1.00000
	19.05	100	0.75000
	9.53	100	0.37520
4	4.76	100	0.18740
10	2.00	100.00	0.07874
40	0.841	99.80	0.03311
60	0.250	99.59	0.00984
100	0.1490	98.57	0.00587
200	0.0740	93.85	0.00291
	0.0539	86.5	0.00212
	0.0388	82.4	0.00153
	0.0285	74.3	0.00112
	0.0173	62.2	0.00068
	0.0114	50.0	0.00045
	0.0082	44.0	0.00032
	0.0060	35.8	0.00024
	0.0040	27.9	0.00016
	0.0029	23.9	0.00011
	0.0021	21.0	0.00008
	0.0013	15.8	0.00005
	0.0013	14.9	0.00005

Figure 158. Particle size distribution in a dispersant for Santa Rosa clay

Date	Time of Reading	Elapsed Time, t (min)	Temperature (°C)	Actual Hydrometer Reading, R_a	Corrected Hydrometer Reading, R_c	% Finer	Hydrometer Correction only for Meniscus, R	L (cm)	L/t	K	D (mm)
5/20/2013	3:31:00 PM	0	-	-	-	-	-	-	-	-	-
5/20/2013	3:31:30 PM	0.5	24.0	17	18.0	34.79	18	13.5	27.0	0.01282	0.066615
5/20/2013	3:32:00 PM	1	24.0	15	16.0	30.92	16	13.8	13.8	0.01282	0.047624
5/20/2013	3:33:00 PM	2	24.0	12	13.0	25.12	13	14.3	7.15	0.01282	0.034280
5/20/2013	3:36:00 PM	5	24.0	9	10.0	19.33	10	14.8	2.96	0.01282	0.022056
5/20/2013	3:46:00 PM	15	23.8	6	6.9	13.41	7	15.3	1.020	0.01285	0.012978
5/20/2013	4:01:00 PM	30	23.8	5	5.9	11.48	6	15.5	0.517	0.01285	0.009237
5/20/2013	4:31:00 PM	60	23.5	3	3.9	7.44	4	15.8	0.263	0.01290	0.006617
5/20/2013	8:01:00 PM	135	23.5	2	2.9	5.51	3	16.0	0.1185	0.01290	0.004439
5/21/2013	12:21:00 AM	270	23.5	1	1.9	3.58	2	16.1	0.05963	0.01290	0.003149
5/21/2013	10:26:00 AM	500	23.2	0	0.8	1.47	1	16.3	0.03260	0.01294	0.002336

$R_c = R_a - \text{Zero Correction} + C_T$; C_T from Table 6-3 of Bowles.

$$\% \text{ Finer} = \frac{R_c a}{W_s}$$

$$D = K \sqrt{L/t}$$

Hydrometer Analysis Parameters	
Hydrometer Number	152H
G_s of Solids	2.70
a	0.99
Dispersing Agent	Distilled Water
Weight of Soil, W_s	51.22699387 grams
Zero Correction	0
Meniscus Correction	1.0

Figure 159. Particle size analysis in water for Santa Rosa clay

Particle Size Distribution in Distilled Water

Sieve #	Particle Diameter (mm)	Percent Finer (%)	Particle Diameter (in)
	76.2	100	3.00000
	50.8	100	2.00000
	38.1	100	1.50000
	25.4	100	1.00000
	19.05	100	0.75000
	9.53	100	0.37520
4	4.76	100	0.18740
10	2.00	100.00	0.07874
40	0.841	99.80	0.03311
60	0.250	99.59	0.00984
100	0.1490	98.57	0.00587
200	0.0740	93.85	0.00291
	0.0666	34.8	0.00262
	0.0476	30.9	0.00187
	0.0343	25.1	0.00135
	0.0221	19.3	0.00087
	0.0130	13.4	0.00051
	0.0092	11.5	0.00036
	0.0066	7.4	0.00026
	0.0044	5.5	0.00017
	0.0031	3.6	0.00012

Figure 160. Particle size distribution in water for Santa Rosa clay

Sodium illite

PINHOLE TEST DATA

Sample No. Sodium Illite
 Compaction Characteristics: compacted using Harvard miniature
 Water Content: optimum at 27%
 Distilled Water Added: Yes No
 Curing Time: 24 hr
 State: remolded using Harvard mini compaction
 Project: Velasco Thesis Site No. _____

Specimen after test



Date 7-Jun
 Page _____
 By EV

Final hole: see picture

Flow started on _____ trial

Clock Time		Head (in)	Flow		Flow Rate (ml/sec)	Turbidity from Side						Completely Clear from Top	Remarks
minutes	seconds		ml	sec		Very Dark	Dark	Moderately Dark	Slightly Dark	Barely Visible	Clear		
1	16	2	25	76	0.329						X		
2	26	2	50	146	0.357					X			
4	34	2	100	274	0.391			X					
5	0	2	110	300	0.385			X					
5	30	2	130	330	0.667			X					
6	0	2	145	360	0.500		X						
6	30	2	160	390	0.500		X						
7	0	2	175	420	0.500		X						
7	30	2	195	450	0.667		X						
8	0	2	210	480	0.500		X						
8	30	2	230	510	0.667		X						
9	0	2	255	540	0.833		X						
9	30	2	275	570	0.667		X						
10	0	2	300	600	0.833		X						
10	30	7	335	630	1.167		X						
11	0	7	380	660	1.500		X						
11	30	7	430	690	1.667		X						
12	0	7	480	720	1.667		X						
12	30	7	545	750	2.167		X						
13	0	7	595	780	1.667		X						
13	30	7	645	810	1.667		X						
14	0	7	700	840	1.833	X							
14	30	7	760	870	2.000	X							
15	0	7	815	900	1.833	X							Under 7 in head and 15 min, flow is distinctly dark, flow rate is between 1.4 and 2.7 mL/s and hole diameter is greater than 1.5-2 needle diameters --> is classified as ND 3

Figure 161. Pinhole test data form for sodium illite

Date	Time of Reading	Elapsed Time, t (min)	Temperature (°C)	Actual Hydrometer Reading, R_a	Corrected Hydrometer Reading, R_c	% Finer	Hydrometer Correction only for Meniscus, R	L (cm)	L/t	K	D (mm)
6/3/2013	12:00:00 PM	0	-	-	-	-	-	-	-	-	-
6/3/2013	12:00:30 PM	0.5	21.5	55	48.8	99.37	56	7.3	14.6	0.01276	0.048767
6/3/2013	12:01:15 PM	1	21.5	55	48.8	99.37	56	7.3	7.3	0.01276	0.034484
6/3/2013	12:02:15 PM	2.25	21.5	54.5	48.3	98.35	56	7.4	3.27	0.01276	0.023068
6/3/2013	12:05:00 PM	5	21.5	54.5	48.3	98.35	56	7.4	1.47	0.01276	0.015474
6/3/2013	12:15:00 PM	15	22.0	54.5	48.4	98.56	56	7.4	0.490	0.01269	0.008882
6/3/2013	12:30:00 PM	30	22.0	54.5	48.4	98.56	56	7.4	0.245	0.01269	0.006280
6/3/2013	1:00:00 PM	60	22.0	54	47.9	97.54	55	7.4	0.123	0.01269	0.004456
6/3/2013	2:30:00 PM	150	22.5	53.5	47.6	96.83	55	7.5	0.0500	0.01246	0.002787
6/3/2013	5:49:00 PM	349	22.8	52	46.1	93.96	53	7.8	0.02235	0.01242	0.001856
6/3/2013	8:43:00 PM	523	23.2	50	44.3	90.13	51	8.1	0.01549	0.01222	0.001520
6/3/2013	10:46:00 PM	646	23.2	49	43.3	88.09	50	8.3	0.01285	0.01222	0.001385
6/3/2013	10:40:00 AM	1240	23.7	47	41.4	84.32	48	8.6	0.00694	0.01214	0.001011
6/3/2013	12:27:00 PM	1467	23.2	45	39.3	79.95	46	8.9	0.00607	0.01222	0.000952

$R_c = R_a - \text{Zero Correction} + C_T$; C_T from Table 6-3 of Bowles.

$$\% \text{ Finer} = \frac{R_c \cdot a}{W_s}$$

$$D = K \sqrt{L/t}$$

Hydrometer Analysis Parameters	
Hydrometer Number	152H
G_s of Solids	2.82
a	0.966
Dispersing Agent	125 mL of Sodium Hexametaphosphate
Weight of Soil, W_s	47.43833017 grams
Zero Correction	6.5
Meniscus Correction	1.0

Figure 162. Particle size analysis in a dispersant for sodium illite

Particle Size Distribution in Dispersant

Sieve #	Particle Diameter (mm)	Percent Finer (%)	Particle Diameter (in)
	76.2	100	3.00000
	50.8	100	2.00000
	38.1	100	1.50000
	25.4	100	1.00000
	19.05	100	0.75000
	9.53	100	0.37520
4	4.76	100	0.18740
10	2.00	100.00	0.07874
40	0.841	100.00	0.03311
60	0.250	100.00	0.00984
100	0.1490	100.00	0.00587
200	0.0740	100.00	0.00291
	0.0488	99.4	0.00192
	0.0345	99.4	0.00136
	0.0231	98.4	0.00091
	0.0155	98.4	0.00061
	0.0089	98.6	0.00035
	0.0063	98.6	0.00025
	0.0045	97.5	0.00018
	0.0028	96.8	0.00011
	0.0019	94.0	0.00007
	0.0015	90.1	0.00006
	0.0014	88.1	0.00005
	0.0010	84.3	0.00004
	0.0010	79.9	0.00004

Figure 163. Particle size distribution in a dispersant for sodium illite

Date	Time of Reading	Elapsed Time, t (min)	Temperature (°C)	Actual Hydrometer Reading, R_a	Corrected Hydrometer Reading, R_c	% Finer	Hydrometer Correction only for Meniscus, R	L (cm)	L/t	K	D (mm)
6/3/2013	12:00:00 PM	0	-	-	-	-	-	-	-	-	-
6/3/2013	12:00:30 PM	0.5	22.8	22	22.6	41.50	23	12.7	25.4	0.01257	0.063341
6/3/2013	12:01:15 PM	1.25	22.8	22	22.6	41.50	23	12.7	10.2	0.01257	0.040060
6/3/2013	12:02:15 PM	2.25	22.8	22	22.6	41.50	23	12.7	5.64	0.01257	0.029859
6/3/2013	12:05:00 PM	5	23.0	22	22.7	41.61	23	12.7	2.54	0.01254	0.019982
6/3/2013	12:15:00 PM	15	23.0	21.5	22.2	40.69	23	12.8	0.853	0.01254	0.011582
6/3/2013	12:30:00 PM	30	23.0	21	21.7	39.78	22	12.9	0.430	0.01254	0.008222
6/3/2013	1:00:00 PM	60	23.0	20	20.7	37.94	21	13.0	0.217	0.01254	0.005836
6/3/2013	2:30:00 PM	150	23.0	20	20.7	37.94	21	13.0	0.0867	0.01254	0.003691
6/3/2013	5:49:00 PM	349	22.8	19	19.6	36.00	20	13.2	0.03782	0.01257	0.002444
6/3/2013	8:43:00 PM	523	23.2	18	18.8	34.39	19	13.3	0.02543	0.01236	0.001971
6/3/2013	10:46:00 PM	646	23.2	18	18.8	34.39	19	13.3	0.02059	0.01236	0.001774
6/3/2013	10:40:00 AM	1240	23.7	16	16.9	31.00	17	13.7	0.01105	0.01229	0.001292
6/3/2013	12:27:00 PM	1467	23.8	15	15.9	29.22	16	13.8	0.00941	0.01228	0.001191

$R_c = R_a - \text{Zero Correction} + C_T$; C_T from Table 6-3 of Bowles.

$$\% \text{ Finer} = \frac{R_c \alpha}{W_s}$$

$$D = K \sqrt{L/t}$$

Hydrometer Analysis Parameters	
Hydrometer Number	152H
G_s of Solids	2.82
α	0.966
Dispersing Agent	Distilled Water
Weight of Soil, W_s	52.7 grams
Zero Correction	0
Meniscus Correction	1.0

Figure 164. Particle size analysis in water for sodium illite

Particle Size Distribution in Distilled Water

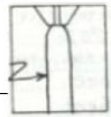
Sieve #	Particle Diameter (mm)	Percent Finer (%)	Particle Diameter (in)
	76.2	100	3.00000
	50.8	100	2.00000
	38.1	100	1.50000
	25.4	100	1.00000
	19.05	100	0.75000
	9.53	100	0.37520
4	4.76	100	0.18740
10	2.00	100.00	0.07874
40	0.841	100.00	0.03311
60	0.250	100.00	0.00984
100	0.1490	100.00	0.00587
200	0.0740	100.00	0.00291
	0.0633	41.5	0.00249
	0.0401	41.5	0.00158
	0.0299	41.5	0.00118
	0.0200	41.6	0.00079
	0.0116	40.7	0.00046
	0.0082	39.8	0.00032
	0.0058	37.9	0.00023
	0.0037	37.9	0.00015
	0.0024	36.0	0.00010
	0.0020	34.4	0.00008
	0.0018	34.4	0.00007
	0.0013	31.0	0.00005
	0.0012	29.2	0.00005

Figure 165. Particle size distribution in water for sodium illite

PINHOLE TEST DATA

Sample No. Sodium Illite with Lime
 Compaction Characteristics: compacted using Harvard miniature
 Water Content: optimum at 27%
 Distilled Water Added: Yes No
 Curing Time: 48 hr
 State: remolded using Harvard mini compaction
 Project: Velasco Thesis Site No. _____

Specimen after test
 Date 7-Jun
 Page _____
 By EV

Final hole: see picture 

Flow started on _____ trial

Clock Time		Head (in)	Flow		Flow Rate (ml/sec)	Turbidity from Side						Completely Clear from Top	Remarks
minutes	seconds		ml	sec		Very Dark	Dark	Moderately Dark	Slightly Dark	Barely Visible	Clear		
1	33	2	25	93	0.269						X		
4	6	2	50	246	0.163						X		
10	0	7	80	600	0.085						X		
11	0	7	85	660	0.083						X		
12	0	7	90	720	0.083						X		
13	0	7	105	780	0.250						X		
14	0	7	120	840	0.250						X		
15	0	7	135	900	0.250						X		
16	0	15	175	960	0.667						X		
16	30	15	200	990	0.833						X		
17	0	15	230	1020	1.000						X		
17	30	15	270	1050	1.333						X		
18	0	15	305	1080	1.167						X		
18	30	15	350	1110	1.500						X		
19	0	15	395	1140	1.500						X		
19	30	15	445	1170	1.667						X		
20	0	15	495	1200	1.667						X		
21	0	40	635	1260	2.333						X		
21	30	40	785	1290	5.000						X		
22	0	40	1000	1320	7.167						X		
23	0	40	1300	1380	5.000						X		
24	0	40	1600	1440	5.000						X		
25	0	40	2000	1500	6.667						X		
													Under 40 in head and 25 min, flow is barely visible, flow rate is greater than 3.0 mL/s and hole diameter is less than 1.5-2 needle diameters --> is classified as ND2

Figure 166. Pinhole test data form for sodium illite treated with 4% lime

